Coordination Chemistry Reviews 540 (2025) 216768

Contents lists available at ScienceDirect

Coordination Chemistry Reviews

journal homepage: www.elsevier.com/locate/ccr

Emerging trends, and prospects in Nanozyme engineering to enhance dual-mode sensing applications

Ragini Singh [a,b,*], Ayush Sharma [c], Oindrila Bainik [d], Bankuru Navyatha [a], Chella Santhosh [e], Earu Banoth [d], Ramachandran Balaji [e], Narendhar Chandrasekar [f], Santosh Kumar [e,**], Hemant Kumar Daima [c,g,h,***]

[a] Department of Biotechnology, Koneru Lakshmaiah Education Foundation, Vaddeswaram, Andhra Pradesh 522302, India
[b] School of Pharmaceutical Sciences and Food Engineering, Liaocheng University, Liaocheng, Shandong Province 252000, China
[c] Amity Center for Nanobiotechnology and Nanomedicine (ACNN), Amity Institute of Biotechnology, Amity University Rajasthan, Jaipur 303002, Rajasthan, India
[d] Opto-Biomedical Microsystems Laboratory, Dept. of Biotechnology and Medical Engineering, National Institute of Technology Rourkela, Odisha 769008, India
[e] Centre of Excellence for Nanotechnology, Department of Electronics and Communication Engineering, Koneru Lakshmaiah Education Foundation, Vaddeswaram 522302, Andhra Pradesh, India
[f] Department of BioNano Technology, Gachon University, 1342 Seongnam-Daero, Sujeong-Gu, 12, Seongnam-si 13120, Gyeonggi-do, Republic of Korea
[g] Nanomedicine and Nanotoxicity Research Laboratory, Department of Biochemistry, School of Life Sciences, Central University of Rajasthan, NH-8, Bandarsindari, Kishangarh 305817, Ajmer, Rajasthan, India
[h] Department of Health Sciences, Interdisciplinary School of Health Sciences, Central University of Rajasthan, NH-8, Bandarsindari, Kishangarh 305817, Ajmer, Rajasthan, India

Abbreviations: AA2P, L-Ascorbic acid 2-phosphate trisodium; ABTS, 2,2′-azino-bis(3-ethylbenzothiazoline-6-sulfonic acid); Aβ, β-amyloid peptide; ACQ, Aggregation-caused quenching; AI, Artificial intelligence; ALP, Alkaline phosphatase; ANN, Artificial neural network; APs, Antioxidant phenolic compounds; AuNPs, Gold nanoparticles; AuNRs, Gold nanorods; BG, Berlin green; BLM, Bleomycin; CAT, Catalase; CcO, Cytochrome c oxidase; CDs, Carbon dots; CDT, Chemodynamic therapy; CeO_2NPs, Cerium oxide nanoparticles; CL, Chemiluminescence; CNTs, Carbon nanotubes; COF, Covalent organic framework; Co-m-ceria, Co-doped mesoporous cerium oxide; CPP, Casein phosphopeptides; CSFs, Carbonized silk fibroin materials; Cu-BTC, Cu-1,3,5-benzenetricarboxylic acid; Cu^{2+}-g-C_3N_4, Copper ion/graphitic carbon nitride nanosheets; CyHMC, Cysteine-hydroxyl merocyanine; DEHP, Di-2-ethylhexyl phthalate; DMCP, Dimethyl chlorophosphite; DPV, Differential pulse voltammetry; DSP, Dithiobis succinimidyl propionate; ECL, Electrochemiluminescence; ELISA, Enzyme-linked immunosorbent assay; EPP, Elm pod polysaccharide; FRET, Förster resonance energy transfer; GC, Glucocorticoids; GCE, Glassy carbon electrode; GO, Graphene oxide; GOx, Glucose oxidase; GPx, Glutathione peroxidase; GQDs, Graphene quantum dots; GR, Glutathione reductase; GSH, Glutathione; H_2O_2, Hydrogen peroxide; H_2S, Hydrogen sulfide; HCR, Hybridization chain reaction; H-Gr, Hemin-graphene; HQ, Hydroxyquinone; HRP, Horseradish peroxidase; IFE, Inner filter effect; IP_6, Inositol hexakisphosphoric; LDA, Linear discriminant analysis; LOD, Limit of detection; LRET, Luminescent resonance energy transfer; LSPR, Localized surface plasmon resonance; MBs, Magnetic beads; MCOF, Magnetic covalent organic framework; MENPs, Melanin nanoparticles; MFN, Manganese ferrite nanoparticles; MG, Malachite green; MI, Molecularly imprinted; ML, Machine learning; MnO_2, Manganese dioxide; MOFs, Metal-organic framework; MPTMS, 3-Mercaptopropyltrimethoxysilane; MRI, Magnetic resonance imaging; MSNs, Mesoporous silica nanoparticles; NAC, *N*-acetyl-L-cysteine; NCDs, Nitrogen-doped carbon quantum dots; NO, Nitric oxide; OPD, *O*-phenylenediamine dihydrochloride; OTA, Ochratoxin A; OVA, Ovalbumin; OXD, Oxidase; PAA, Polyacrylic acid; PAI, Photoacoustic imaging; PAMAM, Polyamidoamine; PBA, Prussian blue analogues; PBNs, Prussian blue nanoparticles; PDT, Photodynamic therapy; PEC, Photoelectrochemical; PEG-HCCs, Poly-(ethylene glycol) hydrophilic carbon clusters; Pep, Pepsin; PFC, Photofuel cell; PLI, Photoluminescence imaging; PLNPs, Persistent luminescence nanoparticles; PM, Parathion-methyl; PMA, Phorbol myristate acetate; POC, Point-of-care; POD, Peroxidase; PTA, 12-phosphotungstic acid; PLTA, Poly(tannic acid); PTI, Photothermal imaging; PVP, Polyvinylpyrrolidone; PW, Prussian white; PY, Prussian yellow; QDs, Quantum dots; RCA, Rolling circle amplification; RES, Reticuloendothelial system; ROS, Reactive oxygen species; RSD, Relative standard deviation; RuNPs, Ruthenium nanoparticles (RuNPs); S/N, Signal-to-Noise ratio; SERS, Surface enhanced Raman spectroscopy; SOD, Superoxide dismutase; TAC, Total antioxidant capacity; TMB, 3,3′,5,5′-Tetramethylbenzidine; TME, Tumor microenvironment; TPs, Tea polyphenols; TRX1, Thioredoxin 1; UA, Uric acid; UCNPS, Upconversion nanoparticles; XOD, Xanthine oxidase.

* Corresponding author at: Department of Biotechnology, Koneru Lakshmaiah Education Foundation, Vaddeswaram, Andhra Pradesh 522302, India.
** Corresponding author at: Centre of Excellence for Nanotechnology, Department of Electronics and Communication Engineering, Koneru Lakshmaiah Education Foundation, Vaddeswaram 522302, Andhra Pradesh, India.
*** Corresponding author at: Nanomedicine and Nanotoxicity Research Laboratory, Department of Biochemistry, School of Life Sciences, Central University of Rajasthan, NH-8, Bandarsindari, Kishangarh 305817, Ajmer, Rajasthan, India.
E-mail addresses: raginisingh@kluniversity.in (R. Singh), santosh@kluniversity.in (S. Kumar), hemant.daima@curaj.ac.in (H.K. Daima).

https://doi.org/10.1016/j.ccr.2025.216768
Received 21 February 2025; Received in revised form 18 April 2025; Accepted 27 April 2025
Available online 8 May 2025

ARTICLE INFO

Keywords:
Nanozymes
Colorimetric
Fluorescence
Electrochemical
Photothermal
Biocompatibility
Integrated technologies

ABSTRACT

Increasing necessity towards the advancement of detection systems has sparked considerable curiosity in integrated dual-modal sensing technologies. The recent progress in the fields of nanozymes and materials chemistry highlights the significance of integrated dual-mode systems for biomedical sensing applications. Interestingly, the combination of two detection signals can enhance diagnostic performance, while minimizing assumptions. Moreover, the integrated technologies boost diagnostic capabilities through immense flexibility, improved accuracy, and broad-range detection. In this perspective, nanozymes have been incorporated into a variety of dual-mode biosensing systems due to their enhanced catalytic activities; and they provide benefits of low cost, high stability, ease of surface tuning, and biocompatibility. Herein, dual-mode biosensing, which leads two output signals can be combination of colorimetric, fluorescent, photothermal, electrochemical, or SERS, owing to their remarkable benefits for sensitive and real-time detection as well as the development of point-of-care (POC) devices. In this seminal review, an in-depth fundamental understanding of different nanozymes-based dual-mode sensing techniques *i.e.* colorimetric/fluorimetric, colorimetric/photothermal, colorimetric/electrochemical, and colorimetric/SERS, has been provided, followed by emphasizing their usage in sensing applications. Here, a comprehensive analysis has also been conducted for the sensing methodologies involving nanozyme-based sensor arrays, synergistic catalytic activities, and the foundational principles of the signal transduction systems, while addressing the challenges and future opportunities for the progress in the domain.

1. Introduction

Enzymes are a class of biological macromolecular catalysts proved to be essential for both industrial and organismal biotransformation processes. However, the wide range applications of natural enzymes have been limited, especially in difficult settings, due to their intrinsic constraints, including susceptibility to environmental influences, low operating stability, high costs, and short lifespans. Therefore, significant attempts have been made to overcome these limitations. In this context, nanozymes (artificial enzymes) can outperform natural enzymes due to their catalytic activity, versatility, and stability under adverse conditions, and nanozymes have prospective uses in chemical engineering, environmental sciences, industrial settings, bio-medical field, and agricultural sectors [1]. The rapid progress in supramolecular chemistry, protein engineering, and nanoscience has escalated the nanozyme engineering approaches to tackle the issues associated with natural enzymes [2]. The tailor-made, specifically designed nanomaterials, which can mimic natural enzymes, are termed as nanozymes, and they have remarkable stability, recyclability, customizable catalytic efficiency, and a blend of classical chemical and biocatalyst benefits [3]. As a result, basic research on nanozymes and their practical applications is becoming significant [4], and over 7500 articles have been published on nanozymes since the discovery of peroxidase-mimic Fe_3O_4 nanoparticles in 2007 [5]. A variety of nanomaterials, including carbon-based nanomaterials, noble metal nanoparticles [6], metal oxides, metal-organic frameworks (MOFs) [7], and polymetallic nanostructures [8] have been reported to mimic natural enzymes, and they are gaining prominence in a broad spectrum of nanotechnology-based applications, including biosensors, food safety, environmental protection, drug delivery, disease diagnosis, imaging and treatment, tissue engineering, and antibacterial/antioxidant agents [9,10]. Approximately 300 distinct types of nanozymes, including oxidoreductases, proteases, hydrolases, DNAs, endonucleases, nitric oxide synthases (NOS), and others, have been developed [11], and because of the small size, high surface area, and adaptable surface characteristics, nanozymes can efficiently bind to biomarkers for improving the speed and sensitivity of illness diagnosis, particularly for infectious, cardiovascular disease, and cancer disorders [12,13].

In the context of above, a multitude of nanomaterials with broad biomedical uses have been discovered with enzyme mimicking actions of catalase (CAT), superoxide dismutase (SOD), oxidase (OXD), peroxidase (POD), glucose oxidase (GOx), and glutathione peroxidase (GPx) [14–16]. Currently, metal and metal oxides nanoparticles are majorly being employed as nanozymes since the metallic active core has demonstrated a remarkable ability of catalytic electronic redox processes, like natural enzymes. Interestingly, the enzyme-mimicking activities of metallic nanozymes can be influenced by a number of variables, including temperature, pH of the surrounding environment, reduction agent, and the oxidation states of the metallic centre [17,18]. Likewise, the characteristics of the disease vary from those of normal tissues, hence offer potentially common therapeutic possibilities for the application and logical designing of nanozymes in biomedicine. For instance, tumor microenvironment (TME) redox potential levels are known to be higher than those of normal tissues, therefore, different tumors can stimulate the nanozymes' functions making it distinct from response of normal tissues [19–21]. It has already been shown that the intracellular glutathione (GSH) can reduce metal ions (Fe^{3+}, Cu^{2+}, Mn^{4+}, *etc.*) to lower-valent ions (Fe^{2+}, Mn^{3+}, and Cu^{+}), and therefore, the catalytic efficiency and peroxidase-like nanozymes activities could be significantly changed in the diseased microenvironment [22].

Like metal nanozymes, the discovery of enzymatic activities in carbon nanotubes (CNTs) and graphene has expanded their biological applications. Fullerene (C_{60}) exhibits distinct catalytic activity, resembling it as a carbon-based nanozyme. Under light, water-soluble carboxylic acid (-COOH) functionalized fullerene can accelerate the breakdown of DNA phosphodiester links [23]. Further, the applications of carbon-bound nanozymes are explored as an interest in the activity of nanomaterials, particularly nanozymes [24–26]. In 2010, Qu's group discovered that graphene has intrinsic peroxidase-mimetic activity and broadened the classification of carbon-based nanozymes [27]. From then on, carbon-based nanozymes with well-defined geometric and electronic structures and a host of other outstanding properties, including mechanical, optical, thermal, and electrical capabilities, have become viable candidates for their use as enzyme-mimics in biomedical applications. In addition to metal, metal oxide, and carbon-based nanozymes, numerous MOF-based nanozymes from the families of hydrolase (such as nuclease, protease, phosphatase, and carbonic anhydrase) and oxidoreductase (such as SOD, peroxidase, oxidase, and catalase) have recently been developed [28]. MOF-based nanozymes have shown great promise in environmental management, analytical chemistry, diagnosis and treatment of diseases. The exceptional catalytic activity of these nanozymes made them useful in the development of colorimetric biosensors, which have become a strong and efficient way for real-time detection. Combining nanozymes with colorimetric sensors has resulted in the development of novel colorimetric sensing techniques [29], and numerous studies have been conducted on MOF-based methods for hydrogen sulfide (H_2S) detection using fluorescence, catalysis, and electrochemical characteristics [30].

From the above discussion, it is apparent that the field of biomedicine has been supported by nanozymes, however, the understanding of factors influencing the catalytic efficiency, enzyme-mimicking properties, and substrate specificity of nanozymes remains a complex

challenge. In particular, the relationship between nanozyme's inherent structural features and external environmental conditions requires deeper exploration to optimize their performance [31,32]. Furthermore, the catalytic mechanisms are essential for the logical design of new nanozymes with innate catalytic capabilities, and this strategy has been extensively used in biomedicine as a controlled multifunctional platform [33,34]. A wide range of biological applications, such as chemodynamic therapy (CDT), oxygen-dependent tumor therapy, radiation therapy, reactive oxygen species (ROS) related diseases, bacterial infection disorders, *etc.*, have recently been reported, which can be achieved by numerous nanoparticles having intrinsic catalytic characteristics [35–37]. The newly explored biomedical capabilities of nanozymes have provided a fresh perspective towards expanding their use in the field of sensing and medical sciences [38,39]. However, biocompatibility, biosafety, scalability, stability, and side effects are among the aspects that require further research attention before explicitly employing nanozymes in sensing and medical sciences [33,34].

Nevertheless, in the recent past, various modes of nanozyme-based biosensing approaches, including colorimetric, fluorescence, electrochemical, photothermal, and photoelectrochemical have been reported for the detection of various target analytes, including biomolecules, microbes, cancerous cells and other disease biomarkers [3]. In comparison to conventional techniques, nanozyme-based biosensing approaches offer several advantages like low detection limit (LOD), enhanced specificity and accuracy, reduced cost, fast, and convenient operation [40]. In this milieu, peroxidase-mimic nanozymes enable the development of colorimetric sensors for qualitative and quantitative detection of analytes. It has drawn wide attention from the scientific community due to cost effectiveness, rapid response, and easy operation with simple instrumentation. However, peroxidase-mimicking nanozymes encounter low catalytic response, influence of surrounding environmental conditions, and weak affinity, which can be overcome by alteration and modification of nanozyme's surface [41]. Secondly, fluorescent properties of nanozymes offer development of fluorometric sensors with enhanced optical and fluorescence properties along with high photostability and broader selection of excitation and emission wavelength, and narrow emission peak [42]. However, this approach suffers several disadvantages due to blinking effect, and aggregation-caused quenching (ACQ), which leads to weakening or disappearance of fluorescence effect. Further, biological systems also cause interference in fluorescence activity and cause high background signal interference [43]. Furthermore, due to biocompatibility and effective photothermal conversion, nanomaterials have become widely popular in photothermal sensing applications [44]. Nanomaterials, particularly those possessing plasmonic characteristics such as gold nanoparticles (AuNPs), demonstrate significant light absorption capabilities, and they are adept at transforming absorbed light energy into heat. Alike, graphene and its derivatives present benefits including easy preparation, distinctive structures, strong photothermal effect, and biocompatibility, all while lacking any inherent biological toxicity [45]. In addition, some nanozymes suffer intrinsic constraints, including limited photothermal conversion efficiency, inadequate photothermal stability, and complex synthesis processes [46]. On the contrary, nanomaterials enhance the response time of electrochemical sensors because of their remarkable reactivity and rapid electron transfer rates [47]. AuNPs enhance electrochemical signals by offering a substantial surface area for biomolecule immobilization, resulting in increased sensitivity for detecting low-abundance biomarkers [48]. Further, high aspect ratio of Au nanowires provides better electrical conductivity for electrochemical applications. Small differences in dimensions, form, and surface characteristics of nanomaterials can greatly influence their electrochemical performance, posing challenges in obtaining consistent and repeatable outcomes. Metal nanoparticles with a rough surface exhibit a more intense electromagnetic field around the surface protrusions. When the molecules being measured are in proximity to these 'tips', their Raman signals have a higher probability of being amplified. The mechanism of chemical strengthening indicates that only molecules that are adsorbed on designated SERS-active sites on the surface of metal nanoparticles can produce robust SERS signals [49]. The process involves a substantial amplification of the Raman scattering signal when analyte molecules adhere to the metal surface, which is predominantly composed of nanoparticles or nanowires exhibiting nanoscale roughness. The application of SERS to examine these isolates on the nano surface significantly amplifies the Raman signal by 10^{14}–10^{15} folds, enabling the detector to assess trace amounts of substances at the molecular level [50]. Despite the significant enhancement provided, noble metal nanostructures utilized as substrates exhibit several inherent limitations, such as low stability, high cost, inconsistent repeatability, and biocompatibility, along with a lack of selectivity for probe molecules. Creating highly sensitive, stable, expansive, and reusable SERS substrates through economical production techniques poses significant challenges [51].

Therefore, nanozyme-based dual-mode sensing strategies like colorimetric/fluorometric, colorimetric/photothermal, colorimetric/electrochemical, and colorimetric/SERS (Fig. 1), which generate two distinct measurable signals in response to chemical or biological stimuli, may offer a highly effective detection platform. Dual-mode approach enhances accuracy through self-validation and self-correction, making it a valuable tool for analytical applications [52]. Notably, the dual-mode system identifies the target analyte by generating two distinct physicochemical signals through synchronized target interactions. This process employs independent detectors rather than relying on multiple techniques for the same sample. Unlike single-mode analysis, dual-mode detection operates efficiently without cross-interference, ensuring enhanced reliability and accuracy [53]. Moreover, utilizing dual-mode methods could prevent inconsistencies in data interpretation inside a complicated matrix and facilitate reciprocal verification, hence improving the diversity, dependability, and precision of sensing [54]. The detection range of the analytes can be increased to enable initial observation of the subject, if the two modes have varying sensitivities. Furthermore, a dual-mode sensing system has the potential to overcome the drawbacks of single-mode approach, including excessive assay usage, restricted information gathering, and diminished reliability and

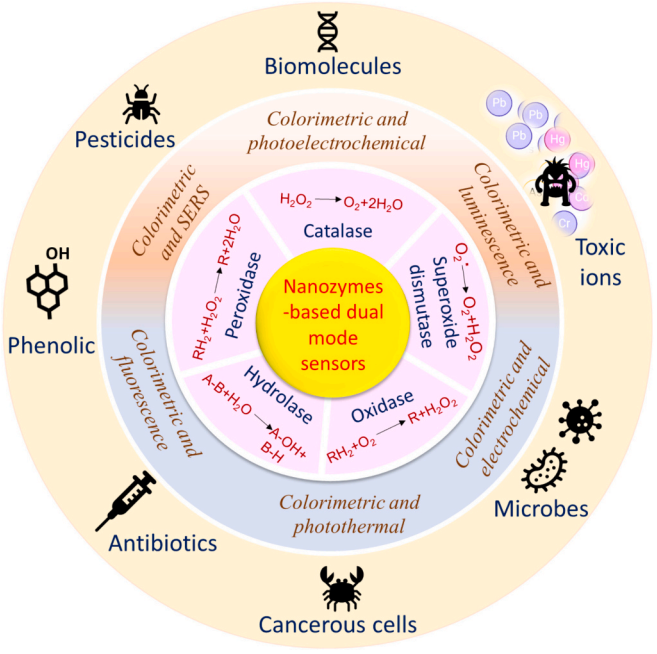

Fig. 1. Schematic representation of reaction mechanisms, mode of actions and nanozyme-based dual-mode sensing techniques used in sensing, biomedical, industrial and environmental applications.

precision [53]. Hence, there is a growing focus on the advancement of dual-mode biosensing systems that are efficient and cost-effective [55]. Although earlier publications have provided an excellent summary of nanozymes' activity [56] and their utilization in the detection of wide range of target analytes employing different sensing strategies for microbial detection [57,58], theranostic purpose [59,60], and development of techniques like sensor array [61], and lateral flow assay [62]. These articles majorly highlight on the nanozymes-based application in particular areas *i.e.*, detection of pathogenic microbes, therapy and diagnostics, and technique development, with their major focus on different target analytes using different classes of nanomaterials. Thus, insufficient emphasis has been placed regarding multi-mode biosensing devices as a novel technique for the detection, leading to a scarcity of available information. Moreover, with the increasing need for enhanced precision and sensitivity in identifying targets due to the generation of two distinct physicochemical signals, the rapid progress of multi-mode assay technology has become a crucial focus of study. Thus, the major focus of this review is to investigate the recent developments in nanozymes dual-mode sensing applications, with an emphasis on their structural properties and how their catalytic activity can be affected by various factors. Further, a summary has been presented about the development and application of nanozyme-based sensor arrays as well as the synergistic effect of smart nanozymes in sensing and biomedical applications.

2. Nanomaterials with enzyme-mimicking characteristics

Each living organism comprises various enzymes that either function independently or collaboratively to facilitate a specific biochemical reaction or a set of reactions in living entities. Peroxidase, catalase, laccase, hydrolase, superoxide dismutase, and oxidase are some of the important enzymes, which are essential for life.

2.1. Peroxidase (POD)-mimetic activity

Peroxidases catalyze the reduction of peroxides by donating an electron to a substrate, which acts as an electron acceptor. Many studies have reported excellent peroxidase-mimetic activity in various nanomaterials, including metal oxide nanoparticles, noble metal nanoparticles, carbon-based nanoparticles, and other nanocomposites [96]. Similar to an enzymatic reaction, the nanozyme reactions follow the standard ping-pong mechanism and Michealis-Menten kinetics [97]. To understand the mechanism underlying peroxidase-like activity of nanomaterials, many studies have been carried out, and it is found that the generation of ROS and electron transfer play a crucial role. This mechanism was first discovered and validated in iron oxide nanoparticles (IONPs), which states the surface Fe^{+2} ions activate the hydrogen peroxide (H_2O_2) and liberate ROS *via* Fenton or Haber-Weiss reactions [2]. Later, this mechanism was observed in MOFs, in which it was proposed that upon the absorption of H_2O_2, O—O bond is disrupted, leading to release ·OH radicals on the surface nanomaterial. Furthermore, the generation of free radicals and the peroxidase-like activity of noble metal-based nanomaterials exhibit pH switchable free radical generation property [98]. In brief, in the first condition, following H_2O_2 absorption at surface, O—O bond in H_2O_2 breaks down to generate OH* radicals, which in turn produces H_2O and O* radicals. In combination with hydrogen atoms from different chromogenic substrates [TMB (3,3′,5,5′-Tetramethylbenzidine), OPD (*o*-phenylenediamine dihydrochloride), or ABTS (2,2′-azino-bis(3-ethylbenzothiazoline-6-sulfonic acid)], the free O* radicals have the ability to oxidize them to produce visible color thus establishing colorimetric applications [99]. This phenomenon contributes to peroxidase-mimic activity following a base-like pathway under acidic conditions which is represented in Eq. (1).

$$H_2O_2{}^{*} \leftrightarrow H_2O^{*} + O^{*} \quad (1)$$

On the contrary, under basic conditions, the adsorbed OH atoms contribute to catalase-like activity by following an acidic-like pathway. In brief, the H_2O_2 breaks down into H* and HO_2* due to breakdown of the O—H bond and the mechanism has been represented in Eq. (2). Here, produced H* combines with pre-adsorbed OH* to produce H_2O molecules.

$$H_2O_2{}^{*} \leftrightarrow H^{*} + HO_2{}^{*} \quad (2)$$

* Denotes the adsorbed species at the nanoparticle's surface.

Vernekar et al. had used vanadia (V_2O_5) nanoparticles to exhibit peroxidase-mimetics in a nanowire system to convert H_2O_2 to water [100]. The mechanism is explained as in Fig. 2A. The work demonstrated the GPx activity of the V_2O_5 nanowires as compared to the other metal oxides in the recycling of glutathione reductase (GR). It further explains the internalization of the V_2O_5 nanowires in mammalian cells through endocytic pathways in low concentrations. Likewise, Rashtbari et al. provided an interesting technique where argon cold plasma is used to modify cobalt oxide (Co_3O_4) nanoparticles for enhanced degradation

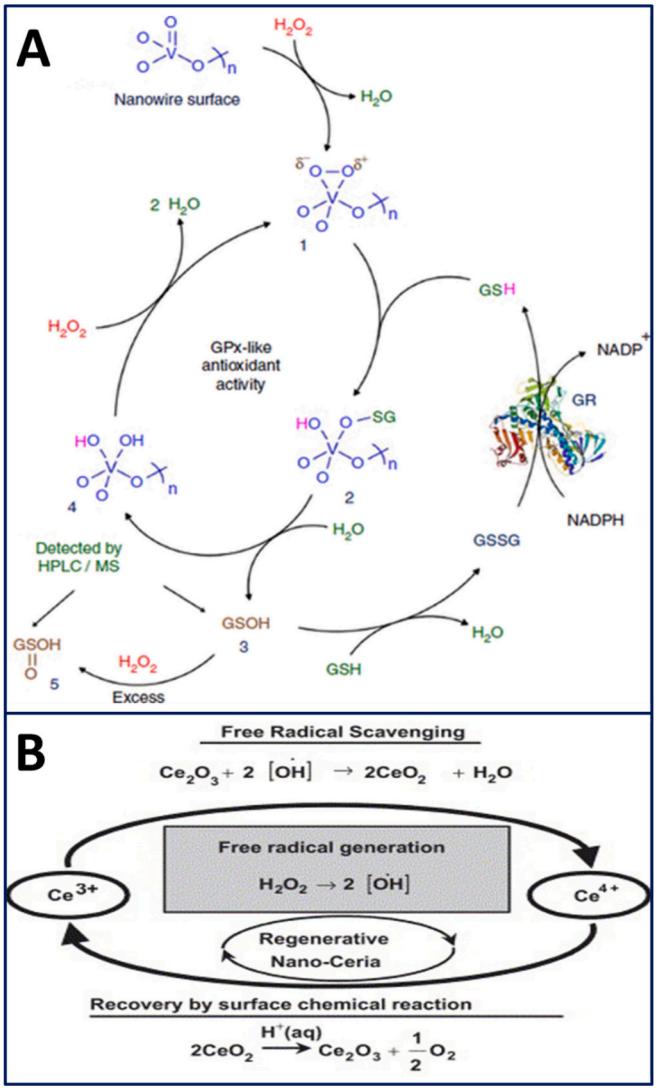

Fig. 2. Schematic illustrating the mechanism of nanozyme activities corresponding to **Panel A:** Peroxidase-mimetic by nanowire surface of vanadium nanozymes. Reprinted with permission from *Nature Communications*, Nature [100] Copyright © 2014. **Panel B:** Mechanism underlying the radical scavenging activity of cerium oxide nanoparticles along with nano-ceria surface chemical reaction. Reprinted with permission from *Biomaterials*, Elsevier [102] Copyright © 2007.

rate of the malachite green (MG) [101]. The degradation mechanism is attributed to Fenton like mechanism by the peroxidase-mimic Ar-Co_3O_4-NPs and it was compared against the pristine Co_3O_4-NPs for their ability to degrade MG.

$$Ar–Co_3O_4 + H^+ \rightarrow Co^{++}/Co^{+++} + H_2O \quad (3)$$

$$Co^{++} + H_2O_2 \rightarrow Co^{+++} + HO^- + HO\cdot \quad (4)$$

$$Co^{+++} + H_2O_2 \rightarrow Co^{++} + H^+ + HOO\cdot \quad (5)$$

$$MG + HO^{\circ} \rightarrow \text{Degraded Product} \quad (6)$$

$$MG + HOO^{\circ} \rightarrow \text{Degraded Product} \quad (7)$$

The dye was subjected to a series of reactions such as reduction, cleavage of ring, methylation as well as amination to form the by-products before undergoing oxidation and reduction to hexadecenoic acid. Peroxidase-mimetic activity of citrate-coated osmium nanoparticles has also been demonstrated for their use in nitrophenol degradation [103]. Addition of osmium oxide (OsO_2) as dopants enhances the peroxidase-like activity of osmium nanozyme [104]. The assays to detect the OPD and TMB turned out to display the increased peroxidase-like activity of the OsO_2doped osmium nanoparticles. The material was also able to degrade 6 mixed phenolic pollutants (2,5-DCP, 2,4-DCP, 4-NP, 4-CP, 2-NP, and 2,6-DCP) by the enhanced catalytic activity. In other study, peroxidase-mimetic nanozyme carrying dual vanadium and iron inspired active catalytic center has been developed [105], and the system was utilized in the detection of H_2O_2 produced intracellularly from cancerous cells, wherein the peroxidase-like activity attributed to the production of both •OH and $•O_2H^-$ radicals.

2.2. Catalase (CAT)-mimetic activity

As the nanozyme behavior exploration continued, the catalase-like nanozymes gained popularity because of their role in restricting ROS. It facilitates the degradation of H_2O_2 to oxygen and H_2O, which leads to preventing oxidative damages to the cells [106,107]. However, it is contingent upon the relative concentrations of nanozymes and substrates, and the decomposition rates rise as the concentrations of these agents increase [108]. By halting the production of ROS, this procedure can successfully shield cells from oxidative stress. The amount of dissolved oxygen present during the reaction process is typically used to gauge the catalase-mimicking activity. Further, temperature and pH also have a significant impact on catalase-like nanozyme activity. While most prefer neutral and alkaline settings, some nanozymes can also function similarly to catalase in slightly acidic environments [109,110], and it adhere to the conventional Michaelis-Menten catalytic process [111]. The structure, shape, and surface valence of nanoparticles, in combination with the pH of surrounding environment, are all strongly related to the catalytic reaction caused by catalase-like activity. Redox reactions and adsorption activation are common examples of catalytic processes. The catalytic mechanism of metal-based catalase-mimicking nanozymes is found to be intimately linked to the free radical chains. On nanozyme surfaces, pre-absorbed OH* (* indicates species that are attached to metal surfaces) play a crucial role in inducing H_2O_2 to favour acid-like decomposition. Subsequently, the decomposed H interacts with pre-adsorbed OH* to give HO_2* and H_2O*. The produced HO_2* then passed H to another H_2O_2*, resulting in an O_2* and changing the H_2O_2* into H_2O* and OH* [112]. Furthermore, because Co_3O_4 nanozyme contains redox forms, the breakdown of H_2O_2 is accompanied by a redox reaction in addition to a free radical reaction. OOH, which is more nucleophilic than H_2O_2, reacts with OH– at a high pH to make O_2H and Co (II), respectively. OOH is also easily able to engage with Co (III), and the resulting O_2H would then react with the OH produced by Co (II), activating H_2O_2. High pH would help both reactions along and speed up Co_3O_4 breakdown of H_2O_2 [113]. In case of Prussian blue nanoparticles (PBNPs), reports showed that at higher pH they exhibited highly efficient catalase-mimetic activity [114]. At alkaline pH, H_2O_2/O_2 redox potential is highly reduced, and thus H_2O_2 is more prone to easy oxidation into O_2. Generally, reduction of PB leads to the formation of Prussian white (PW), whereas oxidation forms the Berlin green (BG) or Prussian yellow (PY). At higher pH, less amount of PBNPs can be oxidized to PY or BG to facilitate the electron transport from TMB to H_2O_2. Therefore, at alkaline pH, catalase-like activity dominated by the following reactions (8–11).

$$3\ PB + H_2O_2 \rightarrow BG + 2OH^- \quad (8)$$

$$2BG + H_2O_2 \rightarrow 6PY + 2OH^- \quad (9)$$

$$6PY + H_2O_2 + 2OH^- \rightarrow 2BG + O_2 + 2H_2O \quad (10)$$

$$BG + H_2O_2 + 2OH^- \rightarrow 3\ PB + O_2 + 2H_2O \quad (11)$$

Cerium oxide nanoparticles (CeO_2) as catalase-mimics unexpectedly, have been reported to demonstrate a redox-state-dependent behavior. Following the electron transfer from H_2O_2 to two Ce^{3+}, the O—O link between the H_2O_2 molecules and the Ce^{3+} site cracks, releasing water molecules [115]. Ce^{4+} then returns to Ce^{3+} by an oxidation reaction, and the catalase activity benefits from the high valence state on nanozyme surfaces [116]. CeO_2 nanoparticles also aid in the hydroxyl ion free radical scavenging activity as explained by Das et al., in a work where they evidenced the autocatalytic behavior of ceria nanoparticles [102]. The work claims in nano dosage amounts, the ceria nanoparticles have a free radical scavenging activity which aids the neurodegenerative condition in rats **(**Fig. 2B**).**

2.3. Oxidase-mimetic activity

Nanozymes exhibiting oxidase-like activity can catalyze the oxidation process on substrates. The reaction follows Michaelis–Menten kinetics, and the catalytic process involves electron transfer that is influenced by pH, temperature, and substrate. The production of reactive species and electron transfer are steps in the reaction pathway of nanozyme oxidase-like activity [117]. The intermediate synthesis of singlet oxygen, oxygen superoxide anion, and electron transfer processes influences the oxidase-type properties of nanomaterials. Nanozymes engage in the electron transfer process, acts both as electron donors and recipients. The activity resembling that of oxidase in naked AuNPs is elucidated by the initial adsorption of the hydrated glucose anion onto the Au surface, resulting in the formation of electron-rich Au species. A nucleophilic attack ensued, activating dissolved oxygen and resulting in a dioxo Au intermediate, facilitating the conversion of electrons from glucose to dioxygen [118]. Studies have revealed that MoO_3 possesses sulfite oxidase activity, and it has been hypothesized that Mo (VI) is reduced to Mo (IV) and that SO_3^{2-} is first bound, then oxidized to SO_4^{2-} on MoO_3 nanoparticles having various oxidation states. Subsequently, Mo (IV) underwent oxidation to revert to Mo (VI) through a series of two one-electron reduction reactions [119].

Interestingly, free radicals are the starting point to produce reactive species, and they can originate from substrates or oxygen molecules. For instance, it has been reported that the free radicals are produced from substrates for the trinuclear complex $[Cu_3(m\text{-}O)_3]^{2+}$, imitating methane monooxygenase [120]. Herein, the antibonding CH orbital [s*(CH)] of methane and the corresponding single-occupied molecular orbital of $[Cu_3(m\text{-}O)_3]^{2+}$ interact to activate methane, followed by the cleavage of the C—H bond, which forms a link with the cluster between the OH group and methyl radical (CH_3). Subsequent CH activation, methanol molecules tend to coordinate with two neighboring copper centers in the trinuclear species. This process occurs without an energy barrier, as CH_3 radicals recombine with the hydroxyl group bound to Cu within the cluster. Reports indicate that activated dissolved oxygen is a source of free radicals. Substrate oxidation is caused by ROS intermediates (such

as O_2•–, $^1O_2$, or •OH), which are produced by enormous dissolved oxygen being absorbed and activated by the huge specific surface area of nanozymes [121–124]. According to Huang et al., the oxygen radical chain reaction generates $O_2^{\cdot}$ first, which is then quickly transformed into H_2O_2 and $^1O_2$ [125].

Likewise, the oxidase-like activity of AuNPs has been explained by employing ultrasmall-sized 3.6 nm particles to evaluate their catalytic behavior [118]. The electron-rich Au species interact with the glucose anion to activate molecular oxygen *via* nucleophilic attack, which is by virtue of the electronic properties of the metallic nanoparticles of size less than 10 nm (Fig. 3**A**). Peng et al. had demonstrated the oxidase-like behavior of Mn_3O_4 nanoparticles coated on top of porous reduced graphene oxide for the detection of ascorbic acid [126]. The work explains that, with increased surface area, faster electron transfer occurs, resulting in the faster oxidation of tetramethylbenzidine. Furthermore, the effect of pH, temperature, and interfering moieties are tested and found to have no effect on the system [126].

2.4. Superoxide dismutase (SOD)-mimetic activity

Superoxide dismutase serves as significant antioxidant enzyme to converts superoxide anion ($O_2^{\bullet-}$) radicals into H_2O_2 and oxygen [1]. Several nanozymes, including CeO_2 nanoparticles, Mn_3O_4, and MnO_2, are known to exhibit SOD-mimetic activity, and the actions of these mimics are elucidated *via* the coupled electron transfer model pertaining to CeO_2 nanoparticles. One of the earliest known nanomaterials to demonstrate SOD-mimicking properties is nanoceria, which is attributed to oxygen vacancies and convertible valence states (Ce^{3+} and Ce^{4+}). While the Ce^{4+} could revert to the original Ce^{3+} through the oxidation of H_2O_2, the oxygen vacancy could react with superoxide to transfer electrons through the formation of H_2O_2 as shown in Fig. 3B [115]. In summary, the $O_2^{\bullet-}$ molecule attaches to the reduced oxygen vacancy site, leading to the release of H_2O_2 as a result of the absorption of two protons and the subsequent transfer of one electron from Ce^{3+} [128]. Alternative theory suggests that SOD activity in CeO_2 nanoparticles is caused by the surface defect locations, where $HO_2^{\bullet}$ adsorbs. CeO_2 nanoparticles regain their original state, followed by the production of H_2O_2 and oxygen as nanoparticles' surface reacts with $HO_2^{\bullet}$. Moreover, iron oxide and cobalt oxide are reported to exhibit SOD-mimetic activity based on Eley-Rideal (ER) and Langmuir-Hinshelwood (LH) mechanisms, respectively.

As discussed earlier, the SOD-mimetic activity of nanozymes may also be attributed to the surrounding pH or the structure and surface ions of nanomaterials. A pH that is too high, suppresses the catalytic activity by creating a stronger electrostatic barrier against superoxide radicals. The primary functions of nanozymes are adsorption, activation, and electron transfer because of the unpaired electrons and multivalent ions on the surface. Nevertheless, surface ions, pH or nanozyme architectures dictate the actual processes. The protonation of O_2 and the adsorption and rearrangement of $HO_2^{\bullet}$ (hydroperoxyl radical) on metal surfaces are the primary routes for the SOD-like activities of metals and alloys. Due to the strong adsorption of $HO_2^{\bullet}$ on the nanozyme surface, O_2^{-} (oxide ion), acting as a Brønsted base, readily accepts a proton from water, leading to the formation of HO_2^{-} (hydroperoxide ion) and OH^{-} (hydroxide ion). Consequently, the rearrangement of HO_2^{-} results in the simultaneous generation of H_2O_2 and O_2 [129]. According to reports, superoxide radicals could be eliminated by tris-malonic acid derivative of the fullerene C_{60} molecule (C_3) by drawing in electron-deficient areas. Superoxide anions are electrostatically driven towards electron-deficient regions of malonic acidic group at nanozyme surface. Further, proton on carboxyl group stabilizes the $O_2^{\bullet-}$ *via* hydrogen bonding until the arrival of second $O_2^{\bullet-}$ to combine with earlier. This leads to dismutation of $O_2^{\bullet-}$ due to protons present on carboxyl group/ water molecules [130]. Similarly, poly-(ethylene glycol) hydrophilic carbon clusters (PEG-HCCs) have shown improved SOD-mimetic catalytic activity, however,

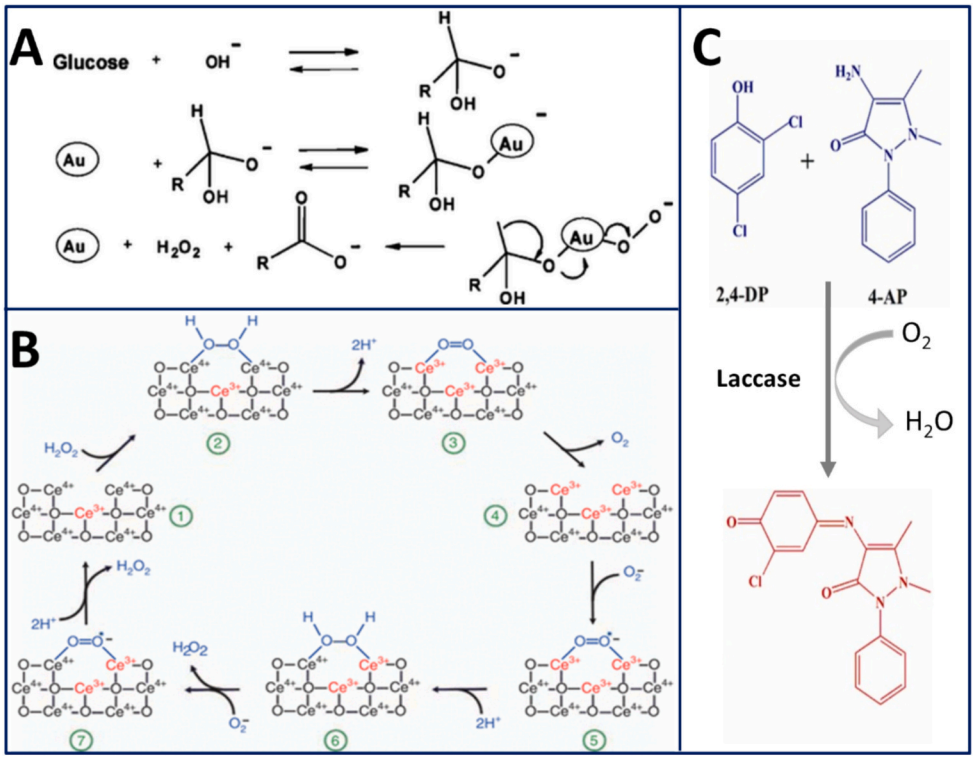

Fig. 3. Schematic illustrating the mechanism of nanozyme activities corresponding to, **Panel A:** Oxidase-mimetic demonstrated by ultrasmall gold (Au) nanoparticles. Reprinted with permission from *Advanced Synthesis & Catalysis*, Wiley [118] Copyright © 2006. **Panel B:** Superoxide dismutase (SOD)-mimetic exhibited by cerium oxide nanoparticles as depicted by electron transfer model. Reprinted with permission from *Chemical Reviews*, American Chemical Society [36] Copyright © 2019. **Panel C:** Laccase-mimetic activity exhibited by Cu—S cluster in detection of hydroxyquinone. Reprinted with permission from *Journal of Hazardous Materials,* Elsevier [127] Copyright © 2023. (For interpretation of the references to color in this figure legend, the reader is referred to the web version of this article.)

they do not have an effect over peroxynitrite ($ONOO^-$) and nitric oxide (NO·) [131]. Herein, two different mechanisms for SOD-mimetic activity of PEG-HCCs are proposed, (i) covalent bond formation among PEG-HCCs graphitic domain and radical, which in turn leads to radical annihilation activity, (ii) PEG-HCCs mediated transformation of $O_2^{\bullet-}$ to O_2. In contrast to the aforementioned nanozymes, melanin nanoparticles (MeNPs) possessing SOD-mimetic activity would be able to scavenge $O_2^{\bullet-}$, NO·, and $ONOO^-$ jointly [132].

2.5. Hydrolases-mimetic activity

One of the most prevalent enzymes, hydrolase, is essential to biological systems because it catalyzes the hydrolysis of chemical bonds. Many nanomaterials (including Ce-AuNPs, Au, CeO_2, ZrO_2, MOFs, and Fe_3O_4) have outstanding hydrolase-like activity. Reaction mainly utilizes water as receptor for the for the transfer group to catalyze the hydrolysis reaction [133]. Despite the catalytic mechanism of hydrolase-like activity in nanozymes, it has received less attention in comparison of others. According to findings, MOF/g-C_3N_4 demonstrates hydrolase-like activity in catalysis of dimethyl chlorophosphate (DMCP) through the process of adsorption and substrate breakdown activity. Cu-BTC (1,3,5-benzenetricarboxylic) and g-C_3N_4-ox can be combined to form a nanocomposite (MOFgCNox) of heterogeneous porosity and chemistry. First, the P═O group of the vaporized DMCP molecules complexes on copper sites, causing the molecules to be adsorbed. Subsequently, distinct interactions occur between DMCP and the copper-based amorphous phase, including hydrogen bond formation and polar interactions. These involve the P═O group interacting with uncoordinated hydroxyl groups of BTC units or positively charged Cu^{2+} ions, respectively. Further, hydroxyl groups in water molecules take the position of DMCP's chlorine atom, causing DMCP to hydrolyze into DMP [134]. Kuang and colleagues also found that CdTe nanoparticles treated with chiral cysteine might resemble restriction endonuclease, enabling it to identify and cut at the restriction site GAT'ATC in double-stranded DNA that has more than 90 base pairs [135]. In this mechanism, DNA acts as an electron acceptor, aiding in the cleavage of phosphodiester bonds, while nanoparticles serve as electron donors, promoting the generation of ROS. In another study, chiral copper sulfide quantum dots (d/l-QDs) are used as photocatalysts to induce protein cleavage. The hydroxyl radicals produced by d/l-QDs selectively disrupt peptide bonds between lysine (K) and leucine (L), facilitating precise protein fragmentation (61 kDa + 5 kDa) [136].

2.6. Laccase-mimetic activity

Laccase enzymes are found in many natural sources, including bacteria, fungi, plants, and insects. As a part of the multi-copper oxidase family, laccase can oxidize various phenolic and non-phenolic compounds due to its broad substrate range and low specificity [137]. To this enzyme, oxygen serves as an electron acceptor to produce water as a byproduct. The reaction mechanism of laccase involves the sequential one-electron oxidation of four reducing substrate molecules, coupled with the simultaneous two-electron reduction of oxygen into water. This process facilitates the catalytic exchange of four protons [138]. Liang et al. synthesized amorphous MOF of guanosine monophosphate coordinated copper [139]. Interestingly, the mechanism of conversion of polyethylene has created a lot of interest in the laccase enzyme, which eventually is being replaced by laccase-mimicking, more robust alternatives like the copper-substituted MOF. The work explains the mechanism of conversion of polyphenols by the laccase-like nanozyme. The catalytic ability of the Cu-GMP is demonstrated with the conversion of 2,4-dichlorophenol (2,4-DP) under a variety of pH, temperature, and saline conditions. In another study, Huang et al. utilized Ag_2O nanoparticles to mimic laccase-like catalysis to detect kanamycin *via* a smartphone-based interface [140]. This work illustrates the calorimetric detection of incremental concentrations of kanamycin by the Ag_2O nanoparticles to an extremely low concentration of 1.3 nM. The phenolic substrates are oxidized to form a semiquinone radical, which is reacted with 4-Aminoantipyrine (4-AAP) to form red solution. The kanamycin reacts electrostatically with the cubic Ag_2O and adsorbed onto the surface, hindering the formation of the semiquinones. The color change correlated with the concentration of kanamycin, which gives the calorimetric signal for the ultra-low levels. Furthermore, Xu et al. employs octahedral Cu—S clusters with a size range of 200–450 nm to evaluate the chromogenic interaction between 2,4-DP and 4-AAP to detect hydroxyquinone (HQ) through advanced oxidation reaction (Fig. 3C) [127]. HQ showed fast reaction kinetics with Cu—S and had rejected interference from metal ions and organic molecules showcasing their selectivity.

3. Characteristics of nanomaterials, and their role in enzymatic activity

The distinct physicochemical properties of nanomaterials, which can be tailored to meet specific application requirements, are closely linked to their enzyme-like properties. Aspects of enzymatic activity like substrate selectivity, catalytic activity, and multienzyme-like activity depend on physicochemical properties of nanomaterials, including their size, shape, crystallographic state, surface modification, and self-assembly [141–145]. In addition to these aspects, pH and temperature are other important parameters which can have significant effect over nanozymes catalytic activity [141,146]. Table 1 summarizes the effect of each of these parameters on nanozyme catalytic activity and efficiency. Interestingly, the key surface properties that influence enzyme-like activities of nanomaterials include surface charge density, hydrophobicity, and binding affinity [147], and all these can be modulated through chemical functionalization or careful nanomaterial synthesis. Furthermore, the small size of nanomaterials allows them to penetrate and interact with biological systems at the molecular level, potentially enabling activities like gene delivery, cell membrane disruption, and targeted formulation delivery [143,148]. Nanomaterials with tailored surface properties could be designed to mimic natural enzymes and catalyze specific reactions, while avoiding drawbacks of natural enzymes, such as limited or low stability and high production costs. This could enable a new field of 'artificial enzymes engineering' to enhanced catalytic efficiency, reusability, and stability compared to natural enzymes. The unique nanoscale properties, particularly high surface area to volume ratios and tunability, make designer-made nanomaterials promising candidates for a wide range of enzymatic-based applications [149]. In the context, it has been discussed that how various factors like, size, shape, chemical composition, and surface modifications matter in the nanozyme-based disease diagnosis and treatment strategies. It has been well indicated that Fe_3O_4 nanozymes' basic catalytic mechanisms is highly essential in the current developments of tumor catalytic therapy, which can be further enhanced by surface modification. Besides, surface modifications effect with polymers, organic small molecules, and inorganic materials can affect the enzymatic properties of nanomaterials [150]. Likewise, Au nanozyme surface modifications aimed at integrating enzyme-like activities, while enhancing or inhibiting catalytic functions in the presence of specific analytes or substrate targets for biosensing and bioassay applications have also been explored [151]. This section explains and provides examples related to size-, shape-, crystallographic state-, surface modifications, as well as pH and temperature-based changes toward nanozymes, including binding affinity, selectivity enhancer, reversible catalytic activity inhibitor, multienzyme-like activity, and catalytic activity enhancer.

3.1. Chemical composition

The chemical composition of nanomaterials is an essential factor influencing their enzymatic activity. Nanozymes can have their catalytic properties fine-tuned through surface modification and doping. For

Table 1
Effect of various factors on catalytic activity of nanozymes.

Factor	Nanoparticles and enzyme-like activity	Variation	Activity	Effect	Refs.
Size	Pd-Ir core-shell nanoparticles Peroxidase	3.3 nm	Kcat: 9.4×10^4 S^{-1}	Increase in Pd—Ir nanoparticles catalytic activity with increases in particle size. Detection sensitivity enhanced by reducing the size.	[63]
		5.9 nm	Kcat: 3.4×10^5 S^{-1}		
		9.8 nm	Kcat: 9.6×10^5 S^{-1}		
		13.0 nm	Kcat: 1.2×10^6 S^{-1}		
Size	Fe_3O_4 nanoparticles Peroxidase	11 nm 20 nm 150 nm	Km: 0.27	Reduced sample size leads to the increased catalytic activity.	[64]
Size	BSA-Pt nanoparticles Peroxidase	3.3 nm	POD Unit: 217 $U{\cdot}g^{-1}$	Smaller-sized nanoparticles possessed higher enzyme-activity	[65]
		1.5 nm	POD Unit: 1009 $U{\cdot}g^{-1}$		
Shape	Platinum nanoparticles	Tetrahedral	14.0 ± 0.6 kJ/mol	Pd icosahedra exhibited significantly superior peroxidase-like activity. Attributed to Pd icosahedra exhibited a higher level of tensile strain compared to compressive strain, resulting in their enhanced effectiveness in the formation of OH radicals.	[66]
		Cubic	26.4 ± 1.3 kJ/mol		
		Spherical	22.6 ± 1.2 kJ/mol		
Shape	Palladium nanoparticles Catalase	Octahedrons	Km: 135.1 mM	Pd octahedrons exhibit significantly greater catalase activity compared to Pd nanocubes.	[67]
		Nanocubes	Km: 102.4 mM		
Shape	AuNPs	Nanoprism	S/V: 0.55 nm^{-1}	Catalytic activity order nanoprisms > nanocubes > nanospheres > nanorod	[68]
		Nanocubes	S/V: 0.14 nm^{-1}		
		Nanospheres	S/V: 0.3 nm^{-1}		
		Nanorods	S/V: 0.54 nm^{-1}		
Surface modification	AuNPs Peroxidase	Unmodified Amino-Modified Citrate-capped		Unmodified AuNPs have stronger catalytic activity than citrate-capped or amino-modified. The surface gold atoms contribute to the observed peroxidase-like activity.	[69]
Surface modification	Co_3O_4 nanoplates	Amino	Kcat: 2.11×10^4 S^{-1}	NH_2-Co_3O_4 has highest catalytic activities followed by SH-Co_3O_4 > COOH-Co_3O_4 > pure Co_3O_4 > OH-Co_3O_4. Variations in functional groups altered electron transport and catalytic activity.	[70]
		Carboxyl	Kcat: 2.25×10^4 S^{-1}		
		Hydroxyl	Kcat: 1.60×10^4 S^{-1}		
		Sulfhydryl	Kcat: 2.39×10^4 S^{-1}		
Surface Modification	Ruthenium or palladium catalysts	Methyl	Kcat: 2.0×10^6 S^{-1}	Cationic nanozymes with hydrophobic surfaces follow the Michaelis Menten model, substrate inhibition exhibited by polar groups.	
		Benzyl	Kcat: 2.7×10^6 S^{-1}		
		Tolyl	Kcat: 4.8×10^6 S^{-1}		
Temperature and pH	Copper peroxide@polydopamine (CuO_2@PDA) nanozyme	High temperature and neutral pH	Laccase-mimetic activity	Potential mechanism for the dual enzymatic activity of CuO_2@PDA has been suggested, highlighting the significant role of the conversion of CuII/CuI active sites in the catalytic cycle of CuO_2@PDA.	[71]
		Low temperature and acidic pH	Peroxidase-mimetic activity		
Temperature and pH	Gold nanoparticles intercalated into the walls of mesoporous silica (AuMS)	pH (2−10)	Peroxidase-mimetic activity	Peroxidase activity rises as pH levels shift from 2 to 4, followed by a decline attributed to the reduced solubility of TMB at elevated pH levels. The change in reaction temperature indicates that the catalytic activity reaches its peak at 40 °C.	[72]
		Temperature (20–80 °C)	Peroxidase-mimetic activity		
pH	Porous coordination network (PCN)s-222-Fe nanozymes	Physiological pH	Peroxidase-mimetic activity	Peroxidase-like activity of PCN-222-Fe nanozymes shows a significant increase at physiological pH.	[73]

instance, the incorporation of different metal ions into the lattice of a metal oxide nanoparticle can significantly alter catalytic activity. Doping, can create surface defects, induce unsaturated vacancies, and regulate the oxidation states of surface metal ions, which play major role in enzymatic properties of nanomaterials [143]. A prominent example is the synthesis of ceria-zirconia nanoparticles (CZ NPs) comprised of different Zr-to-Ce ratios. Result showed that incorporation of Zr ions in the lattice of Ce nanostructure leads to significant enhancement of the vacant oxygen availability, due to fast conversion of Ce^{3+} to Ce^{4+} and *vice versa*. It might be attributed to the reduced capacity of small Zr ions to alleviate lattice strain driven by the Ce^{3+} to Ce^{4+} transition. The findings suggest that the Ce^{3+}/Ce^{4+} ratio rises and there are more surface oxygen vacancies, which increases the nanoparticles' multi-antioxidant capabilities. $Ce_{0.7}Zr_{0.3}O_2$ nanoparticles, in particular, exhibited better and improved ROS scavenging properties required for the treatment of diseases such as lipopolysaccharide-induced endotoxemia [152]. Another heteronanostructure composed of Ce (core) and Mn_3O_4 island has been reported with enhanced oxidase-mimetic activity [153]. Strained Mn_3O_4 island forms on the surface of Ce core as a result of the heterogeneous precipitation of Mn_3O_4, which may enhance the amount of available oxygen in Ce core and accelerates the redox reaction. These nanostructures are more effective at scavenging ROS than individual metal ions because of their bimetallic composition.

Furthermore, it has been demonstrated that CeO_2 nanoparticles coated with 12-phosphotungstic acid (PTA) following exposure to UV light PTA self-reduces to PTA*, which in turn accelerates the transfer of electrons from CeO_2 nanoparticles to AuNPs, where the metal nanoparticle serves as an electron sink. The resulting CeO_2 NPs -PTA*-AuNPs exhibit approximately twice the peroxidase-like activity compared to PTA*-AuNPs alone, attributed to the efficient transfer of electron from CeO_2 nanoparticles to AuNPs facilitated by PTA* [154]. For CeO_2 nanoparticles, our group also showed that the catalase-mimetic activity is robust to the phosphate anions, changes in pH, and the makeup of the media used in cell culture [155].

Report showed that doping of Mo over the Ni—Fe PBA-based nanocages significantly increased the stability and catalytic activity of the nanocages with enhanced peroxidase, and catalase-like activities by 37 and 27 times in comparison to pristine PBNPs [30]. Furthermore, nanocages demonstrated significantly greater stability than normal enzymes in adverse conditions like variable pH, high temperature, and high salt concentration. Incorporation of iridium (Ir) over the palladium (Pd) nanocubes has been demonstrated to develop (Pd—Ir) bimetallic nanostructure [156]. Result showed that These Pd—Ir nanoubes enhances the H_2O_2 degradation as they exhibited ultrathin Ir shell, which has capability to adsorb more OH, in comparison to bare Pd nanocubes. High reactivity and enhanced contact with the Pd nanocubes are attributed to the ultrathin structure of Ir shells. In another study, Liu et al. reported the development of copper-doped carbon dots (Cu-CDs) with high peroxidase-like and catalase-like activity and enhanced biocompatibility [157].

Heteroatom doping, has been shown to improve the catalytic activities of carbon-based nanocatalysts and confer new enzyme-like activity by coordinating their properties. This is because heteroatoms like nitrogen (N), boron (B), sulphur (S), oxygen (O) and phosphorus (P) have significant electron negativity, which may help with electron transit and efficient use of the different nanozyme components [158].Heteroatoms creates defect at surface of nanozyme, thus delocalizing and affecting the total electron density framework which in turn act as active sites for catalytic activity [159]. In consideration to their electron donor behavior, N-doping leads to development of highly active n-type nano-carbons to enhance the catalytic activity. It can be attributed to the fact that lone pair of electrons can produce more surface defects and thus active sites by perturbing the surrounding electronic structure [160]. In a study, Fan et al. demonstrated the doping of "N" over porous carbon nanosphere leads to the inheritance of peroxidase, catalase, oxidase, and SOD-like activity. These nanozymes targets the tumor cell death by producing toxic ROS [161]. In addition to "N", catalytic activity of nanozymes can also be readily enhanced by the doping with oxygen family. In this context, oxygen-doped carbon nitride has been analyzed for their peroxidase-mimetic activity. Result suggests that, oxygen doping has significantly enhanced the catalytic activity nanozymes due to the accelerated electron transfer in comparison to pristine g-C_3N_4 [162].

Further, catalytic activity of carbon-based nanozymes can also be majorly enhanced by the co-doping with mixed heteroatoms or metal or metal oxides. In this context, it was discovered that co-doping with N, S, and P increased the active sites and ROS generating capacity, incorporating the peroxidase-mimicking activity in CQDs (NSP-CQDs). Furthermore, the pH window is expanded by heteroatom doping because of the improved stability and polarity. In addition to having antibacterial properties, these NSPCQDs were active against ABTS oxidation at neutral pH [163]. The edge structure was enhanced by co-doping with N and B in another example by Luo et al. As a result, there were more structural flaws and faster electron transport from N to B, which served as peroxidase activity active sites [164]. Thus, heterogeneous components of the nanozymes work in concert to improve substrate binding and active sites, enable electron transfer, and ultimately increase the nanozymes' selectivity and sensitivity.

3.2. Size

The size of nanoparticles is another critical determinant of their enzymatic activity, as smaller nanoparticles exhibit higher catalytic activities. This effect can be attributed to the fact that with decrease in particle size, corresponds to increased specific surface area and atomic number of the surface which in turn leads to formation of multiple unsaturated and dangled bonds on the particle surface. Due to this, surface energy improved with exposure of many active sites finally enhancing the catalytic activity [165]. For Fe_3O_4 nanozymes, investigation revealed a size-dependent decrease in the peroxidase-like activity in order 30 nm > 150 nm > 300 nm. It might be attributed due to the presence of high Fe(II) on the small-sized particle because of high surface area, which plays crucial role in enhancement of peroxidase-like activity [2]. This fact is further confirmed by size dependent investigation of Peng et al. to different sizes of nanozymes [64]. Here, again catalytic activity of different sized Fe_3O_4 *i.e.* 11 nm, 20 nm, and 150 nm, has been evaluated. As expected, result showed increased catalytic response with decreasing size of nanoparticles. It could be explained, the reduction in particle size exhibited enhanced surface area with more active sites, which in turn facilitate the more efficient contact with the substrate. Ruthenium nanoparticles (RuNPs) also demonstrated the size-dependent antioxidant enzyme-like activity [66]. Result showed that, as expected, in comparison to 3.9 nm and 5.9 nm, RuNPs at small size of ~2 nm, exhibited high enzymatic activity due to dominance of surface-oxidized Ru atoms. Likely, other group also discovered that, in comparison to large-size PBNPs (128 nm), ultrasmall PBNPs of 3.4 nm showed considerably increased peroxidase - and catalase-like activities.

However, this trend does not always hold, as several other factors such as surface defects effects can also influence enzymatic activity of nanoparticles. For example, catalytic activity of citrate AuNPs and polyvinylpyrrolidone (PVP)@AuNPs in size range of 10–15 nm has been evaluated for their catalytic activity [166]. Result indicated that AuNP of varying sizes, while maintaining the same total surface area, exhibited distinct catalytic behaviors. The pattern of catalytic activity shows no dependence on the conjugated ligands for citrate and PVP ligands. Increased defects are observed on the surface of larger AuNP, potentially leading to a greater distribution of active sites on their surface. This observation could elucidate the enhancement of the catalytic reaction based on size dependency. Furthermore, variations in the stabilities of nanoparticles throughout the catalytic process could result in distinct aggregation states, potentially affecting the rate of the reaction. Observation further supported by a recent investigation that thoroughly

examines the size effect on peroxidase-like activities of nanozymes by utilizing Pd—Ir core-shell nanoparticles with different size *i.e.*, 3.3, 5.9, 9.8 and 13.0 nm, but with same surface structure and shape [63]. Result profoundly indicated that catalytic activity increased with particle size, with area-specific activity remaining stable for 3.3–9.8 nm particles but decreasing slightly at 13.0 nm. It was also shown that with increase of particle size K_{cat} value (highest number of substrate conversion to product per second) also increases from 9.4×10^4 to 1.2×10^6 S^{-1}. Smaller nanoparticles showed lower detection limits in ELISA-based biosensing, offering insights into optimizing nanozyme performance. Further, a study was conducted on four different sizes *i.e.*, 2 nm, 4 nm, 8 nm and 12 nm of on AuNPs stabilized with bovine serum albumin (Au@BSA nanoparticles). Result demonstrated that 4 nm-sized nanoparticles possessed higher peroxidase-like activity in comparison to 2, 8, and 12 nm, whereas, GOx-like activities remain constant at all size range. The reason behind this anomaly was not entirely clarified, suggesting that factors beyond mere size, such as the nature of surface ligands or particle agglomeration, might play a significant role [167]. In a recent study, catalytic efficiency of carbon nanotube-supported ultrasmall Pt-based nanozymes (Pt/CNTs) in size range of 0.55–2.81 nm has been evaluated [168]. The observed electronic and kinetic effects that depend on size have been noted for the peroxidase-like reaction, demonstrating a volcano-type relationship between intrinsic activity and the sizes of Pt nanoparticles, with the optimal size identified as approximately 1.69 nm. Result demonstrated that at optimum size Pt nanoparticles facilitate the proper affinity to substrate with excellent catalytic performance.

In addition of regulating catalytic activity and efficiency, size of nanozyme also govern the selectivity in few cases. Interestingly, it has been found that, at optimum size, multienzymatic activity of CeO_2 nanozymes can be governed by the shuttling of electrons from one oxidation to other *i.e.*, Ce^{+3} and Ce^{+4}. Only small-sized CeO_2 nanozymes, typically smaller than 5 nm, tend to acquire the SOD mimicking function. This is most likely because more oxygen vacancies are formed on the surface to maintain a greater Ce^{3+} [11]. Thus, size of nanozymes exhibited a significant impact on their catalytic activity as well as on sensitivity and selectivity enabling wide range of application in diagnostic as well as therapy.

3.3. Morphology and crystallographic state

Several morphology-dependent properties like energy, nanocrystals plane, and surface dimensions are well reported to influence the enzymatic property of nanoparticles [3]. Different morphologies, such as spherical, rod-like, or flower-like structures, provide varying surface areas and active site configurations, which can enhance or inhibit catalytic performances. For instance, flower-shaped Mn_3O_4 nanoparticles exhibited high catalase- and GPx-like activities in comparison to synthesized counterparts (polyhedron, flake-like, hexagonal plate-like, and cuboid structure). This effect might be attributed due to the significantly higher pore size and enhanced surface area of nanoflowers. In another report, catalase- and GPx-like activity of orthorhombic V_2O_5 having different morphologies *i.e.* nanosheets, nanowires, nanospheres, and nanoflowers, has been evaluated [169], and results showed that catalytic activity of nanozyme followed the order of nanospheres > nanoflowers > nanosheets > nanowires, indicating no correlation between available surface area and GPx-like nanozyme activity. This difference in activity might be attributed to the difference in formation rate of V-peroxido species at nanozyme surface due to the reactivity of V═O bond towards H_2O_2. This reaction is highly favored on the nanosphere surface in comparison to all other morphologies. Further, various carbon morphologies like nanoflakes, nanoflowers, dendrites, nanosheets, and nanoleaves have been evaluated for their enzyme-mimetic activity. Results have confirmed that as tentacle of dendrites exhibited high exposed surface area, which in turn accelerates the enzymatic activity by providing more surface-active sites. Further, core-shell structure imparts the additional activity as tubular structure can provide both internal and external site for catalytic activity [160]. A recent study compared the catalytic reactivities of gold nanorods (AuNRs) and gold nanospheres (AuNSs), and it was shown that in presence of sodium borohydride ($NaBH_4$), both AuNRs or AuNSs grown by seed-mediated technique and coated with CTAB were catalytically active. The investigations revealed that the catalytic system utilizing AuNRs exhibits the higher activity, attributed to the greater number of particles and atoms present on the surface compared to spherical particles [170]. Another study on iron oxide nanoparticles demonstrated that flower-like Fe_3O_4 nanoparticles exhibited superior peroxidase-like activity compared to their spherical counterparts. The increased activity is attributed to the higher surface area and more active sites for substrates exposed in the flower-like structure, which facilitates better interaction with substrate molecules. The unique morphology also allows for multi-point attachment of substrates, enhancing the catalytic process. Zhang et al. in another study prepared the different shapes of Co_3O_4 nanoparticles, including nanocubes, nanorods, nanopolyhedrons, and nanoplates [171]. It has been shown that {112} plane is considered as most active and accessible plane out of the three. Co^{3+} is pivotal to the catalytic properties of Co_3O_4 nanoparticles; thus, increasing the surface exposure of Co^{3+} on nanoparticles is advantageous for augmenting their catalytic efficacy. It has been well reported that Co^{3+} do not exist on plane {111} and {100}, whereas each {110} consists of $4Co^{3+}$ and $5Co^{2+}$ and {111} plane contains more Co^{2+} than {100} plane. In the context of above explanation, catalytic activity depending on plane follows the order of {112} > {110} > {111} > {100} and thus Co_3O_4 nanoplates exposing {112} exhibit the highest catalytic activity. The results indicate that Co_3O_4 nanorods reveal an active {110} plane on their lateral surface and a less active {111} plane on their terminal surface, resulting in their catalytic activity being superior to that of Co_3O_4 nanocubes with {100} plane exposure and inferior to that of Co_3O_4 nanopolyhedrons with {110} plane exposure. In another example, {110} plane exposing CeO_2 nanorods exhibited higher oxidase-like activity in comparison to their cuboid counterpart with {100} plane. Whereas CeO_2 nanocubes exhibit enhanced catalase-like activity, with octahedron {111} plane exhibiting lower catalase-like activity [172]. A subsequent mechanistic investigation revealed that the electron density of the surface cerium atoms varied consistently across different crystal facets, resulting in their distinct catalytic activity. Another study on manganese dioxide (MnO_2) nanozymes has shown that nanowires and nanosheets display different levels of catalase-like activity. The anisotropic growth in nanowires exposes specific crystal facets that are more reactive, while the layered structure in nanosheets allows for easier electron transfer, thus affecting the overall enzymatic activity [173]. Thus, the mentioned result suggest that morphology and crystallographic state significantly influence the catalytic performance of nanozymes, necessitating further investigation into their regularity and mechanisms in further research.

3.4. Self-assembly

Self-assembly of nanomaterials is an advanced strategy to enhance their catalytic activity. This involves the spontaneous organization of nanoparticles into structured assemblies, which can exhibit new or improved functionalities and stability. The hierarchical structures formed through self-assembly can provide additional catalytic sites or facilitate multi-step catalytic processes, which may have an impact on multi-enzymatic properties. An illustrative example is the self-assembly of neurotransmitter dopamine and Au nanowire hydrogels, where dopamine cross-linking induces the self-assembly of Au nanowires, resulting in a hydrogel with higher GOx-like and SOD-like activities compared to mildly covered Au-polydopamine or Au-hydrogel without dopamine. This increased activity is attributed to the hydrogel's porous structure and enhanced electron transfer capabilities [174]. Another approach is the engineering of multi-substrate assemblies to create nanozymes with cascade catalytic activities. For instance, the

construction of a multifunctional V_2O_5@pDA@MnO_2 nanozyme assembly has demonstrated improved catalytic ability due to *in-situ* formation of MnO_2 nanoparticles on a V_2O_5 core, providing a synergistic effect from the combined properties of different components. Report showed the development of self-assembled nanozymes Cu-Phen showing electron interplay between cytochrome C [175]. This is designed with a meticulously crafted structure that includes a clearly defined active site, showcasing a receptor-like hydrophobic surface. This design enhances electronic communication with cytochrome C, primarily through hydrophobic interactions, effectively replicating the role of the cyt c oxidase (CcO) enzyme in physiologically relevant conditions. Authors demonstrated for the first time, through kinetic isotopic effects, that electron transfer at the Cu-Phen self-assembled nanozyme and cyt c interface takes place *via* a proton-coupled electron transfer mechanism. This process occurs in a controlled manner, with the phenylalanine ligand potentially playing a combined role in proton relays throughout the catalytic cycle. Other self-assembled MnO_2@PtCo nanoflower-based nanozyme has been reported where MnO_2 exhibited catalase-mimetic activity, whereas, PtCo showed oxidase-mimetic effect [176]. Here, by adjusting the reactant concentration, both the components assembled in to high-ordered nanoflower. PtCo nanozyme has the ability to catalyze oxidation reaction cascades, resulting in intracellular oxidative damage and ultimately achieving an effective therapeutic outcome. In the meantime, the inherent catalase-like activity of the MnO_2 component enables it to swiftly and effectively catalyze the decomposition of H_2O_2 into O_2.

Supramolecular nanozymes, developed through self-assembly methods and diverse non-covalent interactions, have surfaced as another intriguing tool. The organization of biomolecular nanozyme systems through supramolecular self-assembly is crucial factor for the development of structured functional molecular sequences or unit structures in sensing and therapy system [177]. In this context, Xu et al. developed noble metal ion supramolecular nanospheres (Fmoc-His-Au) *via* utilizing the combination of two interactions *i.e.*, electrostatic adsorption and multifarious weak intermolecular forces among $AuCl_4^-$ and amphipathic histidine [178]. Supramolecular nanostructure constitution provided by the noncovalent interaction among $AuCl_4^-$ and histidine. Further, it also facilitates the stabilization of highly active $AuCl_4^-$ centre, which significantly enhances the oxidase and peroxidase-mimetic activity for efficient generation of ROS. In another study, PVP modified Cu single atom nanozyme has been activated by coordination-driven self-assembly strategy using l-cysteine (MoOx-Cu-Cys) [179]. Here, catalase-like activity of nanozyme can be activated by modulation of Cu single atom in acidic condition. Result demonstrated that optimization of catalase-like activity can be performed by well-formed l-Cys-Cu···O active site to align with the active sites of natural catalase *via* a l-Cys bridge that accelerates electron transfer from Cys-Cu to MoOx, as revealed by density functional theory calculations. At the same time, the elevated presence of Cu single atoms in MCCP facilitates the production of •OH through a Fenton-like reaction.

Organic nanozymes requires additional factor such as peptides for their catalytic process, which is considered as major hindrance to their application. Zhang et al. developed the cofactor free organic nanozyme by self-assembly of cyclodextrins modified AuNPs and azobenzene modified peptide chain through host–guest interaction [180]. Developed nanozymes exhibited catalytic activity due to peptide chain ordered assembly on the support surface as well as due to the deprotonation of adjacent histidine imidazole groups. This deprotonation in turn, promotes the proton splitting from water, thereby enhancing nucleophilic attack on incoming substrates. Assembly and disassembly of nanozyme can be regulated by photoisomerization of azobenzene, which further affects the catalytic behavior. Thus, studies conclude that the enzymatic activity of nanozymes can be significantly enhanced by the self-assembly approach. By utilizing this, researchers can design nanozymes with enhanced or tailored catalytic activities suitable for specific biomedical applications, including biosensing, disease therapy, neuro regeneration, and environmental remediation [181].

3.5. Surface modification

Surface modification of nanomaterials plays a pivotal role in determining their enzymatic activity by changing surface chemistry, which can improve interaction with substrates and expand catalytic efficiency [182]. The overall catalytic efficacy and specificity of nanozymes may be impacted by surface modification, which may partially shield or selectively increase their activity [165]. Surface modification can involve the functionalization of nanomaterials with specific molecules like aptamers, antibodies, ligands, or polymers that tailor the surface properties to optimize activity, stability, specificity and selectivity. For instance, modifying the surface of CeO_2 nanoparticles with polyacrylic acid (PAA) notably enhances their peroxidase-like activity. The PAA not only stabilizes the nanoparticles but also increases the number of available active sites by preventing nanoparticle aggregation. Additionally, PAA-modified CeO_2 nanoparticles exhibit increased affinity towards selective substrates, enhancing catalytic efficiency. Such surface modifications are essential for improving the functionality of nanozymes in biological environments, where stability and biocompatibility are crucial [183]. Another example includes the functionalization of Au nanoparticles with thiol-terminated polyethylene glycol (PEG). This modification not only stabilizes the nanoparticles in physiological conditions but also reduces non-specific protein adsorption, thereby improving the selectivity and sensitivity of nanozyme-based biosensors and formulations for neurological applications. The choice of surface modifiers can be tailored to achieve specific interactions with target molecules, thereby enhancing the desired catalytic and multi-enzymatic activity [184].

Fan et al. incorporated the histidine residue at Fe_3O_4 nanoparticles surface in order to provide a similar microenvironment as of natural peroxidase enzyme [185]. Result showed that modification with single amino acid leads to enhanced substrate affinity by ten-folds for H_2O_2 which in turn accelerated the nanozyme catalytic efficiency by twenty-folds. Here, H_2O_2 affinity has been increased due to the formation of a hydrogen bond among imidazole group of histidine and H_2O_2 to provide similar configuration as depicted in natural HRP. In addition to peroxidase-mimetic activity, incorporation of histidine also enhances the catalase-mimetic activity, thus highlighting the increased affinity towards H_2O_2. For instance, CeO_2 nanozymes had been surface modified with poly(tannic acid) (PLTA) to demonstrate their antioxidative behavior [186]. Result showed that PLTA/CeO_2 Nanoparticles exhibited the enhanced SOD-mimetic activity in comparison to bare CeO_2 Nanoparticles which in turn cause high radical scavenging rate in both $ABTS^+$• and DPPH•. This enhancement in SOD-mimetic activity might be attributed to the fact that presence of PTA can increase the content of Ce^{3+} at the nanozyme surface and TA serves as effective radical scavenger. However, peroxidase-mimetic activity of bare CeO_2 nanozyme found to be slightly higher than that of PLTA/CeO_2, which might be attributed to the reduced surface interaction towards H_2O_2 substrate.

In case of multienzymatic activity, surface modification could readily show effect on one type of enzymatic activity without interfering with other [185]. For instance, upon coating with amine-terminal polyamidoamine (PAMAM) dendrimer, gold nanocluster (AuNCs) (AuNCs-NH_2) loses their peroxidase-mimetic activity while retaining catalase-mimetic activity [187]. This result might be attributed to the radical scavenging effect of AuNCs-NH_2, as amines are readily oxidized. Here, highly reactive •OH produced in the system preferably reacts with the abundant amines from the hyper-branched dendrimers (*i.e.*, the periphery 1°-amines and the interior 3°-amines). While amino- and citrate-modified gold nanoparticles demonstrated distinct oxidation behaviors on various substrates (such as TMB and ABTS), unmodified gold nanoparticles were found to have noticeably greater catalytic activity against peroxidase substrates than either of these modifications [188]. The

charge properties of the nanoparticles probably have an impact on the catalytic processes as well as the affinity of enzyme and substrate binding [69].

Carbon-based nanozymes like fullerenes, CNTs are not be properly soluble in water which in turn restricts their enzyme-mimicking activity. This issue can be addressed by coating of nanozyme surface with hydrophilic moieties (polymeric or monomeric amines) or oxygenated functional groups [189]. Peroxidase-mimetic activity of graphene quantum dots has been studied by deactivation of different functional groups *i.e.*, carboxylic (O=C–O–), carbonyl (–C=O), and hydroxyl group (–C–OH) [190]. Here, O=C–O– and –C=O group served as substrate binding site and catalytic active sites, respectively. Whereas –C–OH exhibited inhibitory effect. Result demonstrated that removal of deactivation of carboxyl group leads to reduction in nanozyme affinity towards H_2O_2 substrate, whereas deactivation of hydroxyl and ketonic group increased and decreased the catalytic response, respectively. The catalytic activity of peroxidase-mimetic activity of GQDs was observed to surpass that of GO in the oxidation of TMB. The rise in activity was accomplished through a higher density of functional groups, leading to an abundance of catalytic sites and enhanced electron transport capabilities [191]. Additionally, –COOH group also plays a crucial role in SOD-like activity, majorly owing to its strong interaction with ROS through hydrogen bonding [160]. Thus, surface modification of nanozymes can effectively alter their catalytic response and thus should be chosen carefully according to application prospects.

3.6. pH and temperature

As discussed in earlier sections, like natural enzymes, the impact of external factors such as pH and temperature on nanozymes must be considered that can alter their catalytic activities. Nevertheless, nanozymes demonstrate superior tolerance across a broad spectrum of pH levels, compared to numerous natural enzymes [192]. Generally, nanozymes exhibiting multi-enzymatic action have high chances to depict catalase- or SOD-like activity at high pH, and peroxidase-like activity at low pH [114]. It has been shown that in the case of Fe_2O_3 and Fe_3O_4, different enzymatic activity will be exhibited at different pH conditions. Both nanozymes generate toxic •OH radical at acidic pH due to peroxidase behavior, whereas they showed protective effect in cytosolic conditions by decomposing hazardous H_2O_2 into H_2O and O_2 due to catalase-like activity, and thus suppress the cytotoxic effect [193]. In other report, pH dependence of oxidase- and laccase-like activity has also been monitored. At pH 7.0, CeO_2 oxidase-mimetic activity produces the fluorescent product from non-fluorescent amplify substrate by its oxidation, and at pH 4.0 converts it into non-fluorescent resazurin, which is reliable and sensitive method in cancer-specific biomarker detection for theranostic approach.

Further, it has been widely shown that at acidic condition, nanozymes exhibit effective enzymatic activity, whereas under physiological condition their catalytic efficiency declines. To overcome this, researchers have developed Co-doped mesoporous cerium oxide (Co-m-ceria) nanozymes to effectively work in near-neutral pH for multiple biomarker detection [188]. The Co-m-ceria-incorporated paper microfluidic device allows for the precise and accurate identification of various biomarkers through an image captured by a smartphone. This investigation showcases the possibilities of thoughtfully designing nanozymes and their use in sensing devices, establishing a foundation for application of nanozymes in point-of-care (POC) testing with multiple analytes.

Likewise, inorganic nanozymes typically demonstrate a broader range of temperature tolerance than many natural enzymes, which tend to be sensitive to temperature fluctuations and show the highest catalytic activity at physiological temperature (37 °C) [165]. It has been shown that some nanomaterials like $CuPO_4$ tend to have enhanced peroxidase-mimetic activity over a wide temperature range of 15–65 °C with direct correlation with increasing temperature [194]. In case of multi-enzymatic activity, each enzymatic activity is governed by different optimal temperatures. In the case of cerium-based MOF nanozymes, strong temperature-based peroxidase and oxidase activities have been reported. Herein, oxidase-like activity shows slight increment with the increasing temperature, with sudden decrease at temperature more than 40 °C. Whereas, peroxidase-like activity follows the direct correlation of catalytic activity and temperature with optimum activity at 25 °C [195]. In a similar way, peroxidase- and oxidase-like activity of N-rich carbonized silk fibroin materials (CSFs) has been explored in temperature range from 30 to 80 °C [196]. Both the peroxidase- and oxidase-like activity have optimum catalytic activity at 50 and 60-°C, respectively. Additionally, nanozyme exhibits the highest peroxidase activity at 60 °C, distinct from other reported nanozymes. The catalytic activity resembling that of peroxidase-mimetic activity appears to diminish in high-temperature reactions, likely because of the inadequate thermostability of peroxidase-transformed ox-TMB. Nonetheless, CSF-900, characterized by its stable graphitic structure, demonstrates effective charge transfer capabilities, potentially preventing the disproportionation of oxidized products and contributing to the stabilization of enzyme-like activity at elevated temperatures. In addition to this, temperature also impacts the kinetic energy of the nanozyme active sites, which is attributed to the rate of molecular collisions. The size of a few temperature-sensitive nanozymes is also affected by the change in temperature and represented the hydrodynamic diameter of poly-(vinylcaprolactum-*co*-*N*-methylol acrylamide) [P-VCL-co-NMAM] as a function of temperature. The results indicated that the as-synthesized nanohydrogels shrink from 1250 nm at 20 °C to 380 nm at 57.5 °C, and it can be attributed to the change of PVCL hydrophilicity to hydrophobicity at higher temperatures [146].

All these findings suggest that the functionality of nanozymes, particularly those composed of nanomaterials exhibiting multiple catalytic activities, can be fine-tuned through innovative design and tailored application conditions for targeted objectives. For effective biomedical applications, adjusting nanozyme activity at physiological pH and temperature is essential to maintain consistent catalytic performance. Furthermore, tailored surface modifications using functional groups like polymers, aptamers, or antibodies can significantly enhance specificity, catalytic efficiency, and biocompatibility. These modifications enhance specificity in complex biological samples, leading to improved overall detection. The enhancement of critical elements *via* nanomaterial engineering and hybrid nanozyme designs, along with multi-enzyme cascade reactions, can result in improved sensitivity and selectivity of nanozymes in biomedical detection, thereby further elevating their performance.

4. Nanozymes in dual-mode sensing approaches

Emerging biosensing technologies like colorimetric, electrochemical, fluorometric, *etc.* have been extensively important in sensing applications. However, the shortcomings of single-mode investigations, including but not limited to high assay consumption, restricted information acquisition, and suboptimal reliability and accuracy are major concerns, which could be mitigated by a dual-mode sensing system. In this context, dual-mode biosensing strategies applying nanomaterials like gold, iron, and copper nanoparticles can provide an excellent platform *via* generating two distinct measurable signals, and thus work autonomously, devoid of any reciprocal interference in contrast to single-signal analysis. Further, if two different modes have different sensitivities, it is possible to extend the target's sensing range to conduct primary monitoring. Despite this fact, selection of dual-mode sensing technique is preferred by various factors like analyte types, sample matrix, detection sensitivity, specificity, and instrumentation. For example, metallic (Au, Ag, Pt) nanoparticles, metal oxides (MnO_2, CeO_2, Fe_3O_4) nanoparticles, carbon-based (graphene, carbon dots) nanomaterials, and MOFs can possess specific enzymatic properties that facilitate dual-mode sensing. In this line, colorimetric/fluorescence

dual-mode sensing is of particular importance when both high sensitivity and visual, as well as quantitative readouts are required, such as in biomedical and clinical diagnostics. Even this becomes essential when using biological samples with low analyte concentrations, as fluorescence helps increase sensitivity. On the contrary, this becomes less effective for highly autofluorescent samples (*e.g.*, plant extracts), as the background noise can interfere with the fluorescent signals [197]. Secondly, colorimetric/photothermal dual-mode sensing is best for applications in which temperature-dependent signal enhancement is needed, *e.g.*, pathogen detection, bacterial identification, and food safety detection. It is a useful approach for the detection of trace pathogens or toxins in complicated surroundings, a photothermal effect can entrap false positive results due to background noise. However, it is unsuitable for temperature-sensitive samples, such as living cells or proteins, which are unstable at heating conditions [198]. Further, colorimetric/electrochemical modes of sensing are needed for high-sensitive, real-time monitoring, and ultra-low detection limit applications including heavy metal sensing, toxin analysis, and disease biomarker detection. However, this method demands an electrode fabrication and specialized instrumentation (electrochemical workstations), thus, it is not readily applicable in resource-limited settings [199]. Likewise, colorimetric/SERS mode is highly advanced dual-mode sensing, and it is particularly suitable for ultrasensitive and molecularly specific detection, especially in cancer diagnostics, single-molecule analysis, and forensic applications. This approach is especially applied for trace-level analyte detection in complex biological matrices (blood, urine, tissue extracts) for which sensitivity levels required are not possible by the conventional methodologies. That requires costly Raman spectrometers and complex data interpretation, limiting its utility to high-end research laboratories and clinical environments rather than -field-based use.

Further, another important parameter is selecting an appropriate nanozyme for dual-mode sensing approach. In selecting an appropriate nanozyme for dual-mode sensing, it is essential to consider the catalytic mechanism, electronic properties, and compatibility with detection modalities to achieve optimal sensitivity, selectivity, and dynamic range. The nanozymes utilized for colorimetric/fluorescence dual-mode detection encompass a range of materials, including AuNPs, carbon dots (CDs), QDs, or CeO_2 nanoparticles. These materials inherently exhibit dual functionalities essential for chromogenic reactions, such as the oxidation of TMB and OPD, as well as for fluorescence emission. Specifically, they demonstrate peroxidase-like activity for chromogenic reactions and exhibit fluorescence quenching or enhancement through mechanisms like Förster resonance energy transfer (FRET), inner filter effect (IFE), or charge transfer interactions. Likewise, plasmonic nanozymes (AuNPs, AgNPs, and bimetallic nanostructures) with enhanced localized surface plasmon resonance (LSPR) effects have been utilized in colorimetric or SERS (surface-enhanced Raman scattering) sensing by significantly amplifying Raman signals for ultra-sensitive detection. The nanozyme serves as a catalyst for a colorimetric reaction, while the Raman-active substrate offers spectral fingerprinting for the detection of trace levels of toxins, pesticides, and nucleic acids from complex samples. Whereas, for colorimetric/photothermal dual detection, nanozymes like CuS, MoS_2, Au nanorods, or Pd-based nanomaterials have successfully been utilized due to their NIR absorption and photothermal conversion efficiency. The materials generate a colorimetric signal *via* peroxidase-like or oxidase-like activity, while simultaneously converting light into localized heat when subjected to NIR laser irradiation. In the realm of colorimetric and electrochemical sensing, graphene oxide (GO) or MOFs nanozymes exhibit remarkable catalytic redox activity alongside exceptional electron transfer efficiency. Herein, activity resembling peroxidase is observed, accompanied by the identification of a colorimetric response (derived from peroxidation with chromogenic substrates) and an electrochemical response (utilizing redox-active substrates such as H_2O_2, TMB, and dopamine) that assesses variations in current, impedance, or potential. Thus, for achieving optimal sensing capabilities in biomedical diagnostics, environmental monitoring, and food safety applications, it is essential to consider factors such as stability, catalytic efficiency, compatibility with detection platforms, and environmental conditions when selecting a dual-mode nanozyme sensor. Table 2 provides the recent examples and applications of various nanaozyme-based dual-mode sensing toward different analytes.

4.1. Colorimetric and fluorescent dual-mode sensing

Fluorescent and colorimetric sensing are reported as two major sensing approaches due to their remarkable advantages, like development of more sensitive, efficient, convenient, rapid, and real time sensing applications with advancement in POC devices [52]. Colorimetric sensing, typically relies on change in solution color might be caused due to the aggregation or analyte induced modification. Nanozymes can catalyze the oxidation of chromogenic substrate for development of colored product [41]. If this nanozyme catalyzed oxidation product changes color and emits light or alter the fluorescent activity, the target can be identified through two distinct readout signals *i.e.*, colorimetric and fluorescence. When a compound is exposed to light, electrons in the stable ground state absorb the energy from the light, allowing them to move to higher, unstable excited states. Fluorescence molecules imply on the absorbance of light at one particular wavelength (excited wavelength) and emission at higher wavelength (emission wavelength) while returning to ground state from excited state. Interaction of target analytes with nanozymes can quench their fluorescence, which can be regained upon binding to different targets. In FRET mechanism, nanozymes can be used as electron acceptor and donor, where energy transfer among acceptor and donor can be altered by target molecules [42,52].

Various approaches have been utilized for development of fluorometric and colorimetric-based dual-sensing application. First and main approach is to utilize enzyme-centred catalytic reactions or Fenton reactions and nanozymes for the development of fluorescent/colorimetric biosensors [200]. Second approach includes the incorporation of LSPR acquired plasmonic noble metal (Au, Ag) nanoparticles with fluorescent materials for the development of dual-mode and label-free sensing systems [201]. At last, different fluorescent probes can also be used in the development of dual-mode biosensors. However, various reports have demonstrated that this dual sensing approach has limited practical activity due to complicated integration of fluorescence and color. Taking into consideration, Han et al. demonstrated the sensitive and rapid detection of spike 1 (S1) protein of SARS-CoV-2 based on the fluorescent and colorimetric dual-mode biosensor [201]. Authors developed the dual-mode immune system by coating of QDs and AuNPs over SiO_2 core, exhibiting enhanced stability with high monodispersity. Result showed that the visual identification with rapid screening of virus at infected site can be successfully commenced by colorimetric method, whereas early-stage viral detection can be done by fluorescence signal. Fluorescent and colorimetric dual-mode detection method followed in detection limit of 0.033 and 1 ng/mL, respectively. In addition, the efficacy of the biosensor was assessed in the analysis of real samples. The biosensor that was invented in this study exhibited commendable specificity, accuracy, and repeatability, indicating its potential as a rapid SARS-CoV-2 detection instrument.

In current scenario, nanocomposite containing metal nitrogen-doped carbon (M-N-C) have attracted wide attention due to unique and advantageous characteristics like wide synthesis approaches, enhanced enzymatic activity, and similarity with natural enzymes consisting specific metal active centres [202]. In addition to generating active sites, doping N-doped carbon with metals can enhance its electrical conductivity. In comparison to other fluorescent materials, CDs acquired several advantages like high biocompatibility, water dispersibility, and photostability with low toxicity [203]. In this context, Wu et al. utilized the IFE phenomenon among oxidized-TMB and orange fluorescent CDs for the development of dual-mode sensor for sensitive and rapid

Table 2
Recent studies demonstrating the dual-mode sensing activity of nanozymes in detection of different analytes.

Nanozymes	Analytes	Dual sensing mode	Linear range	LoD	Refs.
Copper/molybdenum bimetallic nanoclusters (Cu/Mo NCs)	Butyrylcholinesterase	Colorimetric	0.5–90 U/L	0.18 U/L	[74]
		Fluorescence	1–100 U/L	0.36 U/L	
Magnetic Fe nanozymes (Fe NZs) and nitrogen-doped carbon quantum dots (NCDs)	α-Glucosidase	Colorimetric	5–100 U/L	2.1 U/L	[75]
		Fluorescence	5–100 U/L	2.4 U/L	
Iron-nitrogen-carbon single-atom nanozyme	Acetylcholinesterase	Colorimetric	0.2–10 U/L	0.11 U/L	[76]
		Fluorescence	0.1–9 U/L	0.057 U/L	
ZIF-8 organometallic frame load with platinum nanoparticles (Pt@ZIF-8)	Silver ion	Colorimetric	1.0–1000.0 nM	0.034 nM	[77]
		Electrochemical	0.1–1000.0 nM	0.322 nM	
Bovine serum albumin templated copper nanoparticles	Dopamine	Colorimetric	10 nM to 10 μM	5 nM	[78]
		Fluorescence	10 nM – 60 μM	5 nM	
Mesoporous polydopamine/MnO_2 nanozymes	*S. aureus*	Colorimetric	5–10^7 CFU/mL	3 CFU/mL	[78]
		Electrochemical	5–10^7 CFU/mL		
Metal–organic frameworks (MOFs-818)	Hydrogen peroxide (H_2O_2)	Colorimetric	4–66 mM	15.37 μM	[79]
		Electrochemical	0.07–3 mM	53.05 nM	
	Hydrogen sulfide (H_2S)	Colorimetric	3 μM to 333 μM	0.8 μM	
		Electrochemical	0.001–0.5 μM	0.76 nM	
Flower-like hierarchical ferrocene metal-organic framework (ZrFc-MOF)	Glyphosate	Colorimetric	0.039–4.73 μg/mL	0.0326 μg/mL	[80]
		Photothermal	0.039–20.16 μg/mL	0.0289 μg/mL	
Ce-UiO-66-NO_2	Phosphate	Colorimetric	20–110 μM	7.60 μM	[81]
		Fluorescence	3–40 μM	1.21 μM	
Er-MOFs@AuNPs	Osteopontin	Colorimetric	1–850 ng/mL	0.04 ng/mL	[82]
		Photoelectrochemical	0.01–25 ng/mL	2.6 pg mL^{-1}	
MnO_2 nanosheets	Alkaline phosphatase	Colorimetric	0.2 to 5 mU/mL	0.08 mU/mL	[83]
		Photothermal	0.2 to 5 mU/mL	0.12 mU/mL	
Covalent organic frameworks (COFs)	Alkaline phosphatase	Colorimetric	0.5–100 μM	0.10 U/L	[84]
		Fluorescence	1–100 μM	0.60 μM	
Iron-based single-atom nanozymes	Epinephrine	Colorimetric	0.01–1.4 mM	2.95 μM.	[85]
		Fluorescence	0.001 mM – 1.0 mM	0.39 μM	
CuNS/Fe_3O_4@MIPs	Vanillin	Colorimetric	1–100 μM	0.11 μM	[86]
		Fluorescence	1–150 μM	0.10 μM	
Fe_3O_4/graphene oxide nanoribbons	Thiophanate-methyl	Colorimetric	0.05–8 μg/mL	28.1 ng/mL	[87]
		Fluorescence	0.02–10 μg/mL	8.81 ng/mL	
Magnetic covalent organic framework (MCOF) with gold nanoparticles	*Salmonella typhimurium*	Colorimetric	10^3–10^8 CFU/mL	1000 CFU/mL	[88]
		Fluorescence	10^1–10^7 CFU/mL	10 CFU/mL	
Fe_3O_4@Cu	Glyphosate	Colorimetric	0.28 to 0.70 μg/mL	0.086 μg/mL	[89]
		Chemiluminescent	0.17–0.42 μg/mL	0.019 μg/mL	
Trimetallic-modified graphitic carbon nitride nanozyme	Acetylcholinesterase	Colorimetric	4–20 μU mL^{-1}	0.13 μU mL^{-1}	[90]
		Fluorescence	4–20 μU mL^{-1}	0.04 μU mL^{-1}	
Pt-Ni alloy nanoparticles	Acid phosphatase	Colorimetric	0.25–15 U/L	0.10 U/L	[91]
		Photothermal	0.25–30 U/L	0.16 U/L	
Iron-cobalt oxide nanosheets (FeCo-ONSs) and gold nanoclusters	Melatonin	Colorimetric	5–800 μM	2.13 μM	[92]
		Fluorescence	5–300 μM	1.17 μM	
Au@AgPt trimetallic nanozyme	*Staphylococcus aureus*	Colorimetric	25–800 U/L	38 CFU/mL	[93]
		SERS	5–1000 U/L	6 CFU/mL	
Bimetallic carbon dots (Fe&Cu@CDs) nanozyme	Methyl mercaptan (CH_3SH)	Colorimetric	0.024–14.4 ppm	0.0072 ppm	[94]
		Photothermal	0.036–14.4 ppm	0.0108 ppm	
Organophosphorus pesticides	Parathion-methyl	Colorimetric	0.01–20	0.004 ng/mL	[95]
		Chemiluminescence	1–100 ng/mL	0.45 ng/mL	

detection of captopril, enzyme inhibitor used for hypertension and heart disease treatment [204]. Sensing principle lies on the ·OH generation upon H_2O_2 degradation which in turn oxidized TMB to blue color product. TMB in oxidized form have absorption spectra overlap with the CDs fluorescence emission spectra, thus leads to IFE induced quenching of CDs fluorescence. Although, in the presence of target analyte, oxidized-TMB reduced to colorless form, and thus causes IFE inhibition between CDs and oxidized-TMB which in turn recovers the quenched fluorescence signal. Result showed the colorimetric and fluorescence sensing approaches have detection limit of 0.56 and 0.47 μM, respectively with linear range from 1 to 50 μM. On this basis, captopril is detected *via* dual-mode "on–off" colorimetric and "off–on" fluorescence detection systems. To prove the real-life clinical applications, pharmaceutical samples were also tested and the result showed relative standard deviation (RSD) of 1.00 % to 3.22 % and 0.46 %-2.38 % for fluorescence and colorimetric sensing, respectively, whereas recovery range is found to be 95.1 % to 104.8 % and 97.6 %-104.0 %, correspondingly. The outcomes validated the suitability of the proposed dual-mode system for captopril assay in pharmaceutical samples with commendable selectivity and accuracy. Further, M-N-C (M = cobalt) was also used in development of dual mode senor for detection of gallic acid as shown in Fig. 4A [205]. Result displayed that Co-N-C possesses oxidase-mimetic property of nanozyme for TMB oxidation to blue color product and blue fluorescence emission property. Further, the oxidized-TMB effectively quenches the nanozyme fluorescence *via* FRET mechanism. However, upon addition of gallic acid, reversed reaction occurs, and thus blue color intensity reduces leading to weakening of FRET mechanism among Co-N-C and oxidized-TMB and recovery of fluorescence intensity at 440 nm (Fig. 4B and C). The developed sensor has LoD of 32.01 nM with linear detection range of 0.1–15 μM. The real sample analysis in tea beverages established the recovery range of 96.44 % ~ 103.48 % and 96.38 % ~ 104.05 % for colorimetric and fluorescence sensing, respectively.

Other reports have also demonstrated the application of Cu-N-CDs (M-N-C) due to their advantages as discussed above, in the development of dual sensing platform for detection of benzenedithiol [208].

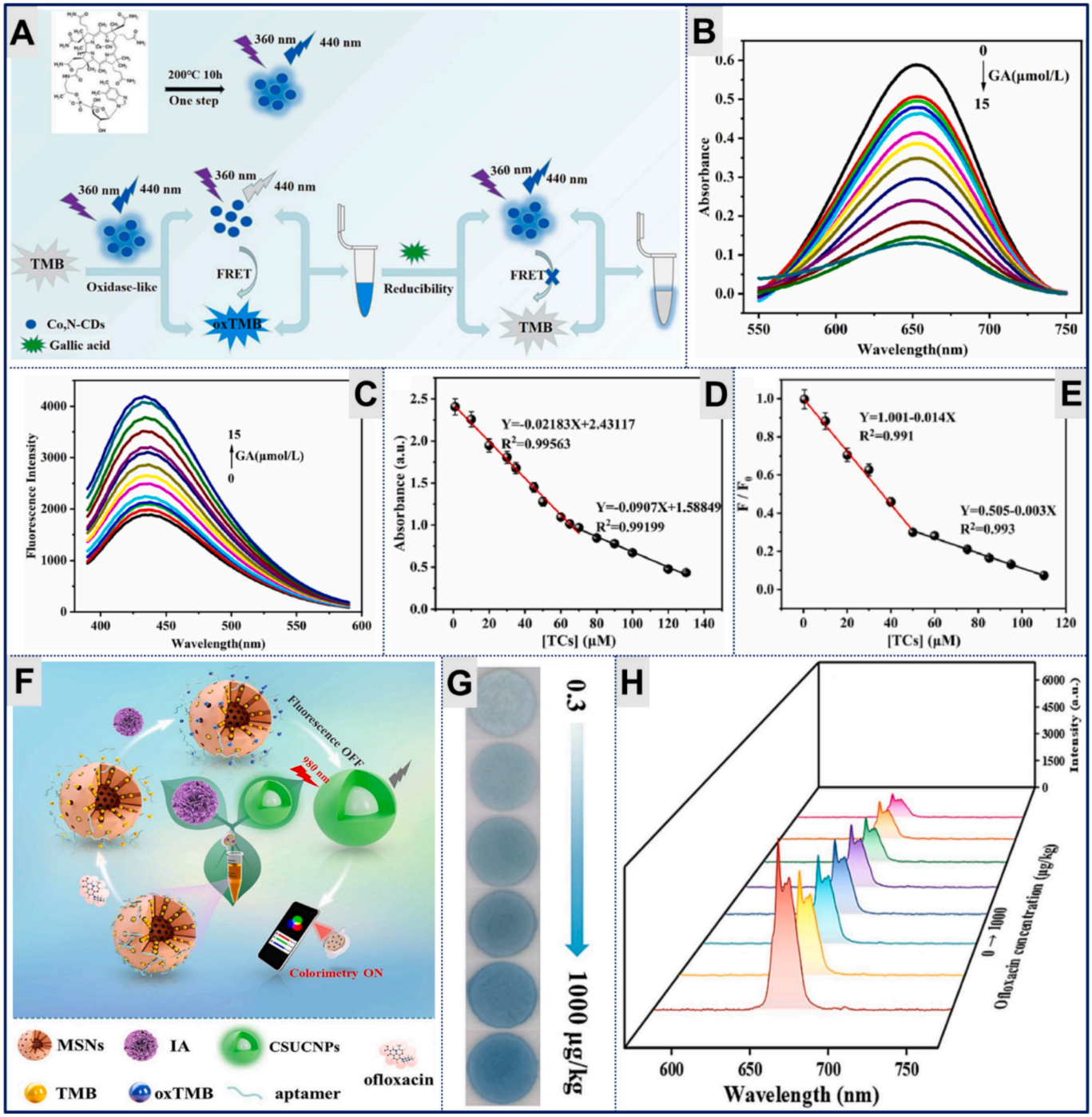

Fig. 4. Panel A: Schematic representation showing the dual-mode detection of gallic acid (GA) by Cobalt-nitrogen co-doped carbon dots; **Panel B:** Colorimetric detection of gallic acid with decreasing color intensity; and **Panel C:** Fluorescence-based detection of gallic acid with increasing fluorescence intensity with increasing gallic acid concentration. Reprinted with permission from *Microchemical Journal, Elsevier* [205] Copyright 2024**. Panel D and Panel E:** Identification of tetracycline using NH2-MIL-88 B nanozymes by colorimetric and fluorometric detection methods, respectively. Reprinted with permission from *Analytica Chimica Acta, Elsevier* [206] Copyright 2024. **Panel F:** Schematic display of dual-mode sensor for detection of ofloxacin; **Panel G:** colorimetric detection with increasing blue color intensity with increasing ofloxacin concentration**, Panel H:** Dual-mode aptasensor showing up-conversion fluorescence spectra with varying concentration of ofloxacin. Reprinted with permission from *Food Chemistry, Elsevier* [207] Copyright 2024. (For interpretation of the references to color in this figure legend, the reader is referred to the web version of this article.)

Here, peroxidase-mimetic activity of Cu and N-CDs coated g-C_3N_4 have been explored in the detection of benzenedithiol, in presence of its chromogenic substrate OPD. Nanostructure catalyzes the ·OH production to oxidize OPD, which emits orange fluorescence under UV irradiation. The findings confirmed the benzenedithiol-mediated inhibition of peroxidase activity of nanozyme, and developed sensor exhibited the LoD of 0.25 μM and 0.32 μM with linear detection range of 0.33–60.0 μM and 0.75–132 μM for fluorescence and colorimetric sensing, respectively. Furthermore, to differentiate the six sulphur-based compounds, smartphone-based colorimetric array sensor has been fabricated with a detection limit of 0.4 μM. The outcomes confirmed that the sensor that was developed functioned as a practical and swift platform, capable of

serving as a dependable portable instrument for the precise and efficient identification of BDT and the differentiation of various sulphur compounds in real water samples.

In this perspective, Zhang et al. showed the NH_2-MIL-88 B (Fe, Ni) based dual-mode detection of tetracycline antibiotic residues and also distinguish between the different tetracycline analogues [206]. As illustrated in Fig. 4D, presence of tetracycline inhibits the ·OH production due to blockage of electron transfer between H_2O_2 and nanozymes, which in turn inhibits the TMB oxidation, and with the increasing tetracycline concentration, fluorescence intensity of nano-system decreases due to IFE phenomenon **(**Fig. 4E**)**. A portable instrument integrating colorimetric and fluorescent signals with a smartphone sensing platform has also been prepared to enable the rapid, and visual quantitative detection of tetracycline. Based on the inhibition of fluorescence and enzyme-like activities by tetracycline, the colorimetric and fluorescent dual-mode nanoplatform enables color change with LoD of 0.182 M and 0.0668 M for the spectrometer and smartphone sensor, respectively. In general, the fluorescent and colorimetric dual-mode detection method exhibits commendable stability, a formidable specificity, and an effective mechanism for mitigating the false-positive concerns that are inherent in a solitary detection mode.

Further, as illustrated in Fig. 4F, Ding et al. developed the aptasensor-based dual-mode ofloxacin detection system with enhanced sensitivity and reliability [207]. In this system, the target analysis majorly depends on the up-conversion nanoparticles (UCNPs) fluorescence properties, iron alkaoxide nanozyme oxidase-like property and TMB release from mesoporous silica nanoparticles (MSNs) coated with aptamer. The intensification of the blue hue of the test paper is readily seen in Fig. 4G as the concentration of ofloxacin increases. The fluorescence intensity decreased gradually as the concentration of ofloxacin increased **(**Fig. 4H**)**. This effect could be linked to the increased release of TMB molecules from the pores of MSNs when exposed to higher concentrations of ofloxacin. The elevated levels of oxidized-TMB, enabled by the iron alkaoxide nanozyme, lead to a more pronounced inhibition of core-shell UCNPs. Result displayed the broad detection range of 0.1–1000 μg/kg and 0.3–1000 μg/kg for fluorescence and colorimetric sensing, respectively, with LoD of 0.048 and 0.165 μg/kg. The developed biosensor showed a satisfactory recovery of 78.24–96.14 % in detection of ofloxacin in real sample.

Thus, all the above examples conclude that the integration of colorimetric/fluorescence dual-mode detection method a single platform not only enhances diagnostic performance by minimizing assumptions, but also boosts diagnostic capabilities through greater application flexibility, improved accuracy, and an expanded detection linear range. The swift advancements in nanotechnology and material chemistry highlight the significant promise of integrated colorimetric/fluorimetric dual-mode systems for detecting various analytes, including biomarkers, microbes, environmental pollutants *etc*. While the integrated dual-mode colorimetric/fluorimetric detection systems offer application flexibility, improve diagnostic capabilities, and enhanced accuracy, there are only a limited number of dual-modal probes that have received approval for practical use. Soon, dual-mode biosensors that integrate the benefits of multiple signal output modes while circumventing their drawbacks will facilitate the dependable, sensitive, and swift detection of various pathogenic bacteria in food. These sensors can be readily utilized for prompt identification.

4.2. Colorimetric and photothermal dual-mode sensing

Photothermal detection generally depends on relation among target analytes and temperature variation using photothermal conversion agent [209]. Portable thermal imager can be used to capture the photothermal temperature image, and it is cost-effective, easy operative technique with enhanced resolution and spatio-temporal effectiveness. Additionally, photothermal assay takeover the colorimetric detection limit of color resolution limitations [210]. Among several photothermal agents, oxidized-TMB has appeared as a novel and potent photothermal agent, exhibiting enhanced photoconversion efficiency in NIR-triggered applications. Herein, oxidized-TMB can be collectively used both as colorimetric and photothermal probe due to its higher absorbance capability in NIR and UV–Visible spectrums. The oxidized-TMB molecules are capable of producing heat energy *via* conversion of NIR wavelength irradiated light energy and the temperature generated is directly or indirectly aligns with the target analyte concentration [211]. Thus, taking into consideration, several studies have used oxidized-TMB as colorimetric and photothermal probe in development of dual-mode biosensor.

In this context, Jiang et al. reported the dual-mode detection of organophosphorus (OP) pesticides using photothermal and oxidase-driven colorimetric detection of platinum-nickel (PtNi) nanoparticles as depicted in Fig. 5A [212]. Author have shown that, PtNi nanoparticles catalyze the TMB oxidation to blue color, which has an excellent photothermal conversion ability for production of heat energy from light energy to increase the solution temperature. Further, acid phosphatase can effectively catalyze the L-ascorbic acid 2-phosphate trisodium (AA2P) hydrolysis, which leads to AA reduction+6 which in turn reduces the blue color intensity of oxidized-TMB to colorless and photothermal effect. Considering the inhibition effect of OP on alkaline phosphatase activity, it limits the ascorbic acid production, and in consequence, blue color of TMB can be restored by the competitive effect. Thus, in presence of OP, TMB can be effectively oxidized to produce blue color and show enhanced photothermal effect **(**Fig. 5B–E**)**. Outcomes of this research have confirmed that the OPs concentration correlated positively with the temperature and color of the probe solution. Moreover, the developed sensor showed the detection limit of 1.66 ng/mL and 1.2 ng/mL for photothermal and colorimetric detection methods, respectively. Therefore, the instrument possesses the capability to precisely identify OPs residues using both colorimetric and photothermal techniques.

Likewise, acetylcholinesterase (AChE) plays crucial role in biological signal transmission and its irregular expression is known to induce several neurodegenerative diseases like Alzheimer's and Parkinson's diseases [213], and taking into consideration the dual-mode sensor for detection of AChE and its inhibitor (paraoxon-ethyl) utilizing Fe-N-C nanozymes has been demonstrated [214]. Fe-N-C effectively catalyzes the degradation of H_2O_2 to •OH to oxidize TMB due to presence of enhanced Fe-Nx sites. Further, conjugation with mercapto group tends to inhibit the peroxidase-mimetic activity due to blockage of Fe-N-C active sites. Thus, developed sensor working mechanism depends on the reduction of peroxidase activity by presence of thiocholine (containing mercapto group), produced due to the action of AChE enzyme over acetylcholine. For AChE sensing, detection limit of developed sensor has been reported to be 2.2 mU/mL and 1.9 mU/mL for photothermal and colorimetric detection methods, respectively, whereas, for the paraxon-ethyl, it is reported to be 0.013 μg/mL and 0.012 μg/mL. Here, proposed assay has the capability to monitor the detection of AChE and its inhibitors. Additionally, it may be expanded to identify additional biomolecules that are involved in the production or consumption of H_2O_2.

Similarly, a dual-mode sensing platform aimed at detecting food grade GSH utilizes CoFeCe nanozyme exhibiting oxidase-like activity, effectively transforming dissolved O_2 into $O_2^{\cdot-}$ [215]. This, in turn, catalyzes the oxidation of TMB, resulting in a visible blue color and photothermal effects. Developed sensor exhibited excellent sensitivity with LoD of 0.092 μM. Oxidase-mimetic activity of nanozymes tends to be governed by factors, like hierarchical hollow sunflower-structure with enhanced active sites, and surface area for immense adsorption of O_2 at surface. CoFeCe three-atom hydroxide facilitates the enormous active sites for generation of $O_2^{\cdot-}$ which in turn oxidize the TMB *via* oxidase-like catalytic activity. In another study, silver palladium (AgPd) bimetallic nanoparticles present the dual-mode sensing for GSH detection [216]. AgPd nanoparticles was synthesized using elm pod

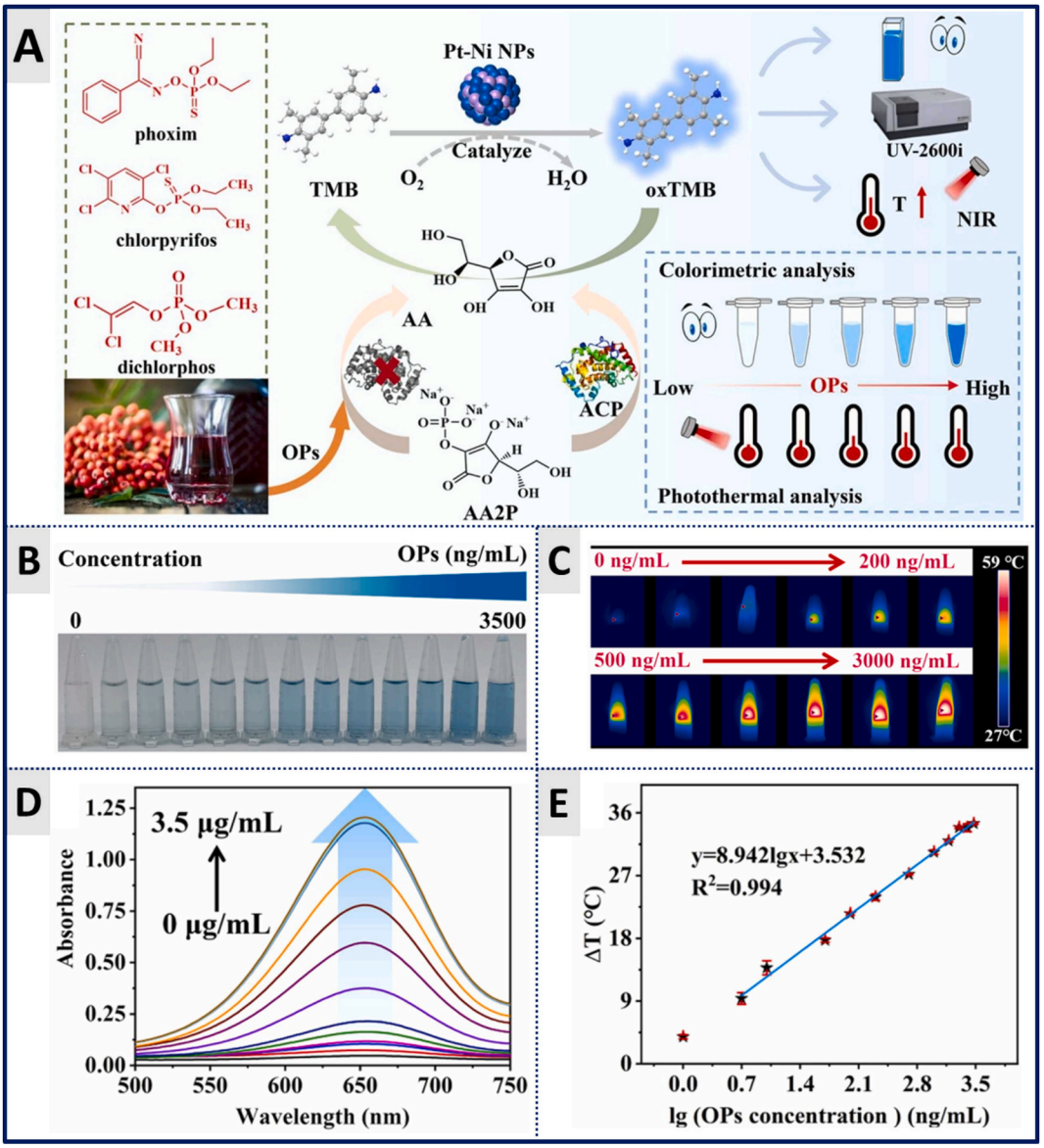

Fig. 5. Panel A: Schematic illustration of application of platinum-nickel (PtNi) nanozymes in colorimetric and photothermal-based detection of organophosphorus (OPs) pesticides. **Panel B:** Colorimetric image at different OP concentration; **Panel C:** Photothermal image at different OP concentration; **Panel D:** Absorbance spectrum showing colorimetric detection with increasing color intensity along with increasing analyte concentration; and **Panel E:** Linear relationships between the OP concentrations and variations in temperature. Reprinted with permission from *Sensors and Actuators B: Chemical, Elsevier* [212] Copyright 2024.

polysaccharide (EPP), which acts as reducing agent and stabilizer because of weak reduction capability and water solubility. Synthesized nanozymes have peroxidase-like activity to produce ·OH radical for conversion of colorless TMB to oxidized blue color products. Addition of GSH can significantly reduce the blue oxidized-TMB to colorless form, and LoD was found to be 0.279 μM with detection in linear range of 0–400 μM. Further, its photothermal properties have been verified and proved to be utilized in photothermal anti-tumor effect. Likewise, Gupta et al. demonstrated the specific and sensitive cholesterol detection using peroxidase-like activity of chitosan-coated cauliflower-like platinum nanostructure (Cs@Pt) [211]. Here, chitosan acts as a stabilizing agent to control the surface property, enhance stability and peroxidase-like activity as well as colloidal dispersion. Results indicated that, oxidized-TMB serves as probe for both photothermal and colorimetric, and due to its excellent absorbance in both NIR and UV–Vis range. Here, cholesterol concentration is directly proportional to the generation of heat produced from absorption of NIR laser light by oxidized-TMB in solution. For colorimetric detection, developed sensor showed LoD of 45 μM with linear detection range of 0–2 mM of cholesterol, whereas for photothermal detection is as low as 25 μM.

Yu et al. developed the dual-mode sensor for prognostic management of patients suffering from myocardial infarction using hollow Prussian blue (h-PB) nanoparticles with the assistance of artificial neural network (ANN) normalization process [217]. In this, liposomes containing h-PB nanoparticles were restricted to the test cell through the application of a traditional immunoassay. The peroxidase-like behavior of h-PB enabled its integration into the TMB-H_2O_2 system, playing a role in amplifying signals for detecting cTnI protein with high sensitivity. When exposed to an 808 nm NIR laser, the corresponding concentration generated a temperature-dependent response, and it was assessed while concurrently monitoring the absorbance of the oxidized-TMB system at 650 nm as a reference. A three-layer ANN comprising 64 neurons was implemented to facilitate bimodal signal processing and regression analysis. Under optimal conditions, the machine learning-enhanced bimodal co-immunoassay demonstrated a broad detection range of 0.02–20 ng/mL, with a sensitivity threshold of 10.8 pg/mL. This research presents a

theoretical foundation for the integration of machine learning in multimodal biosensors, contributing to the advancement of highly sensitive non-enzymatic biosensing technology.

Furthermore, the colorimetric/photothermal dual-mode POC sensing device is demonstrated for mycotoxin detection *i.e.*, aflatoxin in food products, using Pt grafted on N-doped amorphous carbon [218]. Synthesized Pt-CN exhibited excellent peroxidase activity for oxidized-TMB production for colorimetric detection and photothermal sensing. AFB_1-BSA was firstly conjugated to GOx, and competitive immunoassay were performed in the presence of AFB_1. Competitive-type immunoassay was performed for indirect determination of AFB_1 *via* production of H_2O_2 due to catalytic action of GOx on glucose. Generated H_2O_2 are capable of oxidizing TMB to yield a blue color product, with measurable intensity at 652 nm. Additionally, the solution underwent irradiation with an 808 nm laser source for temperature detection, utilizing infrared imaging *via* a smartphone device. Using the oxidized-TMB indication created in the immediate environment, the measurement of target analyte concentration may be done simply by measuring color changes and heat generation. This method offers increased sensitivity without the need for costly analytical instruments. Developed sensor showed the detection limit of 0.76 pg/mL and 0.22 pg/mL for photothermal and colorimetric sensing with linear detection range of 1.0 pg/mL to 10 ng/mL. Further, the approach was effectively utilized to detect AFB1 in peanuts with a satisfactory level of accuracy, when compared to commercially available enzyme-linked immunosorbent assay (ELISA) kits. Notably, the measurement of heat generated by light in this technique is captured using a cell phone, eliminating the need for costly equipment, offering a cost-effective and easy solution for assessing food safety.

Likewise, in early cancer diagnosis, tumor-derived exosomes served as a crucial biomarker as it is responsible for metastasis and proliferation [219]. Thus, it is of great significance to develop accurate and sensitive methods for the detection of exosome for diagnosis and symptomatic treatment of cancer. In this aspect, graphene QDs nanozyme-based dual-mode sensing system is utilized for the detection of exosomes derived from human breast cancer cells [220], wherein the rolling circle amplification (RCA) applied for the development of TMB-loaded graphene QDs nanozymes into DNA flowers (DF). TMB immobilization on the nanozyme surface facilitates the catalytic reaction more efficiently as it enhances its water solubility as well as reduces the distance between nanozymes and TMB. Further, for recognition and capture of MCF-7 derived exosomes, EpCAM corresponding aptamer is immobilized on 96-well plate, and the developed sensor is applied for analysing the real clinical serum sample. Result showed the detection limit of 2170 particles/μL for photothermal approach, whereas 1027 particles/μL for colorimetric detection. Furthermore, the improved sensing platform exhibited exceptional efficacy in accurately differentiating between breast cancer patients and healthy persons during the examination of blood samples. In summary, the proposed dual-readout biosensor has great potential for detecting exosomes in biological research and therapeutic settings.

Given the substantial requirement of meat in people's everyday lives, development of effective methods for assessing its freshness is highly important to ensuring food safety. Novel bimetallic $Fe@CeO_2$ nanozyme has been developed by incorporating ferrocenecarboxylic acid (Fc) into hollow CeO_2 nanospheres. This nanozyme, in combination with xanthine oxidase (XOD), formed a self-sustaining enzymatic cascade catalytic system called $Fe@CeO_2$ + XOD, and it produces a dual-mode analytical platform for hypoxanthine detection to assess meat freshness *via* colorimetric and photothermal modes. The process is aided by TMB, and due to the catalytic properties of XOD, it can transform hypoxanthine into H_2O_2. By activating peroxidase activity induced Fenton-like reaction, $Fe@CeO_2$ quickly breaks down H_2O_2 into •OH, resulting in a typical enzymatic cascade catalytic reaction. Consequently, the TMB without color is oxidized to form the dark-blue oxidized-TMB by •OH. This oxidation process causes an increase in absorption at 652 nm, providing considerable augmentation of chromogenic reaction. Furthermore, the oxidized-TMB exhibits a notable photothermal effect when exposed to a 660 nm laser. A smartphone-based Color Picker App, combined with a handheld thermal imager operating at 660 nm, enables real-time, quantitative, and visually interpretable detection of hypoxanthine with high accuracy and reliability, yielding satisfactory results.

Thus, dual-mode catalytic enhancement, utilizing colorimetric and photothermal methods, significantly boosted both the reliability and sensitivity of the assay. This advancement offers fresh perspectives for effective onsite visual monitoring of various targeted analytes, contributing to the therapeutic and protective effects. Various examples showed that nanozyme-TMB temperature and chromaticity dual-signal sensing platform effectively addresses the limitations associated with single-signal detection, which can result in false positives. At the same time, the dependability of the signal outcomes could be improved through the combined influence of the colorimetric and thermal signals. Consequently, the colorimetric/photothermal dual-signal output sensing system presents an innovative approach for biomolecule detection and holds significant potential for advancement in both biological and clinical sensing fields.

4.3. Colorimetric and surface enhanced RAMAN spectroscopy (SERS) dual-mode sensing

SERS has been considered as an efficient vibrational spectroscopic technique for detection of analytes with high spatial resolution. At nanoscale, Raman signal can be efficiently amplified by the plasmonic property or roughness of SERS active materials enabling single molecule detection. Metals like Au, Ag, and Cu can significantly enhance the Raman signals, while interacting with surface plasmon. Electromagnetic effects and chemical effects are the two major principles that might be attributed to the SERS activity [221]. Electromagnetic effect considered as main mechanism and originated from a substrate due to SPR phenomenon of novel metal nanoparticles because of light concentration in specific region local field enhancement occurs around metal interface, which further leads to enhancement in radiation efficiency [222]. On the other hand, chemical effect induces enhanced Raman signal due to charge transfer between adsorbed molecule and metal. Chemical effect has been reported to show lower signal magnitude in comparison to electromagnetic approach, yet it can play a substantial role under specific circumstances. Thus, SERS plays crucial role in biomedicine, environmental detection, food safety, and pharmaceutical analysis [223,224]. However, real sample molecular concentration determination and identification are not feasible due to the reduced Raman spectra, fluorescence interference or complex behavior of sample matrices. To overcome this, electromagnetic/chemical enhancement can be used to enhance the Raman signal of target analytes. Moreover, a linear equation can be formulated *via* indirect enzymatic reaction for calculation of analyte concentration under analysis (SERS tag) [225,226].

Nanozymes can be effectively integrated with the SERS techniques for development of highly sensitive and selective biosensor. Catalytic activity of nanozymes (conversion of substrate to colored product) combined with SERS provides specific fingerprint peaks deliberating more information about the types and concentration of target analytes, thus enhancing the sensitivity [227]. Secondly, nanozymes exhibiting dual property of catalytic activity and SERS can be designed with Au and Ag [228]. Thirdly, SERS offers an innovative and effective approach for examining the reaction kinetics of nanozymes. It can accurately track alterations in the molecules that are adsorbed on the catalyst surface, along with the catalytic process itself [229]. In the studies, AuNPs are widely employed nanomaterials with SERS and enzyme-like activity [230]. However, the actual applications have been limited due to reduced stability and lower catalytic activity, which need to be improved. Dual-mode colorimetric and SERS-based sensing of analytes depends on the analytes and functionalized nanozymes interaction,

which leads to aggregation of interparticle-crosslinking [231]. Following the same principle, AuNPs modified with *N*-acetyl-L-cysteine (NAC) and dithiobis succinimidyl propionate (DSP) are synthesized for colorimetric and SERS dual-mode detection of serotonin [231]. These two functional AuNPs induce the plasmon coupling due to aggregation, which further leads to visible color change and enhancement of SERS hotspot and thus SERS signal. This system provides several advantages, including enhanced sensitivity with high selectivity and low detection limit of 0.15 mM L^{-1}. Developed system also applied for detection of serotonin in human serum sample with low relative standard deviation of 3.75 %, which evidences its effectiveness in biological sample detection.

As illustrated in Fig. 6A, Qi et al. developed the GeO_2@Fe_3O_4/Au nanocomposite-based colorimetric and SERS dual-mode sensing for ascorbic acid detection [232]. Nanozyme exhibited excellent peroxidase-like activity to convert colorless TMB to blue color oxidized-

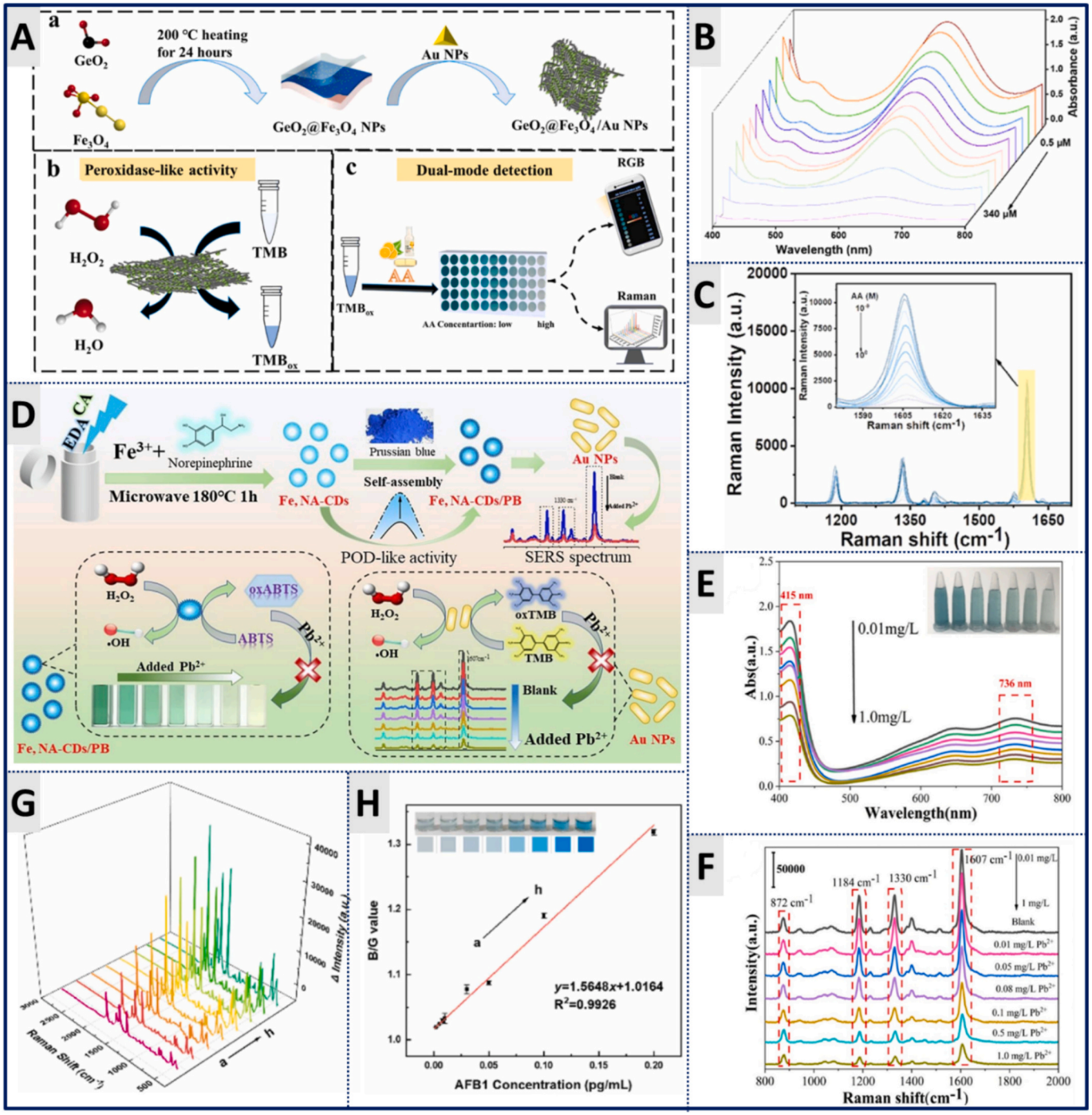

Fig. 6. Panel A: Schematic depiction of synthesis and application of GeO_2@Fe_3O_4/Au nanocomposite and application in detection of ascorbic acid (AA). **Panel B:** Colorimetric detection of ascorbic acid using UV–Visible absorbance spectra. **Panel C:** SERS spectra-based detection of ascorbic acid in sample. Reprinted with permission from *Journal of Food Composition and Analysis, Elsevier* [232] Copyright 2024. **Panel D:** Representation of the fabrication of UV-SERS dual-mode sensor for Pb(II) content detection. Concentration based detection of Pb *via,* **Panel E:** Colorimetric and **Panel F:** SERS-based approaches. Reprinted with permission from *Spectrochimica Acta Part A: Molecular and Biomolecular Spectroscopy, Elsevier* [233] Copyright 2024. **Panel G:** SERS, and **Panel H:** Colorimetric-based detection of AFB_1 using Ag@Au IP6 bifunctional nanozyme. Reprinted with permission from *Sensors and Actuators B: Chemical, Elsevier* [234] Copyright 2024.

TMB, which leads to effective inhibition by ascorbic acid. Based on the above approach, ascorbic acid micro-detection platform using oxidized-TMB as sensing probe is developed, in combination with smartphone-assisted colorimetric (Fig. 6B) and SERS (Fig. 6C) -based sensing. In an ideal condition, with colorimetric approach ascorbic acid detection range is 0.5 μM −340 μM with detection limit of 0.6689 μM. Whereas, SERS approach provides detection range in 10^{-9} μM − 10^{0} M with detection limit of 6.162 × 10^{-13} M. The technique was effectively employed to analyse ascorbic acid in fruits, vitamin C drinks, and vitamin C pills, to demonstrate the findings that align with the recommended levels. In a separate study, Cui et al. designed a dual-mode sensor for detecting Pb(II) in traditional Chinese medicine samples. This sensor utilized iron-doped noradrenaline-based carbon dots (Fe, NA-CDs), combined with Prussian blue (PB) and AuNPs to enhance detection efficiency (Fig. 6D–F) [233]. It has been found that peroxidase activity of nanozymes is inhibited by the addition of Pb(II) both using TMB or ABTS as substrate, and thus can be successfully utilized in its detection. The findings showed that peroxidase-like activity of nanozymes follows “ping-pong catalytic mechanism”, whereas Pb(II) addition induces noncompetitive inhibition imparting modulation in Fe,NA-CDs/PB. SERS and colorimetric detection possess the range of detection is 0.01–1.00 mg/L with detection limit of 8 μg/L and 5 μg/L, respectively. The detecting device, which operates in two modes, has exceptional selectivity. Significantly, the presence of Pb(II) in samples of traditional Chinese medicine has been accurately measured, with satisfactory recovery rates ranging from 90.4 % to 108.9 %.

Similarly, in other study, magnetic ring structure of Fe_3O_4 with AuNPs (R–Fe_3O_4/Au) for SERS and colorimetric detection of biomolecules in human serum is proposed [235]. Peroxidase-like activity of R–Fe_3O_4/Au enables the TMB oxidation for colorimetric analysis, and concomitantly SERS detection *via* sensing Raman signal of oxidized product to provide enzyme kinetics. The outcome showed that for GSH and cholesterol detection, SERS sensing exhibited linear detection range of 1–150 μM and 1–100 μM with detection limit of 0.10 μM and 0.08 μM, respectively. The sensor under consideration has revealed high accuracy and repeatability in measuring the levels of GSH and cholesterol in human blood. The R–Fe_3O_4/Au catalyst exhibited sustained peroxidase-like activity even after five repeated usage cycles, demonstrating its durability. This approach introduces a promising strategy for developing highly efficient SERS substrates and provides an effective means to explore enzyme reaction kinetics. The colorimetric-SERS dual-mode sensors offer a novel approach for using multifunctional sensors and showing promising potential in the field of biosensing.

Ag@Au IP_6 (IP_6 = Inositol hexakisphosphoric micelles) exhibited an excellent SPR effect and thus can act as SERS substrate and also enhance the oxidized-TMB SERS signal *via* combined action of nanogap generated inside its core-shell structure [236]. Tan et al. demonstrated the dual-mode sensor for sensitive and convenient detection of aflatoxin B1 in foodstuff [234]. Bifunctional nanozyme was prepared by combination of hybridization chain reaction (HCR) and alkaline phosphatase (ALP) induced self-assembly reaction. Bimetallic composition of Ag@Au IP_6 nanozyme facilitates TMB oxidation due to its enhanced peroxidase activity. Further, core-shell structured Ag@Au IP_6 nanozyme also served as an excellent SERS substrate for amplification of oxidized-TMB SERS signal (Fig. 6G–H). To tackle the low limit detection of aflatoxin, authors have implemented signal amplification techniques utilizing HCR to greatly improve the sensitivity of the sensing technology. The trigger probe T, modified with an amino group, was attached to carboxyl magnetic beads (MBs) by amide binding and it was then combined with the AFB1 aptamer. Aflatoxin B1 leads to dissociation of aptamer from magnetic beads as it binds to aflatoxin B1 and leads to exposure of T probe. It acts as initial target molecules and initiate HCR amplification to obtain biotin contained multiple long linear DNA chains. Additionally, the incorporation of streptavidin-ALP facilitated its binding to MBs through a biotin-streptavidin interaction, leading to the self-assembly of Ag@Au IP_6 nanoparticles. Under ideal circumstances, the dual-mode aptasensor has linear range from 2 pg/L to 200 pg/L with LoD of 0.58 pg/L, making it suitable for accurately quantifying and detecting AFB1 both in laboratory settings and on-site.

From the above, it is apparent that nanozyme-SERS technology signifies a notable progression in analytical science, providing a highly sensitive, precise, and diversified platform for detecting biomedical markers, environmental pollutants, and food contaminants. The development of complex platforms has further opened new avenues for innovative strategies in biomedical applications, resulting in the utilization of diverse nanomaterials for the precise detection and analysis of different biomarkers. Thus, the combination of nanozymes and SERS principles significantly improves detection limits, enabling the detection of trace amounts of target analytes with exceptional precision. Moreover, synergistic effect among nanozymes and SERS has transformed the domain of biosensing, offering analytical tools that are highly effective and accurate.

4.4. Colorimetric and electrochemical dual-mode sensing

Electrochemical sensing utilizes target-specific recognition and relies on electrochemistry principle for transduction of biochemical signal into measurable electrical signals. Generation of electrochemical signal is directly proportional to the concentration of analytes, thus enabling the quantitative and precise detection. Electrochemical process leads to transferring of electrons between solution and solid electrodes. Here, electrodes play a transducer role to sense electron transfer and hence analyte concentration. Depending on the electroactive and non-electroactive nature of analytes, resultant signals can be directly or indirectly corresponded to the amount present. In the case of non-electroactive analytes, a separate probe having electroactive property should be integrated [237]. Finally, intensity of generated signal relatively depends on the oxidation or reduction of target analyte at electrode surface. Through the alteration of the nanozyme on the electrode surface, it serves as a generator of electrically active probes or signal amplification tags, enabling the acquisition of highly sensitive electrochemical signals *via* the oxidation or reduction of the substrate within the catalytic reaction system. This approach facilitates the development of nano-enzymatic electrochemical sensors. The integration of colorimetric and electrochemical techniques in dual-mode sensing has exhibited the unique benefits of both methods, resulting in a highly effective approach for analytical and diagnostic applications. The colorimetric method fundamentally depends on visible alterations in optical characteristics, including absorbance or color intensity, induced by interactions with the analyte [238]. The measurement of these changes is frequently conducted with spectrophotometers or even smartphone cameras, rendering the method straightforward and widely accessible. The electrochemical mode, conversely, identifies analyte-specific redox reactions by monitoring changes in current, potential, or impedance, thereby delivering accurate, quantitative measurements with exceptional sensitivity [239]. This combination offers notable benefits, as the colorimetric mode facilitates rapid visual screening, allowing for the identification of substantial changes without requiring advanced instrumentation. In the meantime, the electrochemical mode delivers strong quantitative data, guaranteeing specificity and a low limit of detection. Nevertheless, in dual-mode systems, it is crucial that these techniques are frequently crafted to work in harmony with one another. For instance, the identical reaction could yield a chromogenic product suitable for colorimetric detection, while simultaneously producing an electroactive species for electrochemical analysis. This duality facilitates real-time monitoring and cross-validation, minimizing errors and enhancing reliability, particularly in heterogeneous or complex sample matrices. In this context, TMB, as an excellent chromogenic substrate, has also been successfully implicated in development of electrochemical sensor due to its enhanced and strong electrochemical signal [240]. Therefore, TMB functions as a versatile indicator, enabling the development of a dual-mode sensing platform integrating

colorimetric and electrochemical detection [241].

Taking advantage of dual activity of TMB, Zhang et al. demonstrated the dual-mode hemin-graphene (H-Gr) nanocomposite for sensing of Di-2-ethylhexyl phthalate (DEHP), cancer causing agent (Fig. 7A) [242]. Aptamers are utilized to attain great selectivity due to their excellent stability and strong affinity for their target compounds in addition to the preparation of colorimetric platform, DEHP aptamer adsorb to the H-Gr lamella. H-Gr nanocomposite exhibited peroxidase activity to oxidize TMB to blue color product in the presence of H_2O_2. The presence of DEHP solution hinders the catalytic activity of H-Gr by forming complexes with DEHP-aptamer, which leads to a diminished color change. H-Gr nanocomposites are applied to the surface of a glassy carbon electrode (GCE), and DEHP aptamers are introduced onto the H-Gr/GCE. The oxidation current of H-Gr experiences a considerable reduction, which further reduces with the addition of a solution containing DEHP. The inhibition of electron transport of hemin may be attributed to the development of DEHP-aptamer complexes. The developed sensor exhibited linear detection range of $1.00 \times 10^{-10} - 1.00 \times 10^{-7}$ g·L^{-1} and $2.00 \times 10^{-10} - 1.00 \times 10^{-7}$ g·L^{-1} for electrochemical (Fig. 7C) and colorimetric method (Fig. 7B), respectively. Consequently, colorimetric and electrochemical sensor has been developed to detect DEHP with high sensitivity. In another study, recently Lei et al. established the dual-mode detection of H_2O_2 released from live cells (Fig. 7D–F) [243]. This study presents the synthesis of Cu/Zr-MOF nanozymes using the solvothermal method, which exhibit exceptional biocompatibility. The presence of a Cu metal centre significantly enhanced the electrocatalytic activity of Cu/Zr-MOF and its peroxidase-like behavior towards H_2O_2. As shown in Fig. 7D, electrochemical detection demonstrated more sensitivity than colorimetry, with a detection limit as low as 21.3 nM. Colorimetry enabled the identification of H_2O_2 at a concentration of 0.11 μM by detecting the change in color (Fig. 7E). By using a smartphone equipped with a "Color Recognizer" software, it is possible to analyse colours in real-time and with precision using RGB analysis, eliminating the need for additional laboratory equipment. The developed dual-mode sensing technology was effectively utilized for the real-time detection of H_2O_2 emitted by cancer cells. Dual-mode detection is demonstrated to be more dependable and precise compared to traditional single-mode detection, surpassing the constraints of each approach and broadening the scope of dual-mode detection in many fields. It is well known that phorbol myristate acetate (PMA) treatment

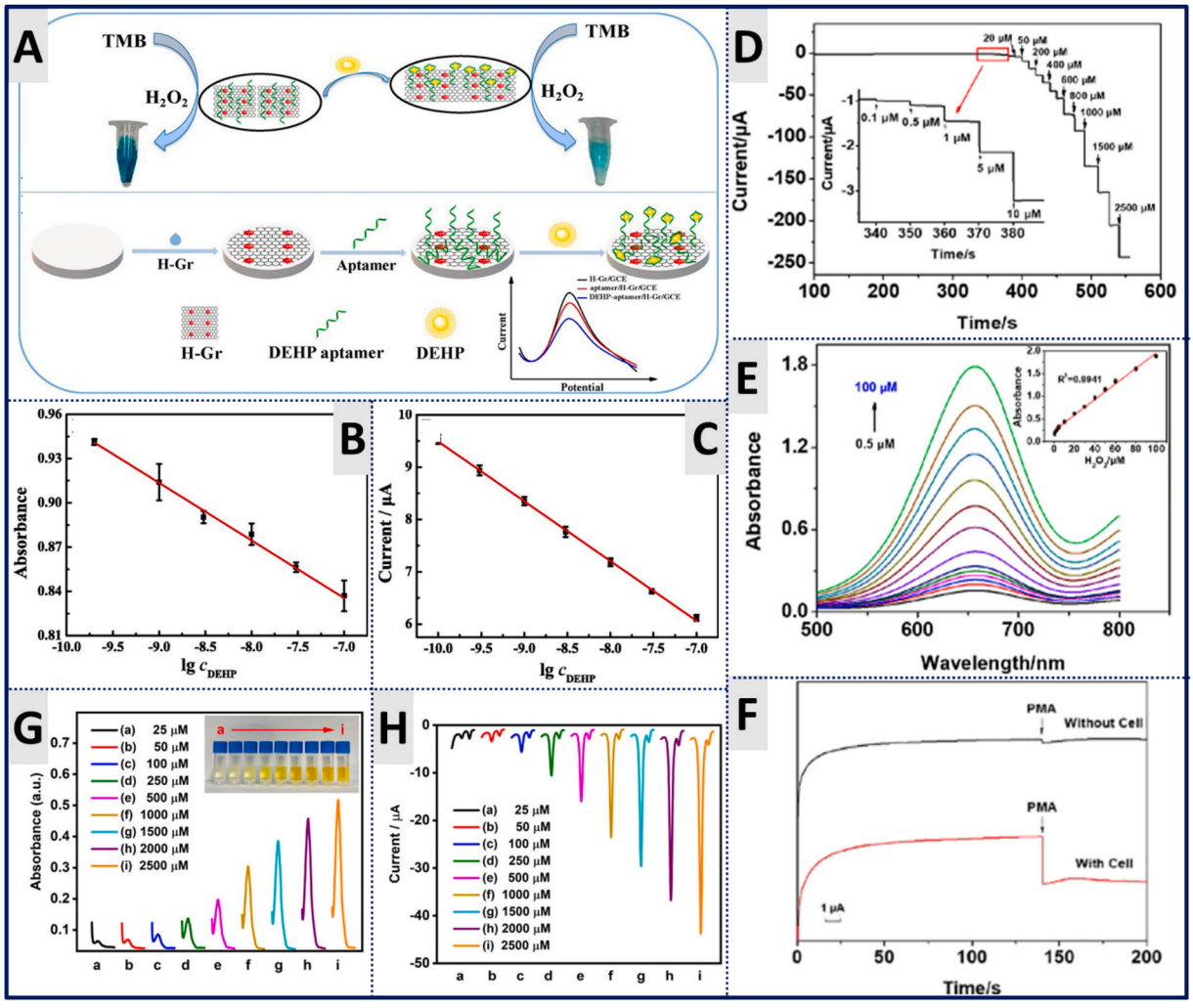

Fig. 7. Panel A: Schematic demonstration of colorimetric and electrochemical sensing of Di-2-ethylhexyl phthalate (DEHP) using hemin-graphene nanocomposites. **Panel B:** The linear correlation between absorbance at 20 min and DEHP concentration, and **Panel C:** The correlation between differential Pulse Voltammetry (DPV) current and DEHP concentration is linear. Reprinted with permission from *Microchemical Journal, Elsevier* [242] Copyright 2023. **Panel D:** Cu/Zr-MOF/SPE chromatographic response upon H_2O_2 injection in system. **Panel E:** UV–vis absorbance spectra at different H_2O_2 concentrations, and **Panel F:** Current response with or without HeLa cells upon PMA addition. Reprinted with permission from *ACS Applied Nano Materials, American Chemical Society* [243] Copyright 2024. **Panel G:** UV–vis absorbance spectrum for colorimetric detection of glucose using CoOOH@Cu nanozymes, and **Panel H:** Difference in DPV current upon addition of different glucose concentrations. Reprinted with permission from *Chem Comm., Royal Society of Chemistry* [245] Copyright 2022.

can stimulate the H_2O_2 production in cells *via* activation of protein kinase C [244]. As presented in Fig. 7F, only small change in current has been observed in presence of PMA alone in the system, whereas current increased significantly when HeLa cells treated with PMA were present.

In the same context, Gu et al. proposed the colorimetric and electrochemical dual-mode sensor for intracellular and extracellular H_2O_2 detection [238], wherein FeS_x/SiO_2 nanoparticles with peroxidase enzyme-like activity are prepared, and TMB is used as multifunctional indicator. Interestingly, TMB can be used both as colorimetric and electroactive probe to build dual-mode detection platform. Result showed that upon addition of H_2O_2, colorless TMB oxidized to blue color product, which leads to a concurrent increase in corresponding absorption peak with decreased electrochemical peak current. The successful integration of the aforementioned two methods resulted in the precise and responsive measurement of intracellular/extracellular H_2O_2.

In another study, synthesis of cobalt copper bimetallic nanoclusters (Co@Cu-BNCs) using a hydrothermal and one-step pyrolysis technique is demonstrated. The synthesized nanoclusters serve as a dual-mode sensing platform for uric acid (UA) detection by colorimetric and electrochemical sensing. Co@Cu-BNCs, when exposed to H_2O_2, exhibit peroxidase-like behavior by transforming the colorless TMB into the blue-colored oxidized-TMB, and the presence of UA in solution leads to reduction in the distinctive absorption peak strength of oxidized-TMB due to its inhibitory influence on the oxidation process of TMB. This research presents a method for detecting UA using a colorimetric assay platform. The method has a linear range of 0.1–195 μM and a low detection limit of 0.06 μM, with a signal-to-noise ratio of 3. Further, the electrochemical approach has a significantly broader detection range due to the prominent electrocatalytic activity of Co@Cu-BNCs, and it has been coated on glassy carbon electrode to develop an electrochemical sensor for UA detection with an expanded linear range from 2 to 1000 μM and a detection limit of 0.61 μM, with a signal-to-noise ratio of 3. Besides, the examination of UA in a human serum sample produced favorable results, indicating utilization of colorimetric and electrochemical dual-mode detection methods for exceptional sensitivity, ease of use, and precision. In this perspective, a novel sensing platform for detecting the breast cancer biomarker thioredoxin 1 (TRX1) has also been proposed [246] employing PBNPs, which are reported to have excellent peroxidase-mimicking and electrocatalytic properties. It can detect TRX1 in physiological fluid using both colorimetric and electrochemical methods. The synthesis of PBNPs was conducted by a hydrothermal method, utilizing $K_3[Fe(CN)_6]$ and PVP as a precursor and capping agent, respectively. In comparison to that of natural horseradish peroxidase (HRP), the synthesized spherical PBNPs exhibited a notable peroxidase-like activity with 20 % and 60 % lower Km values for TMB and H_2O_2, respectively. The presence of PBNPs resulted in an increased efficiency of electron transport on the electrode surface. PBNPs were employed to detect target TRX1 using sandwich-type immunoassay methods, taking advantage of their favorable characteristics. The methodologies employed allowed for the specific and accurate detection of TRX1, with a detection limit as low as 9.0 ng/mL for colorimetric approach and 6.5 ng/mL for electrochemical methods. 10–50 ng/mL has been reported as linear range for detection in both colorimetric and electrochemical approaches. The TRX1 immunoassays, based on PBNP, showed a high level of precision when tested on actual human serum samples. This suggests that they have the potential for replacement of traditional HRP-based immunoassay systems with dual-mode assay systems that are rapid, strong, dependable, and convenient. These new systems can be widely used to identify important target molecules, such as cancer biomarkers.

Further, Cheng et al. offered a dual-mode sensing system for glucose monitoring, which combines colorimetric and electrochemical methods [245]. This method leverages CoOOH@Cu nanosheets as peroxidase-mimics, utilizing OPD as the signaling molecule. The CoOOH@Cu nanosheets were synthesized by introducing Cu^{2+} ions to Co^{2+} ions under alkaline conditions to produce the hydroxide. The CoOOH@Cu nanosheets were synthesized by further oxidation using NaClO. GOx may oxidize glucose, resulting in the conversion of glucose into gluconic acid and H_2O_2. Afterwards, H_2O_2 can oxidize the substrate OPD with the help of CoOOH@Cu nanosheets as a catalyst to produce a brown-yellow oxidized product called OPD-oxidized. The OPD-oxidized product generates both colorimetric (Fig. 7G) and electrochemical signals (Fig. 7H), which may be used to monitor the glucose level. This sensing technique enhances the precision and sensitivity of glucose detection by using the CoOOH@Cu nanosheets strong peroxidase-like activity and the integrated dual-mode output.

The implementation of nanozymes offers significant potential for many applications of electrochemical sensors in biomedicine and medical diagnostics, as well as in the environmental and the food sector. Furthermore, the integration of nanozymes catalytic activity and electrochemical approach enhances the potential for the intelligent utilization of sensors. It has been asserted that with persistent endeavours, nanozymes-based electrochemical sensors will be effectively integrated with smartphones to achieve intelligence and will be extensively utilized in everyday life in the future. In the early phases of development, the transition of nanozyme-based electrochemical biosensor technologies into market-ready products seems to necessitate collaborative efforts that bridge technical and non-technical fields, involving researchers, industry stakeholders, and government entities. These investigations may become especially rigorous in the future for effectively addressing cancer and other illnesses.

4.5. Colorimetric and luminescence/chemiluminescence/electroluminescent dual-mode sensing

Luminescence-based detection is an effective technique due to the variety of modes available for use. Detection can be accomplished by observing a change in luminescence intensity (either turn-off or turn-on), the emission wavelength, or even the excited state lifetime, when a specific chemical is present. The most prevalent techniques for detecting analytes involve luminescence quenching (turn-off) or enhancement (turn-on). The alterations in luminescence may arise from both direct and indirect interactions between the sensing material and the target molecule. Mechanisms involved include photo-induced hole transfer, energy transfer, and/or a chemical reaction [247]. Therefore, in recent times, colorimetric and luminescence technologies have garnered significant interest owing to their appealing benefits, effortless operation, economical nature, and rapid responsiveness [248]. Still, the primary disadvantage of colorimetry is its limited sensitivity. On the contrary, luminescence spectrophotometry is an efficient and sensitive technology, and it has been extensively employed for the detection of analytes [249–251]. Hence, analytes may be detected with high sensitivity using luminescence spectrophotometry, and colorimetric analysis can be used for quick and efficient analytes detection. Using only one detecting method results in a single output signal. The sensitivity and accuracy of a single-mode sensor are inferior to those of multi-mode sensors, as they are unavoidably affected by external influencing factors as discussed earlier. A desirable goal is to create a quick, reliable, and sensitive sensor for the assay of analytes by inventing a dual-mode sensing technique that incorporates both colorimetric and luminescence assays. This approach allows for the accessibility of the benefits offered by both methods, resulting in dual signal readings [252,253].

In this context, Xing et al. proposed the development of covalent organic framework (COF) grafted with lanthanides for dual-mode colorimetric and luminescence detection of tetracycline as shown in Fig. 8A [254]. The selection of Ce^{3+} and Eu^{3+} ions for functionalizing COFs was based on their specific catalytic and luminous properties, which make them suitable for bimodal sensing. COF-Ce-Eu can function as an enzyme-mimic, catalysing the oxidation of TMB in the presence of H_2O_2, and inclusion of tetracycline enhances the catalytic activity of COF-Ce-Eu by forming a complex with tetracycline. As illustrated in Fig. 8B, the catalytic activity and absorbance of COF-Ce-Eu exhibit a

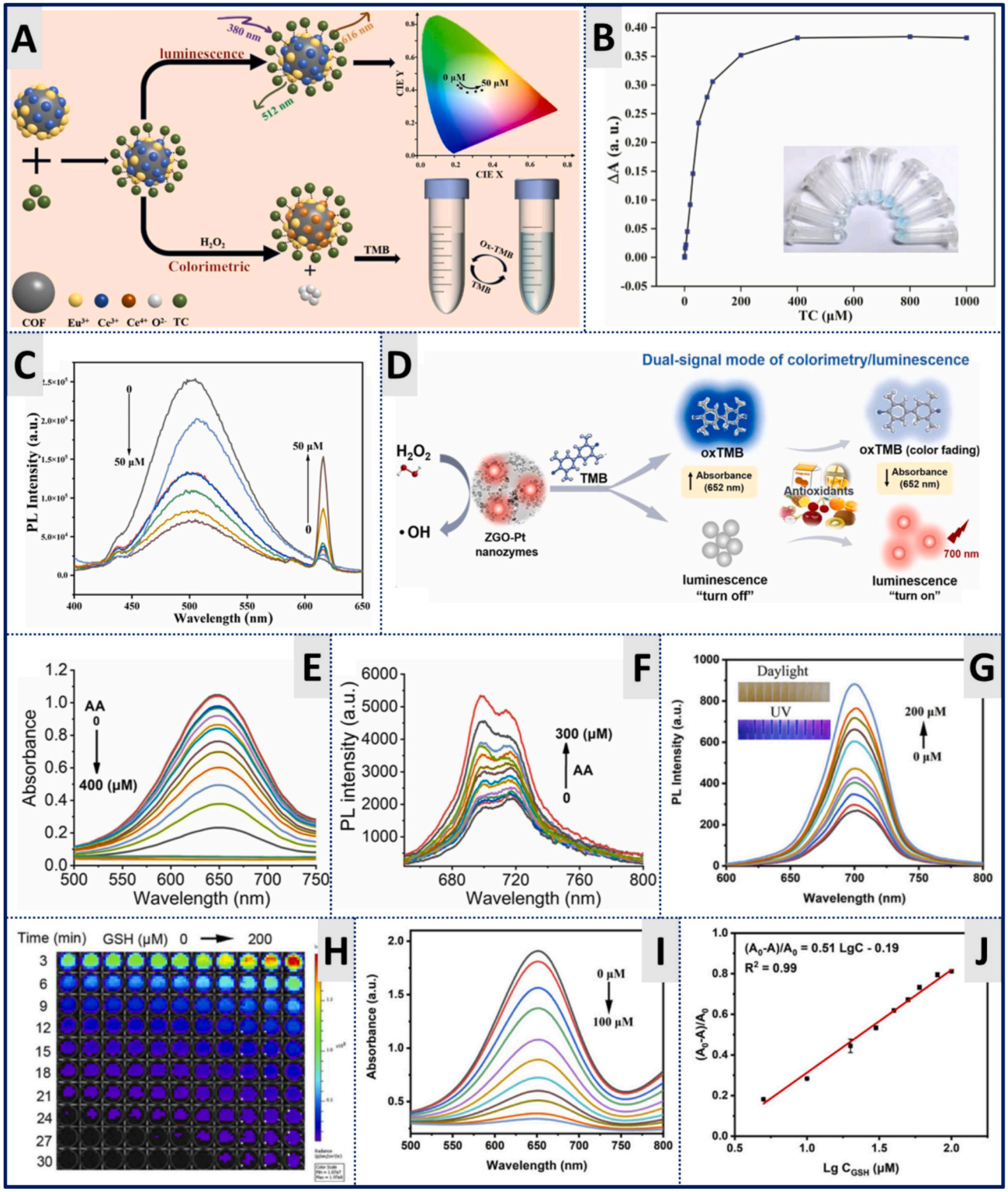

Fig. 8. Panel A: Schematic depiction of lanthanide-grafted covalent organic framework (COF) based colorimetric and luminescence dual-mode sensor for tetracycline detection; **Panel B:** Change in colorimetric, and **Panel C:** Luminescence response in presence of different tetracycline concentrations. Reprinted with permission for *Sensors and Actuators B: Chemical, Elsevier* [254] Copyright 2024**. Panel D:** Illustration of luminescence-colorimetric dual-mode sensing of total antioxidant capacity (TAC); **Panel E:** Colorimetric detection *via* change in UV–Visible absorbance, and **Panel F:** Change of photoluminiscence signal at different AA concentrations. Reprinted with permission for *Sensors and Actuators B: Chemical, Elsevier* [255] Copyright 2024**. Panel G:** PL spectra of ZCGO@MnO_2 with different concentrations of GSH; **Panel H:** PL decay images of ZCGO@MnO_2 with varying concentrations of GSH, both in the absence and presence; **Panel I:** UV–visible spectra for peroxidase activity of ZCGO@MnO_2 reaction system with varying concentration of GSH, and **Panel J:** Linear fitting curves showing change in absorbance at 652 nm *versus* GSH concentration. Reprinted with permission for *Sensors and Actuators B: Chemical, Elsevier* [256] Copyright 2024**.**

direct correlation with the concentration of tetracycline. The ratiometric luminescence response was determined by comparing the intensity ratio of the wide band centred at 512 nm emitted by the COF matrix with the sharp peak at 616 nm emitted by Eu^{3+} (Fig. 8C). The variation in brightness at the wavelength of 512 nm and the rise at 616 nm were contingent upon the concentration of tetracycline. This platform, which combines colorimetric and luminescence-modes, has exceptional selectivity and sensitivity towards tetracycline. Report showed LoD of 24 nM and 3.4 nM, for colorimetric and luminescence approaches, respectively, with broad linear detection range of 0–50 μM. The implemented bimodal sensing technique offers a reliable and effective means of accurately detecting and tracking tetracycline in food and water samples.

Further, in biological and dietary samples, total antioxidant capacity (TAC) is an essential metric for determining the collective antioxidant efficacy. Therefore, precise assessment of TAC has become more crucial for health surveillance and nutritional counselling [257]. As depicted in Fig. 8D, luminescence-colorimetric dual-mode sensor, using a persistent luminous nanozyme called ZGO-Pt has been employed for the specific detection of TAC [255]. The ZGO-Pt material was produced by incorporating platinum nanoflowers as a synthetic addition into $ZnGa_2O_4$:Cr nanoparticles (ZGO). The synthesized ZGO-Pt presented captivating peroxidase-mimetic activity and long-lasting luminescence. It efficiently facilitated the catalysis of the oxidation of colorless TMB into blue oxidized-TMB. At the same time, the generated oxidized-TMB showed a significant absorption at 652 nm, successfully diminishing the luminescence of ZGO-Pt at 700 nm through the inner filter effect. Antioxidants can either compete with oxidizable TMB or convert oxidized-TMB back to TMB. This leads to simultaneous changes in both the blue color and luminescence, which may be used as the foundation for a dual-mode test for TAC (Fig. 8E and F). The ZGO-Pt catalyst demonstrates high efficiency in catalysing reactions, with Km values of 3.12 mM for H_2O_2 and 0.592 mM for TMB. This enables the dual-mode sensor to accurately measure TAC within a wide linear range of 0.5–200 μM in colorimetric mode, whereas 1–300 μM in luminescence mode. Additionally, the sensor has a low detection limit of 0.05 μM and 0.78 μM in colorimetric and luminescence modes, respectively. The dual-mode sensor has been effectively employed for the determination of TAC in fruits, vitamin tablets, and beverages. This study presents a very effective persistent luminous nanoparticle-based nanozyme for a simple TAC test, with potential applications in biosensing and food technology.

Likewise, GSH is a crucial chemical for maintaining the balance of oxidation and reduction in living organisms. Precise monitoring of its fluctuations is beneficial for the early detection and treatment of associated disorders. A novel sensing platform called ZCGO@MnO_2, which has a unique nanoflower structure, has been presented in recent past [256], which exhibits both luminescent resonance energy transfer (LRET) property and oxidase-like activity to detect GSH using two different modes. The sensor comprised of persistent luminescence nanoparticles (PLNPs) that emitted near-infrared light, and MnO_2 had the capacity to quench luminescence and operate as an oxidase. By introducing GSH, luminescence property of nanozymes has been restored with suppression of oxidase-like activity with the reduction of MnO_2 to Mn^{2+}. Thus, the sensor effectively generated dual-mode signal outputs, incorporating both persistent luminescence and colorimetric detection. The use of PLNPs enabled the elimination of background interference from complex biological samples, significantly improving the signal-to-noise ratio. This dual-mode sensing approach further enhanced detection precision, ensuring superior analytical performance. In addition, the sensor can detect alterations in intracellular GSH levels using bioimaging techniques. Fig. 8G elucidates that under the ideal assay circumstances, the system's PL intensity increased gradually as the GSH concentration rose. Indirect evidence that MnO_2 reacted with GSH and caused the manganese layer to degrade was provided by the solution's progressive shift in color from brown to white when exposed to sunshine. As illustrated in Fig. 8H, the intensity of photoluminescence rises, and the duration of afterglow decay extends as the concentration of GSH increases. This suggested the possibility of using the sensing platform for GSH visualization. Additionally, the correlation between [TMB + ZCGO@MnO_2] absorbance and GSH concentration was examined. The absorbance at 652 nm gradually decreased as GSH increased, as shown in Fig. 8I. According to the linear function of $(A_0\text{-}A)/A_0 = 0.51$ LgC GSH - 0.19 ($R^2 = 0.99$), where A = absorbance of the detection system with GSH, and A_0 = absorbance of the detection system without GSH, the absorbance change was linearly correlated with GSH concentration (Fig. 8J). This study introduces novel ideas for creating sensors within complex samples and broadens the application of PLNPs in the field of biosensing.

In another study, biosensing platform had been developed for nucleic acid sensing based on CRISPR-Cas12a-mediated dual-mode up-conversion luminescence and colorimetric-based nanozymes [258]. The system comprised of UCNP@SiO_2/CeO_2 (UNSC) conjugated to single-stranded DNA (ssDNA) probes and exhibited peroxidase activity and acted as luminescence donors. In absence of targeted nucleic acid, luminescence gets quenched due to attachment of ssDNA-UNSC to graphene oxide *via* pi-pi force and no color change has been observed. Whereas, in presence of targeted nucleic acid, Cas12a activation occurs, followed by cleavage of ssDNA probes on UNSCs, which leads to its detachment from graphene oxide surface due to weak binding force. This will lead to restoration of up-conversion luminescence activity and color production in the presence of TMB due to free nanozymes. This biosensing platform demonstrates a limit of detection ~320 fM in the up-conversion luminescence mode and about 28.4 pM in the colorimetric mode for nucleic acid detection, respectively. This dual-mode biosensing system, utilizing UNSC nanozyme and CRISPR-Cas12a, showcases impressive selectivity, excellent repeatability, and straightforward operation, enabling seamless adaptation to other nucleic acid detection methods simply by redesigning the CRISPR RNA sequence.

Chemiluminescent sensing is another important approach to monitor the presence of trace elements. It primarily depends on the redox reaction involving the H_2O_2–luminol system, which produces chemiluminescent signals. Subsequently, the intensity of the luminescence is transformed into a digital signal *via* a converter [259]. Nanozymes exhibiting peroxidase-mimetic activity catalyzes H_2O_2-luminol system to enhance the chemiluminescent signal intensity as well as detection sensitivity to develop colorimetric-chemiluminescent dual-mode sensor [133]. Jing et al. developed colorimetric/chemiluminescence (CL) dual-mode biosensor for aptamer-based detection of Parathion-methyl (PM) pesticide [95] The aptamer specific to PM was affixed to the surface of trimesic acid-Cu (TA-Cu) nanozyme, which can modulate the catalytic capability of nanozyme regarding substrates and also function as a specific recognition unit for PM. In the presence of pesticide, the aptamers attach to PM and release from the surface of the TA-Cu nanozyme, impacting the catalytic capability of the nanozyme with respect to substrates. Result demonstrated that a dual-mode aptasensor method utilizing colorimetric and chemiluminescent techniques for PM detection, featuring linear ranges of 0.01–20 and 1–100 ng/mL, along with detection limits of 0.004 and 0.45 ng/mL, respectively. Significantly, in contrast to many single-mode analysis techniques, this dual-mode sensing system is capable of performing self-inspection by evaluating the detection outcomes of each mode, thereby enhancing the reliability of the detection results. Same dual mode approach has been utilized for detection of glyphosate pesticide using peroxidase-mimetic Fe_3O_4@Cu nanozyme [89]. The synthesized nanozyme initiated the oxidation of luminol/TMB to excited-state 3-aminophthalic acid/blue oxidized TMB due to enhanced peroxidase-like activity, while producing a chemiluminescent signal/visible colorimetric signal. However, the presence of glyphosate hindered this activity, leading to a reduction in signal strength. This inhibitory effect might be attributed through two pathways: one where glyphosate binds with Fe(III)/Cu(II) and occupies the catalytic active sites of Fe_3O_4@Cu, leading to a decrease in the production of •OH, and another where glyphosate competes with TMB

to utilize the generated •OH, thereby diminishing the oxidation of TMB. This mechanism served as the dual-mode colorimetric/CL glyphosate nanosensor, which reached LODs of 0.086 μg/mL and 0.019 μg/mL, thereby showcasing its considerable promise for on-site glyphosate monitoring. Further, Guo et al. demonstrated the development of covalent organic framework (COF)@AuNPs@PDA nanozymes for dual dual-mode colorimetric and chemiluminescent biosensor for detection of *S. aureus* bacteria [260]. Synthesized nanozyme exhibited the nitroreductase and peroxidase-mimetic activity. Result showed that nanozyme can bind to bacteria *via* strong electrostatic interaction, which leads to generation of enhanced chemiluminescent and colorimetric signal. Intensity of generated signals reported to be inversely proportional to the bacterial concentration. Dual-signal method shows a linear response in the concentration range of 10 to 10^7 CFU/mL for *S. aureus*, with a low limit of detection of 7.9 CFU/mL and 8.5 CFU/mL using chemiluminescence and colorimetric approach, respectively. The authors have shown that our proposed method is both feasible and reliable through the analysis of milk and chicken samples. Liu et al. demonstrated inert-remodeling approach for the development of bimetal-confined nitrogen-doped carbon nanozyme for colorimetric/chemiluminescent dual-mode glucose biosensor [261]. A cascade enzyme system of CoNi–CN@GOx was prepared by integrating with GOx, leading to the development of a colorimetric-chemiluminescent imaging sensor for glucose detection based on the CoNi–CN@GOx cascade system. The process involved the catalysis of glucose to produce H_2O_2 *in situ*, which could then be decomposed into •OH by the CoNi–CN nanozyme. This reaction facilitated the oxidation of luminol and TMB, resulting in the generation of visual chemiluminescent and colorimetric imaging signals, respectively. Glucose levels were measured across extensive linear ranges of 0.08–15 mM and 0.1–30 mM using colorimetric and chemiluminescent imaging techniques, respectively. This study presents a promising inert-remodeling approach to develop high-performance nanozymes for dual-mode biosensing applications.

Currently, graphitic phase carbon nitride has attracted considerable interest in the realm of electrochemiluminescence (ECL) sensing because of its chemical stability, non-toxicity, outstanding biocompatibility, and affordability [262]. Tang et al. demonstrated the copper ion/graphitic carbon nitride nanosheets (Cu^{2+}-g-C_3N_4) colorimetric/ECL dual mode biosensor for efficient and sensitive detection of β-amyloid peptide (Aβ) [263]. Here, Cu^{2+}-g-C_3N_4 nanosheets served dual purposes, functioning both as an ECL luminophore and demonstrating remarkable activity akin to a peroxide-like enzyme. Signal-on ECL biosensor was initially developed by utilizing Cu^{2+}-g-C_3N_4 as the ECL signal probe and the aptamer as the capture probe for the target Aβ, leveraging the interaction between Cu^{2+} and Aβ. Additionally, a colorimetric system utilizing peptide segment-functionalized magnetic beads was developed, incorporating Cu^{2+}-g-C_3N_4 as the nanozyme and the peptide segment as the capture motif for Aβ. The suggested approach facilitated the precise identification of Aβ, demonstrating extensive linear ranges of 1.0×10^{-13} M to 1.0×10^{-7} M and 1.0×10^{-12} M to 1.0×10^{-7} M for ECL mode and colorimetric mode, respectively. This work offers significant promise for the timely and precise identification of Alzheimer's disease.

This section outlines the latest advancements in colorimetric and luminescent dual-mode detection utilizing nanozymes. In the nanozyme domain, most activity assays and biosensors utilized chromogenic substrates like TMB and ABTS, known for their cost-effectiveness and ease of detection. Furthermore, the identification of luminescence exhibits a reduced background in contrast to the identification of absorbance. Consequently, luminescent products that can be produced at neutral pH are advantageous for specific applications. A variety of nanozymes have demonstrated the ability to oxidize substrates for use in analytical applications. Nonetheless, most investigations were conducted as proof-of-concept, necessitating significant advancements before practical and effective assays can be established.

4.6. Colorimetric and photoelectrochemical dual-mode sensing

Photoelectrochemical (PEC) sensors have been widely utilized in the sensing of various analytes like biomarkers, heavy metals, antibiotics, organic pollutants, and proteins [264,265]. In general, PEC sensing can be achieved using a photoirradiation in combination with typical three-electrode cell. However, compared to electrochemical sensing, its independent light source and electrochemical detection system offer a reduced background, and a more sensitive signal detection. Most PEC sensors operate in a 'photocurrent' mode, where the transfer of photogenerated electrons between the photoelectrode and analyte is used. Alternatively, electrochemical detection can be combined with photoirradiation using a 'self-powered sensing' mode called photoelectrochemical fuel cell (PFC). In contrast to the conventional three-electrode PEC sensing system, the self-powered sensing system operates efficiently with just two electrodes. Furthermore, it does not require external power sources or intricate equipment, making it a practical solution for creating compact, implantable, or portable devices [266].

A CdS–In_2S_3 heterojunction has been created to boost the PEC performance. This heterojunction was utilized to develop dual-mode biosensors activated by visible light, enabling highly sensitive and selective detection of bleomycin (BLM) [267]. The CdS–In_2S_3 composite demonstrated an increased photocurrent response, when exposed to visible light due to its better absorption in the visible region and decreased recombination of electron-hole pairs in the heterojunction. The sensor exhibited a decline in photocurrent intensity upon interaction with BLM, demonstrating a proportional relationship with its concentration in the range of 5.0–250 nM. Furthermore, the CdS–In_2S_3 photoanode was integrated into a PFC, where it facilitated water oxidation under visible light, while oxygen reduction occurred at Pt cathode, enhancing its functional applicability. This chemical reaction results in the production of electricity. The immobilization of the BLM-binding aptamer on the CdS–In_2S_3 photoanode resulted in an output power of the PFC that decreased as the logarithm of BLM concentration increased from 10 to 250 nM. This created a self-powered sensing platform for BLM detection that could be activated by visible light. Both suggested sensors exhibited exceptional selectivity, commendable repeatability, and remarkable stability. They were effectively utilized for the quantification of BLM in human serum samples.

Further, colorimetric-assisted photoelectrochemical-based sensor has been developed for salicylic acid (SA) detection based on presence of two pairs of cis-diol groups as shown in Fig. 9A [268]. Sandwich-like structure had been prepared by incorporating gold-modified Bi_2S_3 (Au@Bi_2S_3) and metal organic framework (Au@PCN-224) to the electrode. In the presence of TMB substrate, dual sensing approach for colorimetric visualization and photocurrent has been achieved due to nanozyme property and inert electroconductivity of developed sensor. Besides, Ce^{3+} has been incorporated to enhance the colorimetric signal *via* increasing the catalysis activity by energy transformation from PCN-224 surface to the whole system. Fig. 9B illustrates that as the concentration of SA increases; there is a gradual decrease in photocurrent. In addition, the absorption intensity in the UV–visible spectrum at 652 nm has been shown in Fig. 9C. As exemplified in Fig. 9C, the UV–visible intensity progressively increased with the rising concentration of SA (from a to o). Thus, due to the presence of unique SA recognition site and Ce^{3+} as mediator, dual-mode sensing of visualization and photocurrent exhibited high sensitivity. The current approach demonstrated significantly high accuracy, selectivity, and sensitivity for SA detection, achieving a detection limit of 1.44 μM and a 5–1000 μM linear detection range. This method provides an encouraging new framework for identifying SA and suggests a possible tactic for creating advanced biosensors with dual-model readout capabilities. In another study, Wei et al. designed immunosensor for photoelectrochemical/colorimetric dual-mode sensing of ochratoxin A (OTA), ochratoxin B (OTB), and ochratoxin C (OTC) at broad spectrum (Fig. 9D) [269]. Here, bi-functional copper oxide nanoflowers (CuO NFs) attached to corresponding

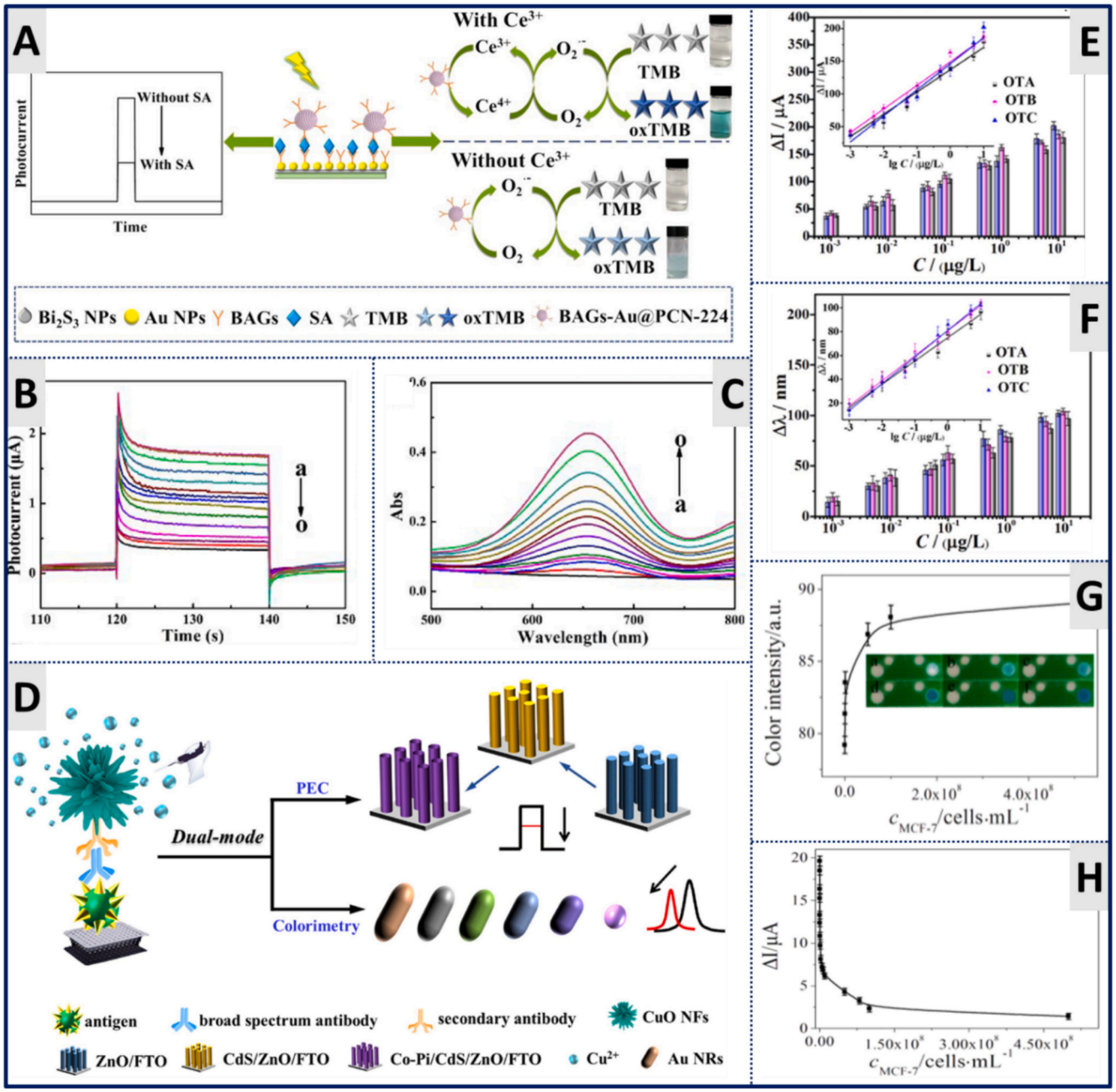

Fig. 9. Panel A: Schematic representation of fabrication process, and dual-mode colorimetric and photoelectrochemical readout of salicylic acid (SA); **Panel B:** Photocurrent response of sensor in presence of different SA concentrations, and **Panel C:** Colorimetric sensing by UV–visible spectrum response at different SA concentrations. Reprinted with permission from *Chinese Chemical Letters, Elsevier* [268] Copyright 2023. **Panel D:** Illustration of dual mode ochratoxin detection; **Panel E:** Variation in PEC current, and **Panel F:** Colorimetric response at various ochratoxin concentrations. Reprinted with permission from *Sensors and Actuators B: Chemical, Elsevier* [269] Copyright 2021. **Panel G:** Colorimetric (Inset: colorimetric response images of MCF-7 cells), and **Panel H:** Photoelectrochemical current response at different MCF-7 cell concentrations. Reprinted with permission from *Analytical Chemistry, American Chemical Society* [270] Copyright 2016.

antibody serves as dual-signal probe for colorimetric and photoelectrochemical detection of ochratoxin. For photoelectrochemical detection, Cd^{2+} in photoactive materials replaced by Cu^{2+} released from CuO nanoflower to form new band gap, which in turn enhances the recombination of electron-hole to vary the respective current. In colorimetric detection, Au nanorods etched by Cu^{2+} induce LSPR shift and multiple color change. As shown in Fig. 9E, there is a positive correlation between PEC current ($\Delta I = I\text{-}I_0$) and ochratoxin concentration, here I represent the PEC current in presence of ochratoxin, whereas I_0 represents in absence of ochratoxin. Additionally, Fig. 9F illustrates that the shift in LSPR position ($\Delta\lambda$) for OTA, OTB, and OTC at identical concentrations is comparable, indicating the feasibility of simultaneous detection of the three ochratoxins. The inset illuminates a strong linear correlation between $\Delta\lambda$ and the logarithm of ochratoxin concentration, spanning the range of 1 ng/L to 10 μg/L. As the concentration of ochratoxins decreases, a greater quantity of CuO NFs-Ab2 can be effectively immobilized in the well. This process resulted in an increased production of Cu^{2+} ions, causing a blue shift in the LSPR peak of Au nanorods. Consequently, the solution underwent a gradual color transition, shifting from brownish-red to grey, then progressing through green, blue, and purple, before ultimately turning to pink. Subsequently, two unique approaches from different detection systems were utilized to precisely and dependably indicate the levels of ochratoxins. This study accomplished the comprehensive identification of OTA, OTB, and OTC,

while presenting an innovative approach for creating a precise, visual, and multi-signal immunosensing platform.

In addition to above, development of photoelectrochemical/colorimetric dual-mode sensor for cyto-analysis of H_2O_2 released from tumor cells using microfluidic paper-based analytical device (μ-PAD) has also been demonstrated [270]. This approach relies on the cleaving of DNA by hydroxyl radicals (•OH). The designed sensor incorporates a layer-by-layer approach featuring concanavalin A, flower-like Au@Pd alloy nanoparticles labelled with graphene quantum dots (GQDs), and tumor cells, all assembled on the surface of vertically aligned bamboo-like ZnO. The structure is supported by a pyknotic platinum nanoparticles modified paper working electrode (ZnO/Pt-PWE). The increased photocurrent response, relative to the bare ZnO/Pt-PWE, was ascribed to the efficient energy level alignment between GQDs and ZnO. Released H_2O_2 induces the DNA strand fragmentation due to generation of •OH through the combined catalytic action of GQDs and Au@Pd alloy nanoparticles. This approach shows decreased photocurrent, and enhanced sensitivity towards H_2O_2 detection in aqueous solutions as represented in Fig. 9H, with a detection limit of 0.05 nM. The released probe facilitates a catalytic chromogenic reaction of substrates, allowing real-time visualization of H_2O_2-related biological processes. Fig. 9G depicts the progressive color change in the chromogenic zone, shifting from colorless to blue and eventually deepening with increasing cancer cell concentrations. Additionally, the cyto-sensor exhibits a linear relationship between grey intensity and the logarithm of cancer cell concentration. This research introduces a novel, cost-efficient, and user-friendly μ-PAD for precise and visual detection of cellular H_2O_2, emphasizing its promising applications in cellular biology and disease pathology.

In short, reports have demonstrated that in comparison to single metal, bimetallic nanomaterials exhibit enhanced chemical and optical properties due to the synergistic effect of two atoms [82]. Consequently, noble metal nanomaterials with unique properties are well-suited for producing colorimetric signals and enhancing PEC signals in dual-mode detection. Nanozyme-based colorimetric and PEC sensors offer the advantages of visual detection alongside highly sensitive electrochemical analysis for biomarker and environmental sensing. Nanozyme-driven colorimetric detection relies on catalytic reactions that produce a color change; PEC sensors employ nanozymes to enhance photocurrent generation when exposed to light, achieving exceptional sensitivity and minimal background detection. The dual-mode approach improves precision, responsiveness, and dependability, rendering it suitable for on-site diagnostics, pathogen identification, and environmental assessment.

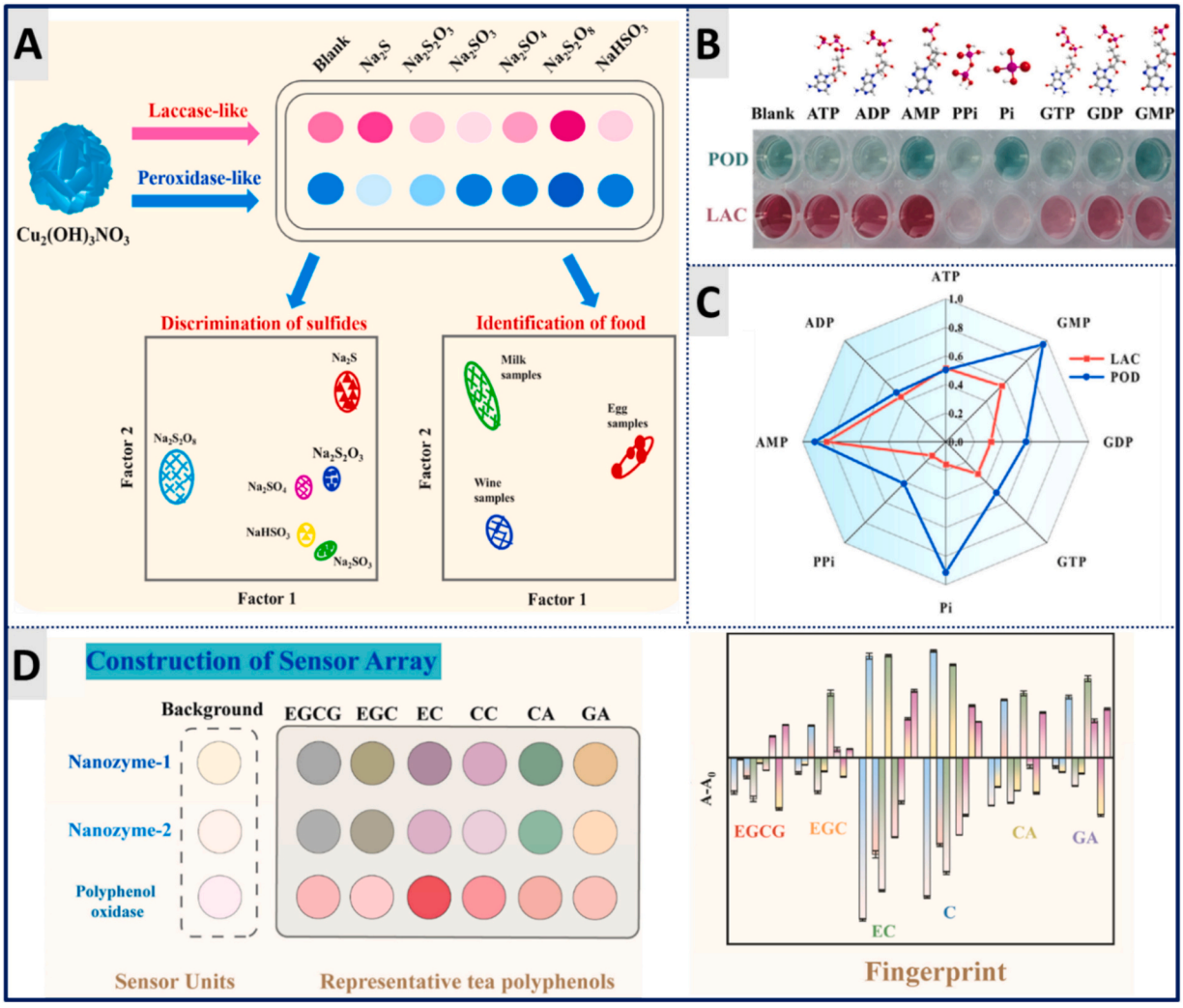

Fig. 10. Panel A: Schematic representation of nanozyme sensor array with dual enzyme-mimetic activity in sensing of different sulfides in various food samples. Reprinted with permission from *Biosensors and Bioelectronics*, Elsevier [273] Copyright © 2024. **Panel B:** Colorimetric response of the $Cu_2Cl(OH)_3$ nanozyme in presence of different phosphates. **Panel C:** Radar Map showing the discrimination of 8 phosphates at 100 μM concentration. Reprinted with permission from *Talanta*, Elsevier [277] Copyright ©2024. **Panel D:** Schematic illustration of nanozyme/enzyme hybrid sensor array with polyphenol oxidase activity for tea polyphenol identification and differentiation of six tea series. Reprinted with permission from *Talanta*, Elsevier [278] Copyright © 2024.

5. Nanozyme-sensor array (artificial nose)

As discussed above, nanozymes with peroxidase-mimetic activity have been employed in construction of various biosensors by conjugation with correspond specific recognition ligands. However, such strategies suffer a major drawback that it cannot be employed in multiplex detection (multiple analytes), and thus lack universality [271]. In order to address this limitation, nanozyme-based sensor arrays have been reported, and they are exhibiting advantageous properties of rapid multiplex detection with high sensitivity and specificity [272]. Sensor array also known as 'artificial nose', is capable of responding to detected objects *via* various signal channels, creating distinct discrimination rules that classify and differentiate samples of unknown species. Recently, 'nanozyme-based sensor array' are considered as "hot spot" in sensing of proteins, microbes, cancer cells, and other analytes.

In the context of above, Jing et al. developed the novel bi-functional copper hydroxide nitrate [$Cu_2(OH)_3NO_3$] nanozyme-based two-channel sensor array exhibiting dual peroxidase- and laccase-like enzymatic properties. As shown in Fig. 10A, the developed array has been utilized in successful identification of six different kinds of sulphides, including Na_2S, $Na_2S_2O_3$, Na_2SO_3, Na_2SO_4, $NaHSO_3$, and $Na_2S_2O_8$ [273]. Herein, except $Na_2S_2O_8$, addition of all other sulfides leads to reduced absorbance of TMB at 652 nm. However, due to its strong oxidizing ability, $Na_2S_2O_8$ further oxidized TMB to show increased absorbance. Further, for sensing based on laccase-like enzyme activity, 2,4-dichlorophenoxyacetic acid (2,4-DP) has been used as a substrate, where except $Na_2S_2O_8$ and Na_2S, addition of all other sulfides leads to reduced absorbance of 2,4-DP. However, similar to peroxidase behavior, here also addition of $Na_2S_2O_8$ shows increased oxidation of 2,4-DP, and leads to increased absorbance. Further, Na_2S known to reduce the Cu^{2+} to $Cu^{+,}$ thus enhancing the laccase-like activity, which corresponds to enhanced absorbance [274]. Additionally, Cu—S bonds also enhance catalytic performance of laccase-like activity by increasing the electron transfer rate [275]. Moreover, the sensor array has successfully recognized and distinguished three actual samples (wine, egg, and milk). This study has been crucial for improving the development of array units and refining the detection of sulfides in complex food samples. Likewise, multi-signal nanozyme-based array by utilizes the peroxidase- and laccase-like activity of Cu-1,3,5-benzenetricarboxylic acid (Cu-BTC) nanozymes for the detection of antioxidant phenolic compounds (APs) has been developed [276]. Due to the laccase-like activity, nanozyme can efficiently catalyze various APs to colored quinone imines products. Peroxidase-like activity of nanozymes leads to oxidation of TMB with excellent photothermal effect which is inhibited due to the strong reducing ability of APs. Thus, colorimetric/photothermal dual-mode sensor array has been developed with integrated ANN algorithm for precise and rapid identification of APs in coffee, black tea and wine. Further, Shi et al. prepared bi-functional di-copper chloride trihydroxide ($Cu_2Cl(OH)_3$) nanozyme-based sensing array system with dual-enzyme-mimetic activity for detection of various phosphates [277]. In order to evaluate the sensing performance, eight different phosphates including ATP, ADP, AMP, GTP, GDP, GMP, PPi and Pi have been tested. It has been reported that phosphates can form metal complex with Cu^{2+} due to its strong interaction activity, which leads to decreased catalytic response of $Cu_2Cl(OH)_3$ by destroying its structure. Additionally, the interaction also alters the charge state, thus significantly altering the enzymatic activity as shown in Fig. 10B and C. Their classification is based on the different phosphates' differing levels of inhibitory effects on $Cu_2Cl(OH)_3$ nanozyme catalytic activity. The results presented in the research provide a possible way to distinguish between different phosphates by evaluating $Cu_2Cl(OH)_3$ dual-enzyme mimicking capabilities.

The sensor array, comprised of zwitterionic dopamine nanoparticle-coated magnetic bimetallic nanoparticles (Fe_3O_4@ZNP@UiO-66) nanozyme for detection and discrimination of phosphoproteins [ovalbumin (OVA), pepsin (Pep), casein phosphopeptides (CPP)] is also developed in recent past [279]. The fabricated nanozymes exhibited enhanced peroxidase-mimic activity, which can readily transfer electrons Zr centre to Fe(II)/Fe(III). Phosphoproteins exert an inhibitory effect over the catalytic activity due to strong interaction between Zr centre and phosphate groups, which can mask the dual active site of nanozymes. Inhibitory effect also might be attributed to ZNP antifouling ability, and due to difference in binding affinity of different proteins towards nanozymes, it leads to generation of different absorbance response at 420 nm in nanozyme-ABTS system. For example, CPP and OVA have comparable isoelectric points; however, because CPP is more phosphorylated than OVA, it inhibits the catalytic activity of the nanozyme strongly. In order to distinguish phosphoproteins from other proteins, linear discriminant analysis (LDA) is used to build a sensor array based on reaction kinetics by merely extracting distinct absorbance intensities at different time periods. Additionally, protein mixture identification and quantitative phosphoprotein determination have been accomplished. Furthermore, the suggested sensor array has tremendous promise in disease diagnosis as it may be used to differentiate cancer cells from normal cells based on the differential amount of phosphoproteins in cells.

In other study, nanozyme-based sensor array had been developed for sensing of tea polyphenols (TPs) using enzyme/ polyphenol oxidase nanozyme-based activity [278]. Here, 4-AAP serves as substrate which can produce different color for accurate detection of TPs at different concentration, ratio, and species **(**Fig. 10D**)**. A dual-output model based on machine learning was additionally employed to accurately predict the concentrations and classes of unknown samples. As a result, it is possible to rapidly and continuously detect TPs both qualitatively and quantitatively. Additionally, Chinese teas were identified using a sensor array that combined a dual-output model based on machine learning. The technique can accurately detect the more specialized tea kinds after differentiating the six tea series in China. An effective and simple method for identifying teas and tea products is offered by this study. Further, fluorescence capillary sensor array based on bimetallic nanozymes with excellent peroxidase-mimetic activity and cross-recognition for rapid discrimination and identification of five glucocorticoids (GCs), namely, hydrocortisone, prednisone, dexamethasone, betamethasone, and cortisone acetate, had been proposed [280]. The MRFCAS was developed by transferring imprinted materials in a single capillary tube, using 18.0 μL of sample each time, to generate distinct response signals and color changes towards five glucocorticoids. The outcomes revealed that in presence of dexamethasone, fluorescence at 455 nm increases with decreased intensity at 571 nm, proving that dexamethasone can enter the imprinted hole to inhibit substrate oxidation. In order to detect five GCs in real time within seven minutes, a smartphone, with the help of MATLAB software, captured the variations in color of MRFCAS that were transformed into digital information. Developed sensor exhibited extremely low detection in nanomolar range with detection accuracy more than 90 % to offer a different approach to multi-target microvolume detection in challenging contexts.

In more advanced study, Dashtian et al. demonstrated the molecularly imprinted (MI) nanozyme sensor array based on $Ce[Fe(CN)_6]$ Prussian blue analogues (PBA) for septicemia detection [281], wherein the developed sensor targets isoleucine, valine, and leucine as a potential indicator of septicemia. The bimetallic nanozyme component, comprising $Fe - CeO_2$, demonstrates strong peroxidase activity, triggering a Fenton-like reaction when activated by the presence of Ce^{4+}/Ce^{3+} and Fe^{3+}/Fe^{2+} cycles. This feature renders it highly appropriate for the activation of persulfate and the following oxidation of TMB, effectively functioning as a colorimetric probe. Furthermore, when valine, leucine, and isoleucine are present, the $MITiO_2$ layer of the nanozyme array exhibits selective binding, resulting in a partial obstruction of cavities and consequently hindering the catalytic reaction of TMB oxidation. The application of $Ce[Fe(CN)_6]$-derived $MITiO_2$ nanozyme arrays presents significant promise in the realm of septicemia detection. This method provides a precise and nuanced way for timely identification and action, ultimately enhancing patient results.

Thus, recent research presented above elucidates how sensor arrays are evolving towards more expansive possibilities. However, because of some intrinsic limitations of the arrays, the actual applications of sensor arrays have not yet been considerably developed. For instance, sensor array detection's sensitivity still needs to be raised. Further, there are restrictions on the range of analytes that sensor arrays can identify, and selective analyte detection is currently not possible. Additionally, the detection device's portability could be enhanced.

6. Synergistic and smart acting nanozymes with cascade action

An enzymatic cascade denotes the combination of multiple enzymatic reactions in one step but not isolating the intermediates. Enzyme cascades are the major class of chemical transformations that assemble metabolic networks and signaling pathways to ensure the survival and growth of life [282–284]. The transformation of biological substrates into desired products is facilitated through a multi-enzyme cascade pathway system. Typically, *in vitro* cascade reactions are carried out by reconstructing natural metabolic pathways extracellularly or assembling diverse artificial enzymes, often incorporating cellular extracts and purified enzymes. However, employing multi-enzyme cascade strategies to achieve controlled co-localization of multiple enzymes on nanoparticles, forming nanoclusters, can significantly enhance reaction rates and overall catalytic efficiency. Nanoparticles displaying natural enzyme-like properties have a bifunctional analog enzyme exhibiting distinctive properties of nanomaterials and the function of biocatalysis as reported in Fe_3O_4, graphene, and Au nanoparticles [285]. The catalytic activity of the nanozymes can be improved by fine-tuning morphology and surface modifications, manipulating the particle size, chemical doping, and composite design as discussed above.

Recently, efforts have focused on highly ordered synergistic applications of nanozymes in cascade systems that drive biological sensing. The nanozymes are developed for independent enzyme-like activity, but several efforts have geared the attention of scientists towards the synergistic activity of nanozymes in cascade systems. Multi-enzyme synergistic activity relies on a single enzyme having two activities for substrate conversion to products. The efficacy and synergistic effects of nanozymes can be boosted significantly by combining with other enzymes, such as, GO_X and peroxidase, implying a higher capability of ROS release. The performances of multi-enzymatic nanozymes can be regulated by pH, H_2O_2, and GSH concentrations, and the level of oxygenation for improved diagnostics and therapeutic roles of nanozymes [33]. In this context, it has been found that the pH levels of the nanozymes can remarkably influence the catalytic reactions with the same substrate. Furthermore, the efficiency of the catalytic activity of nanozymes can be improved by mimicking the MOF system or utilizing its strong restriction framework as a carrier for biomimetic enzymes, since it provides solid support (as a carrier), where the enzymes are dispersed within the framework to realize high stability and reaction activity [286]. Huang et al. developed MOF nanosheets of Au nanoparticles as GOx peroxidase and loaded them with CuTCPP (Fe) to exhibit cascade catalysis. The MOF acts as a template for nanoparticles to grow and receives H_2O_2 from glucose oxidation by Au nanoparticles. This cascade system is more effective and tolerant to various pH environments and opens more options for glucose detection [287]. Conventional photodynamic treatment (PDT) utilizes light-generating ROS to regulate tumor growth but hypoxia in TME limits ROS production, and hence restricts the PDT efficacy for cancer therapy. In this regard, single-atom iron-containing (SAF) nanoparticles are developed to encapsulate DOX and A549 cell membranes as a nanoagent drug carrier. This nanoagent acts as peroxidase that initiates a Fenton-like reaction for toxic hydroxyl radicals generation in an acidic TME for CDT. The peroxidase activity of SAF nanoparticles has been compared with $Fe(NO_3)_3$@ZIF-8 but the latter cannot catalyze H_2O_2 into ·OH, indicating that MOFs as SAF nanoparticles enhance the catalytic activity of nanozymes in accordance with the pH of TME [33]. Moreover, Mn MOF has been successful in exhibiting catalytic activity after PEGylation of MnMOF (PEG-MnMOF) that serves as a catalase-mimicking and peroxidase-like nanozyme activities by incorporating a photosensitizer, indocyanine green (ICG) into the dual-enzyme-based PEG-Mn-MOF to demonstrate the enhanced PDT treatment of tumors. This nanoagent establishes comparable peroxidase- and catalase-like catalytic activities in addition to oxygen production and hydroxyl radical generation to kill cancer cells. This supports Fenton reactions to alleviate anticancer effects and improves the therapeutic efficiency of PDT by synergistic series-parallel catalytic pathways [288].

Kim et al. developed Ce6-loaded manganese ferrite nanoparticles (MFN) coupled with mesoporous silica nanoparticles that function as catalase and deliver oxygen to alleviate hypoxia, making PDT treatment more effective. Furthermore, MFN can also be employed as magnetic resonance imaging (MRI) contrasting agent, enabling non-invasive tracking of the nanozymes. Thus, MFN show a promising theranostic agent for cancer diagnosis and treatment [289]. Ultrasound (US)-enhanced enzyme dynamic (enzyodynamic) therapy is another means to treat cancer. Chang and his team reported a $LaFeO_3$ (LFO) perovskite nanozyme that possesses quadruple enzyme-mimicking activities – oxidase, peroxidase, catalase, and GPx. They trigger a series of reactions to reverse the hypoxic microenvironment, reduce the natural antioxidant and release ROS that effectively induce cell death in breast cancer cells. This work determines the ability to circumvent apoptosis resistance by coupling with nanocatalytic enzymes in treating pyroptosis-dominant breast cancer [290]. In another work, PEGylated $Cu_xMn_yS_z$ (PCMS) is reported to promote cascade catalytic reactions in TME without affecting normal tissues. This catalyzes the cascade conversion of endogenous H_2O_2 to oxygen by catalase-like activity followed by oxidase-like activity of superoxide radical to produce O_2 in the TME (Fig. 11A). It also effectively reduces intracellular GSH through glutathione oxidase-like activity. As shown in Fig. 11B, photoacoustic imaging clearly reveals enhanced signal at tumor site, up to 5.8-fold after 24 h following PCMS treatment. Furthermore, PCMS demonstrates significant photothermal effects under NIR-II 1064 nm laser irradiation, which further improves CDT in tumor treatment. The excellent photothermal effect of PCMS benefits MRI, infrared thermal imaging, and photoacoustic imaging and its biodegradation in TME helping to track the drug *in vivo* [291]. Besides, a novel nanorods by coating Bi_2S_3 on dendritic mesoporous silica and subsequent infusion with CeO_2 nanozymes is developed. This enables the nano-agent to mimic peroxidase- and catalase-like activity, while effectively regulating the TME and has increased GSH-consumption capability, improving the OH-mediated tumor nano-catalyst therapy. This synergistic capability elevates oxidative stress and reduces hypoxia, making it a promising strategy for targeted cancer therapy [292].

Advances in nanotechnology, microfabrication, and biotechnology are driving further evolution in *in-vitro* biosensing, resulting in methods of detection that are more sensitive and precise. Xu et al. developed carbon fiber microelectrodes modified with GQDs and AuPd alloy nanoparticles as nanozymes. The catalytic efficiency of GQDs in H_2O_2 decomposition is attributed to their aromatic structure and surface functional groups. Additionally, the quantum confinement effect of GQDs facilitates the nucleation of AuPd nanoparticles on the microelectrodes, enhancing their peroxidase-mimicking activity. This improved sensor exhibits high selectivity and sensitivity in detecting H_2O_2 variations across different human breast cancer cells, making it a valuable tool for monitoring peroxide levels in clinical breast cancer tissues. Their as-prepared microelectrodes a low limit of detection of approximately 0.5 μM with a large linear detection range (1.0 μM to 18.4 μM). This sensor demonstrated a distinct response to different concentrations of H_2O_2 in live human breast cancer cells, exhibiting remarkable sensitivity and selectivity for *in situ* monitoring of H_2O_2 at trace levels in clinical breast cancer tissues [294]. Xia and his colleagues developed a systematic approach to a cascade nanozyme for regulated self-assembly, fluorescent detection, and sequential catalysis involving cyclodextrin modified with Au nanoparticles. Rhodamine B fluorescence

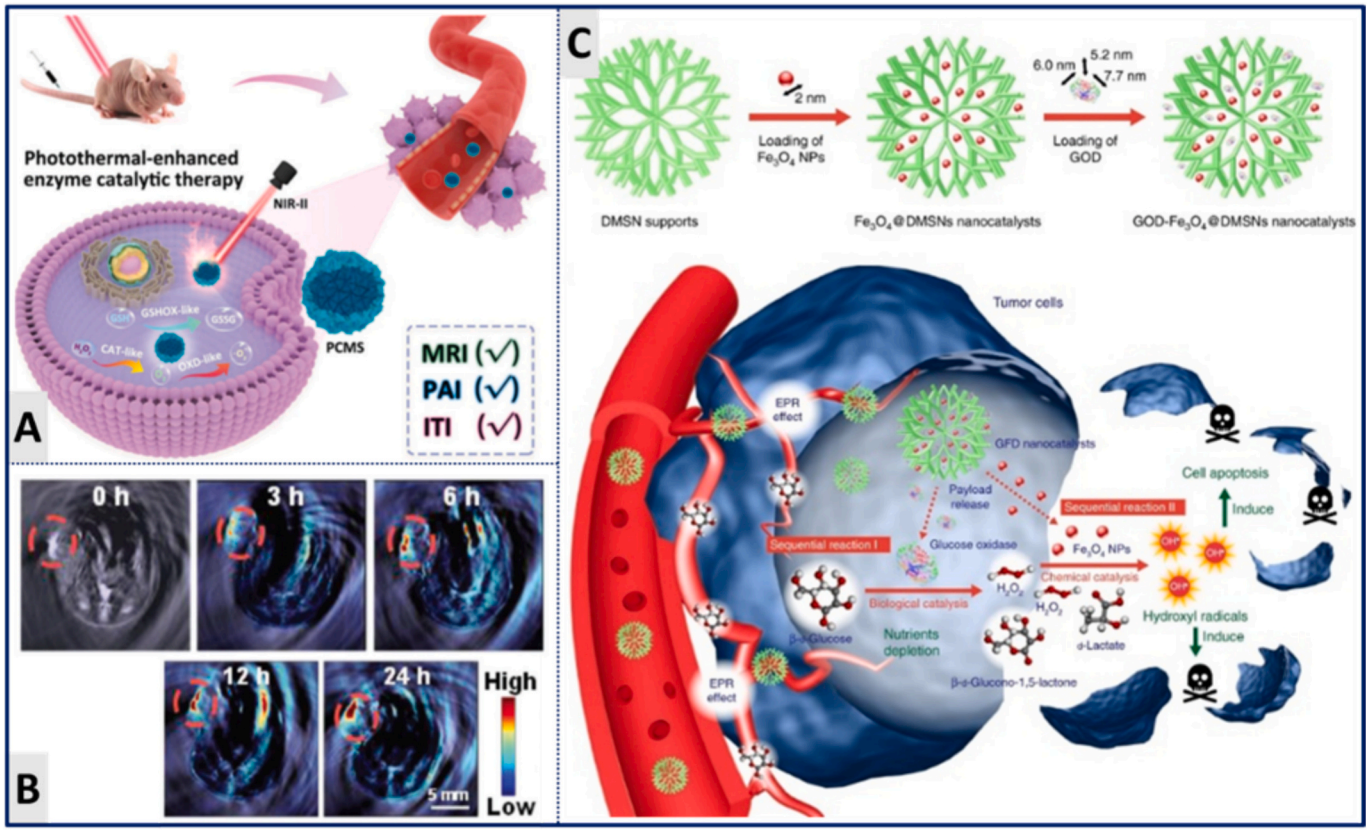

Fig. 11. Panel A: Schematic showing PCMS-induced mechanism for photothermal-enhanced cascade catalytic therapy. **Panel B** Photoacoustic imaging showing increased tumor signal in time time-dependent manner following PCMS injection. Reprinted with permission from *Advanced Healthcare Materials*, John Wiley and Sons [291]Copyright © 2022. **Panel C:** Schematic of fabrication and catalytic therapy of sequential cascade nanozyme, and sequential catalytic-therapeutic mechanism of the nanozyme, schematic shows the generation of hydroxyl radical to kill cancer cells. Reprinted with permission from *Nature Communications*, Springer Nature [293] Copyright © 2017.

is quenched upon interaction with CD molecules on the surface of Au nanoparticles. In the presence of cholesterol, rhodamine B is released, leading to fluorescence signal recovery. This approach facilitates the selective and sensitive detection of cholesterol in blood samples. CD@AuNPs nanozyme facilitates the oxidation of glucose into gluconic acid, generating H_2O_2 under alkaline conditions (pH 9). Furthermore, at acidic pH (4.5), CD@AuNPs catalyzes the oxidation of TMB in the presence of H_2O_2. This pH-regulated self-synergistic CD@AuNPs nanozyme system initially oxidize glucose and produces H_2O_2 that in turn oxidizes TMB to produce a colorimetric reaction. This unveils the synergistic properties of nanozymes in biosensing and detection of various substances, like, proteins, cancer cells *etc.*, opening an avenue in biomedical and biotechnology engineering [295]. The GO intrinsic peroxidase-mimicking properties can also be employed to measure glucose concentration by the synergistic effects of GO_x and GO. The GO_x-GO system provides excellent selectivity towards glucose while GO offers higher affinity to TMB molecule through π-π stacking and hydrophobic interaction [24]. The acidic environment of the TME initiates the oxidase- and peroxidase-like activities to generate ROS. Furthermore, magnetic Fe_3O_4 nanoparticles combined with GO_x can be developed for *in vivo* cancer treatment as reported by Huo and co-workers. They presented a novel approach to tumor therapy by sequential catalytic nanomedicine that involves delivery of biocompatible nano-catalyst into tumor site. Fe_3O_4 nanoparticles and natural GOx have been integrated into large pore-sized biodegradable dendritic silica nanoparticle to develop the sequential nano-catalyst. The acidic environment of the TME triggers GO_x to consume glucose in tumor cells and produces a significant amount of H_2O_2 catalyzed by peroxidase-like Fe_3O_4 nanoparticles. These successive reactions generate lethal hydroxyl radicals, leading to apoptosis and death of tumor cells as shown in Fig. 11C. This work manifests the indulgence of nanozymes for cancer theranostics in a synergistic manner and highlights the deeper understanding of synergistic effects of nanozymes for sensing diseases and subsequent treatments [293].

Research has also been focused on biological systems indulging CeO_2 nanoparticles with GOx that forms an effective catalytic cascade for glucose detection in serum [296], and a multiple enzyme/nanozyme system within the MOFs of GOx and PVI -Hemin encapsulated in ZIF-8 is developed. This system improves the cascade reactions exhibiting high catalytic efficiency for glucose with a low LOD, high selectivity, and stability. Additionally, this system can also work for other oxidases like cholesterol oxidase, thereby opening a new approach for industrial biocatalysts, biomedical engineering, and biosensing applications [297]. The idea of the synergistic effect of nanozymes with cascade catalysis reactions is further realized in the immobilization of proteins onto the nanozymes.

Smart nanozymes: Numerous investigations have revealed the responsiveness of nanozymes for a wide range of biomedical applications under the influence of stimuli like pH, GSH-concentration, light, and temperature. Herein, pH-, temperature-, glucose-, ROS-and GSH-responsive nanozymes have been recognized as 'smart nanozymes' to identify and destroy tumor cells [298,299]. The pH of the surrounding environment can fine-tune the structures and composition of pH-sensitive nanozymes. They benefit the controlled release systems modulated by pH change that affects the charge distribution and protonation state of the functional groups of the nanozymes. A slight variation in pH can influence the surface charge, aggregation state, and the conformation of the nanozymes. It has been reported that TME exhibits

an acidic pH environment condition in comparison to normal tissues. Taking advantage of this, nanozymes can be effectively used in the colorimetric detection of tumor cells due to the enhanced peroxidase-like activity in acidic conditions [300]. Apart from acidic pH, few other crucial abnormal characteristics also represent TME, like high temperature, increased level of enzymes and biomolecules (glucose and GSH). Thus, in the context of developing nanozyme-bearing systems for cancer theranostics, the ability to modulate enzyme-mimetic activities through varying environmental pH, temperature, biomolecules like glucose, and GSH, presents a significant targeting strategy. This approach aims to improve treatment efficacy and safety of normal tissues, thereby minimizing side effects. In this context, Li et al. developed pH/glucose/GSH triple-responsive bismuth−manganese-based nanozyme (BDS-GOx@MnOx) for breast cancer theranostic application [301]. Here, MnOx shell provides pH responsiveness and degrades gradually in acidic TME to release GOx to induce glucose starvation as well as H_2O_2 generation in tumor cells. Subsequently, GSH reduces the high valent manganese to $Mn^{2+,}$ which leads generation of ·OH in presence of H_2O_2 to induce chemotherapy. Furthermore, developed nanozymes influence tumor ablation due to inhibition of mitochondrial activity, which in turn inhibits ATP. Moreover, BDS-GOx@MnOx is shown to enhance the computed tomography (CT) as well as MRI to establish the sensing application. Thus, engineered nanozyme has the potential to fulfill the requirements for both diagnosing and ablating malignant tumors. Liang et al. developed nitrogen-doped graphene nanomaterials (N-GNMs), which exhibited enhanced peroxidase-mimetic activity in TME for tumor-specific therapy [302]. Result indicated that developed nanosystem induces tumor cell death by producing highly toxic •OH in acidic TME, whereas, normal cells remain at neutral pH remains in healthy condition. N-GNMs exhibit significant catalytic activity and can react to trace amounts of endogenous H_2O_2 in the TME, leading to enhanced efficacy in tumor treatment.

Furthermore, Wen et al. demonstrated the application of lysosomal-targeted AuNRs- CyHMC (cysteine-hydroxyl merocyanine) nanozymes *in situ* SERS pH monitoring as well as multimodal imaging-guided phototherapy [303]. AuNRs are well known to exhibit GOx mimetic activity as well as frequently used as the SERS active substrate [36]. Here, AuNRs played a role of SERS substrates as well as photoacoustic/photothermal reagents, whereas, CyHMC considered for self-fluorescence localization and generation of pH-sensitive Raman signal. The suggested nano-theranostics demonstrated the ability to monitor pH changes through SERS during photothermal therapy. As anticipated, this resulted in the development of AuNRs-CyHMC, which features fluorescence and Raman signals that are non-interfering, offering innovative concepts for monitoring the localization of gold-based nano-theranostics within subcellular organelles.

Supramolecular nanozyme is another very effective and efficient technique that has shown promising effect in biomedical applications by altering the redox state and ROS in a cancer environment. Nanozymes designed using supramolecular assembly tend to offer high flexibility and responsiveness towards cancer microenvironment in comparison of existing covalent linkages [304]. Additionally, the host-guest nanosystem-based selectivity allows supramolecular assemblies to circumvent the detrimental impacts on normal cells and tissues by selectively sensing and destroying them. In a supramolecular nanozyme, there are diverse forms of nano-architecture alterations found in nanoparticles, nanovesicles or hydrogels. Regarding supramolecular nanovesicles, the intrinsic photosensitizer within these structures can maintain a monomolecular configuration without any quenching due to aggregation. The nanovesicles exhibit the ability to load drugs and respond reversibly to stimuli in complex TME. Following the assembly into nanovesicles and subsequent cross-linking with 3-mercaptopropyltrimethoxysilane (MPTMS) along with PEGylation, these GSH/pH dual-responsive nanovesicles effectively consume GSH while simultaneously up-regulating ROS in tumors [305].

Zhang et al. designed Fe_3O_4 nanocomposite as peroxidase-mimic as activable ROS platform for enhanced cancer theranostic approach [306]. Due to intrinsic peroxidase-mimetic activity of nanozymes, it showed therapeutic activity due to generation of toxic •OH and O_2 for PDT. Further, Fe_3O_4 was modified with CuS and porphyrin, enabling synergistic therapeutic effect and multimodal imaging. *In vivo* multimodal imaging techniques, such as PAI, MRI, photoluminescence imaging (PLI), and photothermal imaging (PTI), utilize the tumor-targeting characteristics of chitosan-encapsulated Fe_3O_4 nanoparticles modified with CuS and porphyrin (FCCP) nanoparticles following intravenous administration. It has the potential to effectively induce cancer cell death both *in vitro* and *in vivo* through a synergistic approach combining PDT and PTT. This investigation highlights the potential of activatable generation of ROS and O_2 for PDT, utilizing nanotechnology to address a significant limitation in cancer treatments. All these strategies, together, overcome the problem faced in cancer treatment due to limited H_2O_2 and overexpression of GSH. This multifunctional nanoplatform may enable self-boosting CDT and synergistic therapy.

7. Conclusion and prospects

Nanozymes are specifically designed nanomaterials, and they can perform functions of natural enzymes. Due to the novel characteristics of nanomaterials and unique enzyme-mimicking properties, the nanozymes are extensively being employed in the field of biomedicine, sensing, and catalysis. In recent times, significant efforts have been made to dictate nanozymes for sensing applications, wherein special emphasis is given on the enhanced dual-mode sensing. The amalgamation of nanozymes and dual-mode sensing strategies has significantly enhanced the sensitivity, specificity, accuracy, and versatility of biomedical diagnostics. Using integration approach of colorimetric detection with complementary techniques such as fluorescence, photothermal, SERS, electrochemical, luminescence, and photoelectrochemical methods, scientists have developed highly efficient platforms for detecting biomarkers, pathogens, and disease-related molecules. These hybrid approaches offer improved signal amplification, real-time monitoring, and multifunctional capabilities.

In this context, the most studied nanozymes exhibit SOD-, catalase, GPx-, and peroxidase-like activities. Moreover, biological systems offer a vast array of molecular catalysts that are emerging as potential agents for futuristic nanozyme studies. Notably, heme-based enzymes, GOx, DNase, and RNase are of current interest. Thus, the development of nanozymes with a broader spectrum of enzyme-mimetic activities remains imperative. However, the key challenge in the field of nanozymes is achieving catalytic efficiency along with specificity comparable to that of natural enzymes, necessitating further advancements in nanozyme design and functionality. Moreover, there are a range of different challenges for further development of nanozymes towards their clinical translation in biosensing and disease conditions.

While broad range of nanozymes are engineered to effectively mimic natural enzymes, there remain several limitations and challenges. Firstly, special attention is required to improve the nanozyme activity and specificity for higher efficiency and effectivity. Additionally, the ongoing concerns about nanozyme toxicity and biocompatibility highlight the urgent need to create biocompatible nanozymes with minimal cytotoxic effects for therapeutic and biosensing applications. For instance, nanozymes are being deposited in reticuloendothelial system (RES), which leads to high toxicity and specificity loss, thus restricting their application in clinical purposes. Some nanozymes, like nickel disulfide, show significant biodegradability; however, their prolonged presence due to slow degradation in the bloodstream limits their use in biomedical applications. The structural and functional aspects of composite nanozymes significantly impact their pharmacokinetics, selectivity, and biosafety. In addition to this, the use of H_2O_2, which can induce damage beyond a certain threshold, is essential for the peroxidase activity of nanozymes. It would be advantageous and well-received to utilize pro-oxidative nanozymes that operate independently of H_2O_2.

Secondly, it is important to eliminate the interference and negative effect caused by opposite enzymatic activity of single nanozyme like pro-oxidative and antioxidative activity at the same time. It has been reported that numerous nanozymes demonstrate both ROS-producing and ROS-scavenging enzymatic characteristics, whether under identical or varying conditions. Determining an appropriate equilibrium between these contrasting activities and replicating the intricacies of natural enzyme systems will be crucial for advancing intelligent nanozyme-based therapeutics in the future. Thirdly, in addition to several advantages, multifunctionality of nanozymes may also induce the severe side effects and complications specifically in the case of condition dependent switchable activity of nanozymes. It might be caused due to the targeting more than single analyte for multifaceted effect. Therefore, a thorough 'polypharmacology' approach should be utilized to assess the possible negative impacts of multienzymatic nanozymes.

At next, one of the major concerns of nanozyme catalytic activity is their low selectivity in comparison to natural enzymes, particularly in detection of interconvertible or multivalent ions. Introduction of recognition element and molecular imprinting techniques can be effectively applied to answer the problem. Ultimately, advancements have been achieved in the differentiation and simultaneous detection of analogues through the development of nanozyme sensor arrays. This approach can successfully address the issue of interference caused by coexisting substances. Further, detection in the presence of real biological samples can lead to nonspecific protein adsorption on nanozymes, which negatively impacts their catalytic activity and ultimately yields unsatisfactory detection outcomes. In order to promote the development of innovative nanozymes with enhanced efficiency, it is essential to delve deeper into the resistance of their enzyme-like functions to interference.

Moreover, an in-depth comprehension of the catalytic mechanisms and the interconnectedness of distinct enzymatic properties for the same nanoparticles should be explored. Due to the complex environmental conditions, various nanozymes-based detection mechanism is still ambiguous. Reactive radicals produced due to catalytic activity thought to be the main reason of oxidation response, however, in a few instances electron transfer thought to be the main factor. However, these two mechanisms may also coexist in the same reaction conditions. Likewise, phosphates are thought to promote oxidase activity when TMB serve as substrate, while inhibitory effect in case of ABTS. Understanding the relationship between the activity and structure of nanozymes requires a thorough exploration of their catalytic mechanisms. This insight will be beneficial for the technical design of nanozymes that possess the desired characteristics. For the successful execution of the necessary activity, it is crucial that nanozymes are transported to the infected site with precision and targeted control. In addition, nanozymes have been applied in detection of wide range of analytes; however, in ion sensing its target range is rather restricted to detection of few ions like Ag^{+}, Hg^{2+}, F^{-}, Cr^{6+}, and Pb^{2+}. This might be attributed to the fact that the range of analytes that interact with nanozymes, whether directly or indirectly, remains quite restricted. Thus, it is essential to methodically examine the effects of various analytes on the catalytic performance of nanozymes.

At last, the aggregation and instability of nanomaterials present significant challenges. Therefore, enhancing the catalytic activity and stability of nanozymes has emerged as a critical issue that requires immediate attention. Consequently, altering the nanomaterial surface to create effective nanozymes with enhanced catalytic activity and strong affinity will be the primary emphasis of upcoming investigations.

Thus, advancements in this field could pave the way for next-generation artificial enzymes, positioning and designing nanozymes, as a ground-breaking tool in theranostics innovation. In this perspective, several innovative strategies have been utilized including design inspiration from naturally occurring enzymes, meticulous physicochemical properties and exterior corona development, self-assembly, endogenous/exogenous stimulation responsive control, *in-situ* synthesis of tailor-made nanozymes, and integration of artificial intelligence (AI) and machine learning (ML) to enhance the specificity and safety of smart nanozymes during their use in biomedicine application. As research in this field continues to evolve and advance, the development of more selective, biocompatible, and scalable nanozyme-based sensing systems with minimal toxicity will pave the way for next-generation diagnostic tools with broad applications in biomedical research, point-of-care testing, and personalized medicine.

Declaration of competing interest

The authors declare that they have no known competing financial interests or personal relationships that could have appeared to influence the work reported in this paper.

Acknowledgements

HKD acknowledges the Central University of Rajasthan, India, for Seed Grants (2023, and 2025) and the Indian Council of Forestry Research and Education (ICFRE), Dehradun, India, for a research grant (ICFRE/RFRI/2023–24/SFM-2). Further, HKD expresses his gratitude to the Department of Science and Technology, Government of India, New Delhi, for providing the FIST grant (SR/FST/LS-I/2023/1153) to the Department of Biochemistry, School of Life Sciences, Central University of Rajasthan, India. AS and HKD acknowledge Department of Science and Technology, Government of India, New Delhi for providing FIST grant (SR/FST/LS-I/2017/56) to Amity Institute of Biotechnology, and PURSE grant (SR/PURSE/2021/77) to Amity University Rajasthan, Jaipur, India.

Data availability

No data was used for the research described in the article.

References

[1] R. Singh, A. Umapathi, G. Patel, C. Patra, U. Malik, S.K. Bhargava, H.K. Daima, Nanozyme-based pollutant sensing and environmental treatment: trends, challenges, and perspectives, Sci. Total Environ. 854 (2023) 158771, https://doi.org/10.1016/j.scitotenv.2022.158771.

[2] L. Gao, J. Zhuang, L. Nie, J. Zhang, Y. Zhang, N. Gu, T. Wang, J. Feng, D. Yang, S. Perrett, X. Yan, Intrinsic peroxidase-like activity of ferromagnetic nanoparticles, Nat. Nanotechnol. 2 (2007) 577–583, https://doi.org/10.1038/nnano.2007.260.

[3] S. Singh, N. Rai, H. Tiwari, P. Gupta, A. Verma, R. Kumar, V. Kailashiya, P. Salvi, V. Gautam, Recent advancements in the formulation of nanomaterials-based nanozymes, their catalytic activity, and biomedical applications, ACS Appl. Bio Mater. 6 (2023) 3577–3599, https://doi.org/10.1021/acsabm.3c00253.

[4] Y. Chen, P. Wang, H. Hao, J. Hong, H. Li, S. Ji, A. Li, R. Gao, J. Dong, X. Han, M. Liang, D. Wang, Y. Li, Thermal atomization of platinum nanoparticles into single atoms: an effective strategy for engineering high-performance nanozymes, J. Am. Chem. Soc. 143 (2021) 18643–18651, https://doi.org/10.1021/jacs.1c08581.

[5] S. Ji, B. Jiang, H. Hao, Y. Chen, J. Dong, Y. Mao, Z. Zhang, R. Gao, W. Chen, R. Zhang, Q. Liang, H. Li, S. Liu, Y. Wang, Q. Zhang, L. Gu, D. Duan, M. Liang, D. Wang, X. Yan, Y. Li, Matching the kinetics of natural enzymes with a single-atom iron nanozyme, Nat. Catal. 4 (2021) 407–417, https://doi.org/10.1038/s41929-021-00609-x.

[6] Y. Chen, B. Jiang, H. Hao, H. Li, C. Qiu, X. Liang, Q. Qu, Z. Zhang, R. Gao, D. Duan, S. Ji, D. Wang, M. Liang, Atomic-level regulation of cobalt single-atom Nanozymes: engineering high-efficiency catalase mimics, Angew. Chem. Int. Ed. 62 (2023) e202301879, https://doi.org/10.1002/anie.202301879.

[7] C. Hong, X. Meng, J. He, K. Fan, X. Yan, Nanozyme: a promising tool from clinical diagnosis and environmental monitoring to wastewater treatment, Particuology 71 (2022) 90–107, https://doi.org/10.1016/j.partic.2022.02.001.

[8] H.W. Kroto, J.R. Heath, S.C. O'Brien, R.F. Curl, R.E. Smalley, C60: Buckminsterfullerene, Nature 318 (1985) 162–163, https://doi.org/10.1038/318162a0.

[9] S. Iijima, Helical microtubules of graphitic carbon, Nature 354 (1991) 56–58, https://doi.org/10.1038/354056a0.

[10] K.S. Novoselov, A.K. Geim, S.V. Morozov, D. Jiang, Y. Zhang, S.V. Dubonos, I. V. Grigorieva, A.A. Firsov, Electric field effect in atomically thin carbon films, Science (New York, N.Y.) 306 (2004) 666–669, https://doi.org/10.1126/science.1102896.

[11] J. Wu, X. Wang, Q. Wang, Z. Lou, S. Li, Y. Zhu, L. Qin, H. Wei, Nanomaterials with enzyme-like characteristics (nanozymes): next-generation artificial enzymes (II), Chem. Soc. Rev. 48 (2019) 1004–1076, https://doi.org/10.1039/C8CS00457A.

[12] M. Yang, Z. Wang, M. Su, S. Zhu, Y. Xie, B. Ying, Smart Nanozymes for diagnosis of bacterial infection: the next frontier from laboratory to bedside testing, ACS Appl. Mater. Interfaces 16 (2024) 44361–44375, https://doi.org/10.1021/acsami.4c07043.

[13] Y. Huang, X. Guo, Y. Wu, X. Chen, L. Feng, N. Xie, G. Shen, Nanotechnology's frontier in combatting infectious and inflammatory diseases: prevention and treatment, Signal Transduct. Target. Ther. 9 (2024) 34, https://doi.org/10.1038/s41392-024-01745-z.

[14] D. Wang, D. Jana, Y. Zhao, Metal–organic framework derived nanozymes in biomedicine, Acc. Chem. Res. 53 (2020) 1389–1400, https://doi.org/10.1021/acs.accounts.0c00268.

[15] Y. Fan, S. Liu, Y. Yi, H. Rong, J. Zhang, Catalytic nanomaterials toward atomic levels for biomedical applications: from metal clusters to single-atom catalysts, ACS Nano 15 (2021) 2005–2037, https://doi.org/10.1021/acsnano.0c06962.

[16] R. Singh, S. Singh, Redox-dependent catalase mimetic cerium oxide-based nanozyme protect human hepatic cells from 3-AT induced acatalasemia, Colloids Surf. B: Biointerfaces 175 (2019) 625–635, https://doi.org/10.1016/j.colsurfb.2018.12.042.

[17] L. Zhang, L. Zhang, H. Deng, H. Li, W. Tang, L. Guan, Y. Qiu, M.J. Donovan, Z. Chen, W. Tan, In vivo activation of pH-responsive oxidase-like graphitic nanozymes for selective killing of helicobacter pylori, Nat. Commun. 12 (2021) 2002, https://doi.org/10.1038/s41467-021-22286-x.

[18] L. Gao, X. Yan, Nanozymes: Biomedical applications of enzymatic Fe_3O_4 nanoparticles from in vitro to in vivo, in: S. Perrett, A.K. Buell, T.P.J. Knowles (Eds.), Biological and Bio-Inspired Nanomaterials: Properties and Assembly Mechanisms, Springer Singapore, Singapore, 2019, pp. 291–312.

[19] M. Yang, J. Li, P. Gu, X. Fan, The application of nanoparticles in cancer immunotherapy: targeting tumor microenvironment, Bioact. Mater. 6 (2021) 1973–1987, https://doi.org/10.1016/j.bioactmat.2020.12.010.

[20] F. Liu, L. Lin, Y. Zhang, Y. Wang, S. Sheng, C. Xu, H. Tian, X. Chen, A tumor-microenvironment-activated nanozyme-mediated theranostic nanoreactor for imaging-guided combined tumor therapy, Adv. Mater. 31 (2019) 1902885, https://doi.org/10.1002/adma.201902885.

[21] Z. Wang, Z. Li, Z. Sun, S. Wang, Z. Ali, S. Zhu, S. Liu, Q. Ren, F. Sheng, B. Wang, Y. Hou, Visualization nanozyme based on tumor microenvironment "unlocking" for intensive combination therapy of breast cancer, Sci. Adv. 6 (2020) eabc8733, https://doi.org/10.1126/sciadv.abc8733.

[22] P. Liu, L. Hao, M. Liu, S. Hu, Glutathione-responsive and -exhausting metal nanomedicines for robust synergistic cancer therapy, Front. Bioeng. Biotechnol. 11 (2023) 1161472, https://doi.org/10.3389/fbioe.2023.1161472.

[23] Y. Song, K. Qu, C. Xu, J. Ren, X. Qu, Visual and quantitative detection of copper ions using magnetic silica nanoparticles clicked on multiwalled carbon nanotubes, Chem. Commun. 46 (2010) 6572–6574, https://doi.org/10.1039/C0CC01593H.

[24] Y. Song, K. Qu, C. Zhao, J. Ren, X. Qu, Graphene oxide: intrinsic peroxidase catalytic activity and its application to glucose detection, Adv. Mater. 22 (2010) 2206–2210, https://doi.org/10.1002/adma.200903783.

[25] H. Sun, Y. Zhou, J. Ren, X. Qu, Carbon nanozymes: enzymatic properties, catalytic mechanism, and applications, Angew. Chem. Int. Ed. 57 (2018) 9224–9237, https://doi.org/10.1002/anie.201712469.

[26] H. Ding, B. Hu, B. Zhang, H. Zhang, X. Yan, G. Nie, M. Liang, Carbon-based nanozymes for biomedical applications, Nano Res. 14 (2021) 570–583, https://doi.org/10.1007/s12274-020-3053-9.

[27] P. Wang, S. Liu, M. Hu, H. Zhang, D. Duan, J. He, J. Hong, R. Lv, H.S. Choi, X. Yan, M. Liang, Peroxidase-like nanozymes induce a novel form of cell death and inhibit tumor growth in vivo, Adv. Funct. Mater. 30 (2020) 2000647, https://doi.org/10.1002/adfm.202000647.

[28] Q. Cheng, X. Du, Z. Fu, Z. Ding, J. Xie, Dual-mode Ce-MOF Nanozymes for rapid and selective detection of hydrogen sulfide in aquatic products, Polymers 16 (2024) 1747, https://doi.org/10.3390/polym16121747.

[29] X. Du, G. Wu, X. Dou, Z. Ding, J. Xie, Recent advances of fluorescence MOF-based sensors for the freshness of aquatic products, Microchem. J. 203 (2024) 110901, https://doi.org/10.1016/j.microc.2024.110901.

[30] C. Wang, G. Ren, B. Yuan, W. Zhang, M. Lu, J. Liu, K. Li, Y. Lin, Enhancing enzyme-like activities of prussian blue analog nanocages by molybdenum doping: toward cytoprotecting and online optical hydrogen sulfide monitoring, Anal. Chem. 92 (2020) 7822–7830, https://doi.org/10.1021/acs.analchem.0c01028.

[31] S. Liang, X.-L. Wu, J. Xiong, X. Yuan, S.-L. Liu, M.-H. Zong, W.-Y. Lou, Multivalent Ce-MOFs as biomimetic laccase nanozyme for environmental remediation, Chem. Eng. J. 450 (2022) 138220, https://doi.org/10.1016/j.cej.2022.138220.

[32] L.-S. Lin, J. Song, L. Song, K. Ke, Y. Liu, Z. Zhou, Z. Shen, J. Li, Z. Yang, W. Tang, G. Niu, H.-H. Yang, X. Chen, Simultaneous Fenton-like ion delivery and glutathione depletion by MnO_2-based nanoagent to enhance chemodynamic therapy, Angew. Chem. Int. Ed. 57 (2018) 4902–4906, https://doi.org/10.1002/anie.201712027.

[33] D. Jiang, D. Ni, Z.T. Rosenkrans, P. Huang, X. Yan, W. Cai, Nanozyme: new horizons for responsive biomedical applications, Chem. Soc. Rev. 48 (2019) 3683–3704, https://doi.org/10.1039/c8cs00718g.

[34] R. Zhang, X. Yan, K. Fan, Nanozymes inspired by natural enzymes, Acc. Mater. Res. 2 (2021) 534–547, https://doi.org/10.1021/accountsmr.1c00074.

[35] S. Ahmadi, K. Rahimizadeh, A. Shafiee, N. Rabiee, S. Iravani, Nanozymes and their emerging applications in biomedicine, Process Biochem. 131 (2023) 154–174, https://doi.org/10.1016/j.procbio.2023.06.014.

[36] Y. Huang, J. Ren, X. Qu, Nanozymes: classification, catalytic mechanisms, activity regulation, and applications, Chem. Rev. 119 (2019) 4357–4412, https://doi.org/10.1021/acs.chemrev.8b00672.

[37] H. Wang, K. Wan, X. Shi, Recent advances in nanozyme research, Adv. Mater. 31 (2019) 1805368, https://doi.org/10.1002/adma.201805368.

[38] Q. Zeng, H. Zhong, J. Liao, Q. Huo, B. Miao, L. Zeng, B. Zhang, G. Nie, Antioxidant activities of metal single-atom nanozymes in biomedicine, Biomater. Sci. 12 (2024) 5150–5163, https://doi.org/10.1039/D4BM00978A.

[39] H. Dong, Y. Fan, W. Zhang, N. Gu, Y. Zhang, Catalytic mechanisms of nanozymes and their applications in biomedicine, Bioconjug. Chem. 30 (2019) 1273–1296, https://doi.org/10.1021/acs.bioconjchem.9b00171.

[40] F. Arshad, N.F. Mohd-Naim, R. Chandrawati, D. Cozzolino, M.U. Ahmed, Nanozyme-based sensors for detection of food biomarkers: a review, RSC Adv. 12 (2022) 26160–26175, https://doi.org/10.1039/D2RA04444G.

[41] Z. Chi, Q. Wang, J. Gu, Recent advances in colorimetric sensors based on nanozymes with peroxidase-like activity, Analyst 148 (2023) 487–506, https://doi.org/10.1039/D2AN01850K.

[42] W. Zhong, Nanomaterials in fluorescence-based biosensing, Anal. Bioanal. Chem. 394 (2009) 47–59, https://doi.org/10.1007/s00216-009-2643-x.

[43] D. Xiao, H. Qi, Y. Teng, D. Pierre, P.T. Kutoka, D. Liu, Advances and challenges of fluorescent nanomaterials for synthesis and biomedical applications, Nanoscale Res. Lett. 16 (2021) 167, https://doi.org/10.1186/s11671-021-03613-z.

[44] M. Zhang, Z. Xu, J. Chen, Z. Ju, Y. Ma, Z. Niu, Z. Xu, T. Zhang, F. Shi, Recent advances on nanomaterials-based photothermal sensing systems, TrAC Trends Anal. Chem. 177 (2024) 117801, https://doi.org/10.1016/j.trac.2024.117801.

[45] Z. Wang, M. Wang, X. Wang, Z. Hao, S. Han, T. Wang, H. Zhang, Photothermal-based nanomaterials and photothermal-sensing: an overview, Biosens. Bioelectron. 220 (2023) 114883, https://doi.org/10.1016/j.bios.2022.114883.

[46] H.S. Han, K.Y. Choi, Advances in nanomaterial-mediated photothermal cancer therapies: toward clinical applications, Biomedicines 9 (2021) 305, https://doi.org/10.3390/biomedicines9030305.

[47] A.R. Jalalvand, M.M. Karami, Roles of nanotechnology in electrochemical sensors for medical diagnostic purposes: a review, Sens. Bio-Sens. Res 47 (2025) 100733, https://doi.org/10.1016/j.sbsr.2024.100733.

[48] L. Dykman, N. Khlebtsov, Gold nanoparticles in biomedical applications: recent advances and perspectives, Chem. Rev. 41 (2012) 2256–2282, https://doi.org/10.1039/C1CS15166E.

[49] Z. Huang, A. Zhang, Q. Zhang, D. Cui, Nanomaterial-based SERS sensing technology for biomedical application, J. Mater. Chem. B 7 (2019) 3755–3774, https://doi.org/10.1039/C9TB00666D.

[50] S. Mahanty, S. Majumder, R. Paul, R. Boroujerdi, E. Valsami-Jones, C. Laforsch, A review on nanomaterial-based SERS substrates for sustainable agriculture, Sci. Total Environ. 950 (2024) 174252, https://doi.org/10.1016/j.scitotenv.2024.174252.

[51] Y. Xu, Q. Dong, S. Cong, Z. Zhao, SERS materials with small-molecule sensitivity for biological diagnosis, Anal. Sens. 4 (2024) e202300067, https://doi.org/10.1002/anse.202300067.

[52] R.O. Saleh, Y.Q. Almajidi, S. Mansouri, A. Hammoud, P. Rodrigues, S.O. Mezan, H.G. Maabreh, M. Deorari, M.N. Shakir, M.Q. Alasheqi, Dual-mode colorimetric and fluorescence biosensors for the detection of foodborne bacteria, Clin. Chim. Acta 553 (2024) 117741, https://doi.org/10.1016/j.cca.2023.117741.

[53] R. Moldovan, E. Vereshchagina, K. Milenko, B.-C. Iacob, A.E. Bodoki, A. Falamas, N. Tosa, C.M. Muntean, C. Farcău, E. Bodoki, Review on combining surface-enhanced Raman spectroscopy and electrochemistry for analytical applications, Anal. Chim. Acta 1209 (2022) 339250, https://doi.org/10.1016/j.aca.2021.339250.

[54] J. Neng, Q. Zhang, P. Sun, Application of surface-enhanced Raman spectroscopy in fast detection of toxic and harmful substances in food, Biosens. Bioelectron. 167 (2020) 112480, https://doi.org/10.1016/j.bios.2020.112480.

[55] M. Chen, A. Qileng, H. Liang, H. Lei, W. Liu, Y. Liu, Advances in immunoassay-based strategies for mycotoxin detection in food: from single-mode immunosensors to dual-mode immunosensors, Compr. Rev. Food Sci. Food Saf. 22 (2023) 1285–1311, https://doi.org/10.1111/1541-4337.13111.

[56] Y. Ouyang, M.P. O'Hagan, I. Willner, Functional catalytic nanoparticles (nanozymes) for sensing, Biosens. Bioelectron. 218 (2022) 114768, https://doi.org/10.1016/j.bios.2022.114768.

[57] Z. Jin, G. Huang, Y. Song, C. Liu, X. Wang, K. Zhao, Catalytic activity nanozymes for microbial detection, Coord. Chem. Rev. 534 (2025) 216578, https://doi.org/10.1016/j.ccr.2025.216578.

[58] S. Mansouri, Detection of pathogenic bacteria with nanozymes-based colorimetric biosensors: advances, challenges and future prospects, Microchem. J. 205 (2024) 111392, https://doi.org/10.1016/j.microc.2024.111392.

[59] S. Shahraki, E. Vaziri, A.A. Saboury, K. Fan, Biomedical potential of nanozymes: harnessing redox enzyme mimicry for theranostic applications, Coord. Chem. Rev. 517 (2024) 215937, https://doi.org/10.1016/j.ccr.2024.215937.

[60] X. Yuan, X. He, J. Fan, Y. Tai, Y. Yao, Y. Luo, J. Chen, H. Luo, X. Zhou, F. Luo, Q. Niu, W. Hu, X. Sun, B. Ying, Advances in nanozymes with peroxidase-like activity for biosensing and disease therapy applications, J. Mater. Chem. B 13 (2025) 1599–1618, https://doi.org/10.1039/D4TB02315C.

[61] M. Wang, H. Zhang, S. Yan, Y. Zhou, X. Guo, D. An, W. Zhong, Y. Zhang, Fabrication of MOF-based nanozyme sensor arrays and their application in disease diagnosis, Coord. Chem. Rev. 532 (2025) 216506, https://doi.org/10.1016/j.ccr.2025.216506.

[62] H. Li, Y. Peng, X. Huang, R. Wan, L. Zhang, X. Wang, L. Han, L. Li, C. Wang, J. Chen, Advances in design and preparation of nanozymes and their applications

for constructing higher sensitive lateral flow assays, Coord. Chem. Rev. 510 (2024) 215797, https://doi.org/10.1016/j.ccr.2024.215797.
[63] Z. Xi, W. Gao, X. Xia, Size effect in Pd−Ir Core-Shell nanoparticles as Nanozymes, ChemBioChem 21 (2020) 2440–2444, https://doi.org/10.1002/cbic.202000147.
[64] F.F. Peng, Y. Zhang, N. Gu, Size-dependent peroxidase-like catalytic activity of Fe_3O_4 nanoparticles, Chin. Chem. Lett. 19 (2008) 730–733, https://doi.org/10.1016/j.cclet.2008.03.021.
[65] S.-B. He, R.-T. Chen, Y.-Y. Wu, G.-W. Wu, H.-P. Peng, A.-L. Liu, H.-H. Deng, X.-H. Xia, W. Chen, Improved enzymatic assay for hydrogen peroxide and glucose by exploiting the enzyme-mimicking properties of BSA-coated platinum nanoparticles, Microchim. Acta 186 (2019) 778, https://doi.org/10.1007/s00604-019-3939-y.
[66] F. Xia, X. Hu, B. Zhang, X. Wang, Y. Guan, P. Lin, Z. Ma, J. Sheng, D. Ling, F. Li, Ultrasmall ruthenium nanoparticles with boosted antioxidant activity upregulate regulatory T cells for highly efficient liver injury therapy, Small 18 (2022) 2201558, https://doi.org/10.1002/smll.202201558.
[67] C. Ge, G. Fang, X. Shen, Y. Chong, W.G. Wamer, X. Gao, Z. Chai, C. Chen, J.-J. Yin, Facet energy versus enzyme-like activities: the unexpected protection of palladium nanocrystals against oxidative damage, ACS Nano 10 (2016) 10436–10445, https://doi.org/10.1021/acsnano.6b06297.
[68] H.L.K.S. Stolle, J.J. Kluitmann, A. Csáki, J.M. Köhler, W. Fritzsche, Shape-dependent catalytic activity of gold and bimetallic nanoparticles in the reduction of methylene blue by sodium borohydride, Catalysts 11 (2021) 1442, https://doi.org/10.3390/catal11121442.
[69] S. Wang, W. Chen, A.-L. Liu, L. Hong, H.-H. Deng, X.-H. Lin, Comparison of the peroxidase-like activity of unmodified, amino-modified, and citrate-capped gold nanoparticles, ChemPhysChem 13 (2012) 1199–1204, https://doi.org/10.1002/cphc.201100906.
[70] J. Huo, J. Hao, J. Mu, Y. Wang, Surface modification of Co_3O_4 Nanoplates as efficient peroxidase nanozymes for biosensing application, ACS Appl. Bio Mater. 4 (2021) 3443–3452, https://doi.org/10.1021/acsabm.1c00017.
[71] H. Zhang, Y. Chen, Y. Wei, X. Zhang, H. Ma, Construction of a CuO2@PDA nanozyme with switchable dual enzyme-mimic activities for colorimetric sensing of catechol and hydroquinone, ACS Appl. Mater. Interfaces 17 (2025) 15886–15895, https://doi.org/10.1021/acsami.5c00904.
[72] S. Ray, R. Biswas, R. Banerjee, P. Biswas, A gold nanoparticle-intercalated mesoporous silica-based nanozyme for the selective colorimetric detection of dopamine, Nanoscale Adv. 2 (2020) 734–745, https://doi.org/10.1039/C9NA00508K.
[73] T. Li, X. Wang, Y. Wang, Y. Zhang, S. Li, W. Liu, S. Liu, Y. Liu, H. Xing, K.I. Otake, S. Kitagawa, J. Wu, H. Dong, H. Wei, Microenvironmental modulation breaks intrinsic pH limitations of nanozymes to boost their activities, Nat. Commun. 15 (2024) 10861, https://doi.org/10.1038/s41467-024-55163-4.
[74] J. Qiang, C. Zhou, B. Wang, Z. Huo, X. Su, A highly sensitive dual-mode detection platform based on the novel copper/molybdenum bimetallic nanoclusters and co–Fe layered doubled hydroxide nanozyme for butyrylcholinesterase activity sensing, Talanta 282 (2025) 126973, https://doi.org/10.1016/j.talanta.2024.126973.
[75] Y. Lv, C. Zhou, M. Li, Z. Huo, Z. Wei, N. Wang, G. Wang, X. Su, A dual-mode sensing system based on carbon quantum dots and Fe nanozymes for the detection of α-glucosidase and its inhibitors, Talanta 268 (2024) 125328, https://doi.org/10.1016/j.talanta.2023.125328.
[76] Z. Han, C. Zhou, Y. Lv, N. Wang, X. Su, A dual-signal sensing platform based on single atomic iron-nitrogen-carbon nanozyme for the detection of neurodegenerative disease-related bioactive molecules acetylcholinesterase and dopamine, Sensors Actuators B Chem. 425 (2025) 136969, https://doi.org/10.1016/j.snb.2024.136969.
[77] C. Zhang, Y. Yi, Y. Zhou, R. Zhou, G. Zhu, Homogeneous electroanalysis coupled with colorimetry dual-mode sensing of silver ion in water based on target-inhibited peroxidase activity of Pt@ZIF-8 nanozyme, Microchem. J. 197 (2024) 109839, https://doi.org/10.1016/j.microc.2023.109839.
[78] D.-Q. Feng, S. Wang, Z. Yu, W. Zhang, G. Liu, Dual-recognition driven sensing platform based on a BSA-cu NP nanozyme combined with smartphone-assistance for fluorometric/colorimetric monitoring of dopamine, RSC Adv. 15 (2025) 199–206, https://doi.org/10.1039/d4ra07209j.
[79] K. Yu, M. Li, H. Chai, Q. Liu, X. Hai, M. Tian, L. Qu, T. Xu, G. Zhang, X. Zhang, MOF-818 nanozyme-based colorimetric and electrochemical dual-mode smartphone sensing platform for in situ detection of H_2O_2 and H_2S released from living cells, Chem. Eng. J. 451 (2023) 138321, https://doi.org/10.1016/j.cej.2022.138321.
[80] X. Luo, Y. Yan, F. Zhang, G. Huang, Z. Li, J. Huang, Interface engineered self-induced and cascading nanozyme for colorimetric and photothermal dual-mode pesticide sensing, Mater. Today Chem. 40 (2024) 102202, https://doi.org/10.1016/j.mtchem.2024.102202.
[81] Y. Qin, S. Li, L. Liang, J. Wu, Y. Zhu, S. Zhao, F. Ye, Regulating the redox and non-redox enzyme-mimicking activities of Ce-UiO-66-NO_2 nanozyme for dual-mode sensing of phosphate, Sensors Actuators B Chem. 412 (2024) 135782, https://doi.org/10.1016/j.snb.2024.135782.
[82] H. Liang, L. Chen, X. Chen, H. Zhang, X. Wang, H. Deng, X. Xiong, Y. Wang, C. Li, Near-infrared photoelectrochemical and colorimetric dual-mode aptasensor for determining osteopontin based on Er-MOF nanoballs@gold nanoparticles and Au_2Pt nanozymes, Sensors Actuators B Chem. 414 (2024) 135887, https://doi.org/10.1016/j.snb.2024.135887.
[83] Y. Zhang, T. Zhao, B. Zhao, B. Sun, X. Zhang, Y. Gu, Q. Zhang, M. Li, Development of MnO_2 nanosheets nanozyme-based colorimetric and photothermal dual-signal platform for monitoring alkaline phosphatase activity, Microchem. J. 207 (2024) 111656, https://doi.org/10.1016/j.microc.2024.111656.
[84] C. Hu, G. Li, Y. Xue, J. Liu, Z. Cai, Z. Lin, Light-activated bifunctional nanozymes based on three-component covalent organic frameworks for colorimetric and ratiometric fluorescence dual-mode detection of alkaline phosphatase, Sensors Actuators B Chem. 422 (2025) 136593, https://doi.org/10.1016/j.snb.2024.136593.
[85] Y.-H. Shi, W.-C. Jiang, J. Zeng, S.-Y. Wang, W. Wu, S.-D. Xie, Y. Zhao, Z.-H. Xu, G.-Q. Zhang, Non-pyrolytic synthesis of laccase-like iron based single-atom nanozymes for highly efficient dual-mode colorimetric and fluorescence detection of epinephrine, Anal. Chim. Acta 1322 (2024) 343031, https://doi.org/10.1016/j.aca.2024.343031.
[86] C. Zhang, Y. Zhou, L. Ming, L. Chen, M. Xue, J. Zhang, H. Zhang, Dual–mode strategy for the determination of vanillin in milk–based products based on molecular-imprinted nanozymes, Food Chem. 469 (2025) 142615, https://doi.org/10.1016/j.foodchem.2024.142615.
[87] S. Tai, H. Cao, Y. Cui, C. Peng, J. Xu, Z. Wang, Sensitive colorimetric and fluorescence dual-mode detection of thiophanate-methyl based on spherical Fe_3O_4/GONRs composite nanozyme, Food Chem. 450 (2024) 139258, https://doi.org/10.1016/j.foodchem.2024.139258.
[88] H. Li, H. Xu, S. Yao, S. Wei, X. Shi, C. Zhao, J. Li, J. Wang, Colorimetry/fluorescence dual-mode detection of salmonella typhimurium based on self-assembly of MCOF with au NPs nanozyme coupled AIEgen, Talanta 270 (2024) 125505, https://doi.org/10.1016/j.talanta.2023.125505.
[89] K. Deng, H. Hu, Y. Li, X. Li, H. Deng, Y. Chen, X. Yang, L. Wang, X. Chen, Mechanistic investigation and dual-mode colorimetric-chemiluminescent detection of glyphosate based on the specific inhibition of Fe_3O_4@cu nanozyme peroxidase-like activity, Food Chem. 443 (2024) 138501, https://doi.org/10.1016/j.foodchem.2024.138501.
[90] M. Zheng, M. Liu, Z. Song, F. Ma, H. Zhu, H. Guo, H. Sun, High-precision colorimetric-fluorescent dual-mode biosensor for detecting acetylcholinesterase based on a trimetallic nanozyme for efficient peroxidase-mimicking, J. Mater. Sci. Technol. 191 (2024) 168–180, https://doi.org/10.1016/j.jmst.2024.01.013.
[91] T.T. Li, H.X. Li, Q. Yu, W.Q. Jia, S.T. Li, W. Zhu, Z. Chen, L. Han, Colorimetric and photothermal dual-mode sensing platform for point-of-care testing of acid phosphatase activity and inhibitor screening based on oxidase-mimetic activity of Pt-Ni alloy nanoparticles, Microchem. J. 207 (2024) 112258, https://doi.org/10.1016/j.microc.2024.112258.
[92] Y. Guo, Y. Lv, C. Zhou, J. Wang, X. Su, Dual-channel sensing strategy for melatonin detection based on iron-cobalt oxide nanosheets with peroxidase-like activity and gold nanoclusters, Microchem. J. 201 (2024) 110655, https://doi.org/10.1016/j.microc.2024.110655.
[93] X. Huang, Y. Yang, H. Zhou, L. Hu, A. Yang, H. Jin, B. Zheng, J. Pi, J. Xu, P. Sun, H.-H. Cai, X. Liang, B. Pan, J. Zheng, H. Zhou, Coupling of an au@AgPt nanozyme array with an micrococcal nuclease-specific responsiveness strategy for colorimetric/SERS sensing of Staphylococcus aureus in patients with sepsis, J. Pharm. Anal. 15 (2024) 101085, https://doi.org/10.1016/j.jpha.2024.101085.
[94] X. Gao, H. Chen, H. Qiu, Y. Zhang, J. Cheng, Y. Shen, Portable hydrogel kit driven by bimetallic carbon dots nanozyme for H_2O_2-self-supplying dual-modal monitoring of atmospheric CH_3SH, J. Hazard. Mater. 469 (2024) 133871, https://doi.org/10.1016/j.jhazmat.2024.133871.
[95] W. Jing, Q. Shi, S. Qiang, Y. Wang, Y. Li, T. Zhao, Y. Li, D. Liu, Y. Liu, F. Liu, Dual-mode colorimetric and chemiluminescence aptasensor for organophosphorus pesticides detection using aptamer-regulated peroxidase-like activity of TA-cu, Talanta 285 (2025) 127410, https://doi.org/10.1016/j.talanta.2024.127410.
[96] A. Sen, J. Oswalia, S. Yadav, M. Vachher, A. Nigam, Recent trends in nanozyme research and their potential therapeutic applications, Curr. Res. Biotechnol. 7 (2024) 100205, https://doi.org/10.1016/j.crbiot.2024.100205.
[97] M.F. Gustavo, E. Székely, J. Tóth, Kinetic modeling of a consecutive enzyme-catalyzed enantioselective reaction in supercritical media, ACS Omega 5 (2020) 26795–26806, https://doi.org/10.1021/acsomega.0c02405.
[98] S. Makkar, N. Sarawagi, N. Priyadarshi, S. Kaul, P.K. Sodhi, A.K. Srivastava, N. K. Singhal, Recent advancements in nanozyme hydrogel based system for enhanced sensing applications, Biosens. Bioelectron. X, 21 (2024) 100548, https://doi.org/10.1016/j.biosx.2024.100548.
[99] R.V. Lloyd, P.M. Hanna, R.P. Mason, The origin of the hydroxyl radical oxygen in the Fenton reaction, Free Radic. Biol. Med. 22 (1997) 885–888, https://doi.org/10.1016/S0891-5849(96)00432-7.
[100] A.A. Vernekar, D. Sinha, S. Srivastava, P.U. Paramasivam, P. D'Silva, G. Mugesh, An antioxidant nanozyme that uncovers the cytoprotective potential of vanadia nanowires, Nat. Commun. 5 (2014) 5301, https://doi.org/10.1038/ncomms6301.
[101] S. Rashtbari, G. Dehghan, S. Khorram, M. Amini, A. Khataee, Y. Yoon, Plasma modified Co_3O_4 nanoparticles for catalytic degradation process through enhanced peroxidase-like activity, J. Ind. Eng. Chem. 121 (2023) 114–123, https://doi.org/10.1016/j.jiec.2023.01.015.
[102] M. Das, S. Patil, N. Bhargava, J.-F. Kang, L.M. Riedel, S. Seal, J.J. Hickman, Auto-catalytic ceria nanoparticles offer neuroprotection to adult rat spinal cord neurons, Biomater 28 (2007) 1918–1925, https://doi.org/10.1016/j.biomaterials.2006.11.036.
[103] C. Tang, T. Fang, S. Chen, D. Zhang, J. Yin, H. Wang, Citrate-functionalized osmium nanoparticles with peroxidase-like specific activity for highly efficient degradation of phenolic pollutants, Chem. Eng. J. 464 (2023) 142726, https://doi.org/10.1016/j.cej.2023.142726.
[104] S. He, L. Yang, P. Balasubramanian, S. Li, H. Peng, Y. Kuang, H. Deng, W. Chen, Osmium nanozyme as peroxidase mimic with high performance and negligible

interference of O_2, J. Mater. Chem. A 8 (2020) 25226–25234, https://doi.org/10.1039/D0TA09247A.
[105] S. Sahar, A. Zeb, Z. Mao, A.-W. Xu, W. Wang, PBA-derived heteroatom-doped mesoporous graphitic spheroids as peroxidase Nanozyme for in vitro tumor cells detection, ACS Appl. Bio Mater. 7 (2024) 1778–1789, https://doi.org/10.1021/acsabm.3c01179.
[106] O. Ighodaro, O. Akinloye, First line defence antioxidants-superoxide dismutase (SOD), catalase (CAT) and glutathione peroxidase (GPX): their fundamental role in the entire antioxidant defence grid, Alex. J. Med. 54 (2018) 287–293, https://doi.org/10.1016/j.ajme.2017.09.001.
[107] P. Mathur, M. Kumawat, R. Nagar, R. Singh, H.K. Daima, Tailoring metal oxide nanozymes for biomedical applications: trends, limitations, and perceptions, Anal. Bioanal. Chem. 416 (2024) 5965–5984, https://doi.org/10.1007/s00216-024-05416-4.
[108] S. Lin, Z. Yu, D. Chen, Z. Wang, J. Miao, Q. Li, D. Zhang, J. Song, D. Cui, Progress in microfluidics-based exosome separation and detection technologies for diagnostic applications, Small 16 (2020) 1903916, https://doi.org/10.1002/smll.201903916.
[109] J. Dong, L. Song, J.-J. Yin, W. He, Y. Wu, N. Gu, Y. Zhang, Co_3O_4 nanoparticles with multi-enzyme activities and their application in Immunohistochemical assay, ACS Appl. Mater. Interfaces 6 (2014) 1959–1970, https://doi.org/10.1021/am405009f.
[110] B. Xu, Y. Cui, W. Wang, S. Li, C. Lyu, S. Wang, W. Bao, H. Wang, M. Qin, Z. Liu, W. Wei, H. Liu, Immunomodulation-enhanced nanozyme-based tumor catalytic therapy, Adv. Mater. 32 (2020) 2003563, https://doi.org/10.1002/adma.202003563.
[111] M. Wang, M. Chang, Q. Chen, D. Wang, C. Li, Z. Hou, J. Lin, D. Jin, B. Xing, Au_2Pt-PEG-Ce6 nanoformulation with dual nanozyme activities for synergistic chemodynamic therapy/phototherapy, Biomater 252 (2020) 120093, https://doi.org/10.1016/j.biomaterials.2020.120093.
[112] J. Li, W. Liu, X. Wu, X. Gao, Mechanism of pH-switchable peroxidase and catalase-like activities of gold, silver, platinum and palladium, Biomater 48 (2015) 37–44, https://doi.org/10.1016/j.biomaterials.2015.01.012.
[113] J. Mu, L. Zhang, M. Zhao, Y. Wang, Co_3O_4 nanoparticles as an efficient catalase mimic: properties, mechanism and its electrocatalytic sensing application for hydrogen peroxide, J. Mol. Catal. A Chem. 378 (2013) 30–37, https://doi.org/10.1016/j.molcata.2013.05.016.
[114] W. Zhang, S. Hu, J.-J. Yin, W. He, W. Lu, M. Ma, N. Gu, Y. Zhang, Prussian blue nanoparticles as multienzyme mimetics and reactive oxygen species scavengers, J. Am. Chem. Soc. 138 (2016) 5860–5865, https://doi.org/10.1021/jacs.5b12070.
[115] I. Celardo, J.Z. Pedersen, E. Traversa, L. Ghibelli, Pharmacological potential of cerium oxide nanoparticles, Nanoscale 3 (2011) 1411–1420, https://doi.org/10.1039/C0NR00875C.
[116] T. Pirmohamed, J.M. Dowding, S. Singh, B. Wasserman, E. Heckert, A.S. Karakoti, J.E.S. King, S. Seal, W.T. Self, Nanoceria exhibit redox state-dependent catalase mimetic activity, Chem. Commun. 46 (2010) 2736–2738, https://doi.org/10.1039/B922024K.
[117] Y. Chong, Q. Liu, C. Ge, Advances in oxidase-mimicking nanozymes: classification, activity regulation and biomedical applications, Nano Today 37 (2021) 101076, https://doi.org/10.1016/j.nantod.2021.101076.
[118] M. Comotti, C. Della Pina, E. Falletta, M. Rossi, Aerobic oxidation of glucose with gold catalyst: hydrogen peroxide as intermediate and reagent, Adv. Synth. Catal. 348 (2006) 313–316, https://doi.org/10.1002/adsc.200505389.
[119] R. Ragg, F. Natalio, M.N. Tahir, H. Janssen, A. Kashyap, D. Strand, S. Strand, W. Tremel, Molybdenum trioxide nanoparticles with intrinsic sulfite oxidase activity, ACS Nano 8 (2014) 5182–5189, https://doi.org/10.1021/nn501235j.
[120] S. Grundner, M.A.C. Markovits, G. Li, M. Tromp, E.A. Pidko, E.J.M. Hensen, A. Jentys, M. Sanchez-Sanchez, J.A. Lercher, Single-site trinuclear copper oxygen clusters in mordenite for selective conversion of methane to methanol, Nat. Commun. 6 (2015) 7546, https://doi.org/10.1038/ncomms8546.
[121] Q. Wang, H. Wei, Z. Zhang, E. Wang, S. Dong, Nanozyme: An emerging alternative to natural enzyme for biosensing and immunoassay, TrAC Trends Anal. Chem. 105 (2018) 218–224, https://doi.org/10.1016/j.trac.2018.05.012.
[122] L. Wang, S. Li, X. Zhang, Y. Huang, $CoSe_2$ hollow microspheres with superior oxidase-like activity for ultrasensitive colorimetric biosensing, Talanta 216 (2020) 121009, https://doi.org/10.1016/j.talanta.2020.121009.
[123] X. Zhang, A. Yuan, X. Mao, Q. Chen, Y. Huang, Engineered Mn/co oxides nanocomposites by cobalt doping of Mn-BTC - new oxidase mimetic for colorimetric sensing of acid phosphatase, Sensors Actuators B Chem. 299 (2019) 126928, https://doi.org/10.1016/j.snb.2019.126928.
[124] Z. Jin, G. Xu, Y. Niu, X. Ding, Y. Han, W. Kong, Y. Fang, H. Niu, Y. Xu, Ti_3C_2Tx MXene-derived TiO_2/C-QDs as oxidase mimics for the efficient diagnosis of glutathione in human serum, J. Mater. Chem. B 8 (2020) 3513–3518, https://doi.org/10.1039/C9TB02478F.
[125] X.J. Yang, R.S. Li, C.M. Li, Y.F. Li, C.Z. Huang, Cobalt oxyhydroxide nanoflakes with oxidase-mimicking activity induced chemiluminescence of luminol for glutathione detection, Talanta 215 (2020) 120928, https://doi.org/10.1016/j.talanta.2020.120928.
[126] D. Peng, M. Que, X. Deng, Q. He, Y. Zhao, S. Liao, X. Li, H. Qiu, Mn_3O_4 nanoparticles decorated porous reduced graphene oxide with excellent oxidase-like activity for fast colorimetric detection of ascorbic acid, Microchim. Acta 190 (2023) 243, https://doi.org/10.1007/s00604-023-05822-y.
[127] W. Xu, Y. Zhang, X. Zhang, X. Xu, Q. Wang, One stone, two birds: a cu-S cluster as a laccase-mimicking nanozyme and sulfite activator for phenol remediation in marine environments, J. Hazard. Mater. 457 (2023) 131776, https://doi.org/10.1016/j.jhazmat.2023.131776.
[128] Q. Liu, A. Zhang, R. Wang, Q. Zhang, D. Cui, A review on metal- and metal oxide-based nanozymes: properties, mechanisms, and applications, Nano-Micro Lett. 13 (2021) 154, https://doi.org/10.1007/s40820-021-00674-8.
[129] X. Shen, W. Liu, X. Gao, Z. Lu, X. Wu, X. Gao, Mechanisms of oxidase and superoxide dismutation-like activities of gold, silver, platinum, and palladium, and their alloys: a general way to the activation of molecular oxygen, J. Am. Chem. Soc. 137 (2015) 15882–15891, https://doi.org/10.1021/jacs.5b10346.
[130] S.S. Ali, J.I. Hardt, K.L. Quick, J. Sook Kim-Han, B.F. Erlanger, T.-T. Huang, C. J. Epstein, L.L. Dugan, A biologically effective fullerene (C60) derivative with superoxide dismutase mimetic properties, Free Radic. Biol. Med. 37 (2004) 1191–1202, https://doi.org/10.1016/j.freeradbiomed.2004.07.002.
[131] E.L. Samuel, D.C. Marcano, V. Berka, B.R. Bitner, G. Wu, A. Potter, R.H. Fabian, R. G. Pautler, T.A. Kent, A.L. Tsai, J.M. Tour, Highly efficient conversion of superoxide to oxygen using hydrophilic carbon clusters, Proc. Natl. Acad. Sci. USA 112 (2015) 2343–2348, https://doi.org/10.1073/pnas.1417047112.
[132] Y. Liu, K. Ai, X. Ji, D. Askhatova, R. Du, L. Lu, J. Shi, Comprehensive insights into the multi-antioxidative mechanisms of melanin nanoparticles and their application to protect brain from injury in ischemic stroke, J. Am. Chem. Soc. 139 (2017) 856–862, https://doi.org/10.1021/jacs.6b11013.
[133] X. Cheng, S. Liu, Y. Hu, Recent advances in nanozyme sensors based on metal–organic frameworks and covalent–organic frameworks, Biosensors 14 (2024) 520, https://doi.org/10.3390/bios14110520.
[134] D.A. Giannakoudakis, Y. Hu, M. Florent, T.J. Bandosz, Smart textiles of MOF/g-C_3N_4 nanospheres for the rapid detection/detoxification of chemical warfare agents, Nanoscale Horiz. 2 (2017) 356–364, https://doi.org/10.1039/C7NH00081B.
[135] M. Sun, L. Xu, A. Qu, P. Zhao, T. Hao, W. Ma, C. Hao, X. Wen, F.M. Colombari, A. F. de Moura, N.A. Kotov, C. Xu, H. Kuang, Site-selective photoinduced cleavage and profiling of DNA by chiral semiconductor nanoparticles, Nat. Chem. 10 (2018) 821–830, https://doi.org/10.1038/s41557-018-0083-y.
[136] C. Hao, R. Gao, Y. Li, L. Xu, M. Sun, C. Xu, H. Kuang, Chiral semiconductor nanoparticles for protein catalysis and profiling, Angew. Chem. Int. Ed. 58 (2019) 7371–7374, https://doi.org/10.1002/anie.201902673.
[137] L. Arregui, M. Ayala, X. Gómez-Gil, G. Gutiérrez-Soto, C.E. Hernández-Luna, M. Herrera de los Santos, L. Levin, A. Rojo-Domínguez, D. Romero-Martínez, M.C. N. Saparrat, M.A. Trujillo-Roldán, N.A. Valdez-Cruz, Laccases: structure, function, and potential application in water bioremediation, Microb. Cell Factories 18 (2019) 200, https://doi.org/10.1186/s12934-019-1248-0.
[138] K.M. Polyakov, S. Gavryushov, S. Ivanova, T.V. Fedorova, O.A. Glazunova, A. N. Popov, O.V. Koroleva, Structural study of the X-ray-induced enzymatic reduction of molecular oxygen to water by Steccherinum murashkinskyi laccase: insights into the reaction mechanism, acta crystallographica. section D, Struct. Biol. 73 (2017) 388–401, https://doi.org/10.1107/s2059798317003667.
[139] H. Liang, F. Lin, Z. Zhang, B. Liu, S. Jiang, Q. Yuan, J. Liu, Multicopper laccase mimicking nanozymes with nucleotides as ligands, ACS Appl. Mater. Interfaces 9 (2017) 1352–1360, https://doi.org/10.1021/acsami.6b15124.
[140] L. Huang, Y. Tang, J. Wang, X. Niu, J. Zhou, Y. Wu, Cubic Ag_2O nanoparticles as robust laccase mimetics in a smartphone-assisted colorimetric sensor for rapid and ultrasensitive detection of kanamycin in environment, Sensors Actuators B Chem. 391 (2023) 134052, https://doi.org/10.1016/j.snb.2023.134052.
[141] M. Kumawat, A. Umapathi, E. Lichtfouse, H.K. Daima, Nanozymes to fight the COVID-19 and future pandemics, Environ. Chem. Lett. 19 (2021) 3951–3957, https://doi.org/10.1007/s10311-021-01252-5.
[142] S. Jeyachandran, R. Srinivasan, T. Ramesh, A. Parivallal, J. Lee, E. Sathiyamoorthi, Recent development and application of “nanozyme” artificial enzymes—a review, Biomimetics 8 (2023) 446, https://doi.org/10.3390/biomimetics8050446.
[143] M. Wei, J. Lee, F. Xia, P. Lin, X. Hu, F. Li, D. Ling, Chemical design of nanozymes for biomedical applications, Acta Biomater. 126 (2021) 15–30, https://doi.org/10.1016/j.actbio.2021.02.036.
[144] M. Matur, H. Madhyastha, T.S. Shruthi, R. Madhyastha, S.P. Srinivas, P.N. Navya, H.K. Daima, Engineering bioactive surfaces on nanoparticles and their biological interactions, Sci. Rep. 10 (2020) 19713, https://doi.org/10.1038/s41598-020-75465-z.
[145] M. Kumawat, H. Madhyastha, M. Singh, D. Jain, H.K. Daima, Functional silver nanozymes regulate cell inflammatory cytokines expression in mouse macrophages, Colloids Surf. A Physicochem. Eng. Asp. 650 (2022) 129294, https://doi.org/10.1016/j.colsurfa.2022.129294.
[146] Y. Wang, W. Wang, Z. Gu, X. Miao, Q. Huang, B. Chang, Temperature-responsive iron nanozymes based on poly(N-vinylcaprolactam) with multi-enzyme activity, RSC Adv. 10 (2020) 39954–39966, https://doi.org/10.1039/D0RA07226E.
[147] S.L. Hooe, J.C. Breger, I.L. Medintz, Enhancing enzymatic activity with nanoparticle display – an updated compendium and engineering outlook, Mol. Syst. Des. Eng. 9 (2024) 679–704, https://doi.org/10.1039/D4ME00017J.
[148] J. Golchin, K. Golchin, N. Aliadadian, S. Ghaderi, S. Eslamkhah, M. Eslamkhah, A. Akbarzadeh, Nanozyme applications in biology and medicine: an overview, Artif. Cells Nanomed. Biotechnol. 45 (2017) 1069–1076, https://doi.org/10.1080/21691401.2017.1313268.
[149] W. Yang, X. Yang, L. Zhu, H. Chu, X. Li, W. Xu, Nanozymes: activity origin, catalytic mechanism, and biological application, Coord. Chem. Rev. 448 (2021) 214170, https://doi.org/10.1016/j.ccr.2021.214170.
[150] G. Tang, J. He, J. Liu, X. Yan, K. Fan, Nanozyme for tumor therapy: surface modification matters, Exploration 1 (2021) 75–89, https://doi.org/10.1002/EXP.20210005.

[151] S. Garehbaghi, A.M. Ashrafi, V. Adam, L. Richtera, Surface modification strategies and the functional mechanisms of gold nanozyme in biosensing and bioassay, Mater. Today Bio. 20 (2023) 100656, https://doi.org/10.1016/j.mtbio.2023.100656.
[152] M. Soh, D.-W. Kang, H.-G. Jeong, D. Kim, D.Y. Kim, W. Yang, C. Song, S. Baik, I.-Y. Choi, S.-K. Ki, H.J. Kwon, T. Kim, C.K. Kim, S.-H. Lee, T. Hyeon, Ceria–zirconia nanoparticles as an enhanced multi-antioxidant for sepsis treatment, Angew. Chem. Int. Ed. 56 (2017) 11399–11403, https://doi.org/10.1002/anie.201704904.
[153] W. Lu, J. Chen, L. Kong, F. Zhu, Z. Feng, J. Zhan, Oxygen vacancies modulation Mn_3O_4 nanozyme with enhanced oxidase-mimicking performance for l-cysteine detection, Sensors Actuators B Chem. 333 (2021) 129560, https://doi.org/10.1016/j.snb.2021.129560.
[154] F. Shah, N. Yadav, S. Singh, Phosphotungstate-sandwiched between cerium oxide and gold nanoparticles exhibit enhanced catalytic reduction of 4-nitrophenol and peroxidase enzyme-like activity, Colloids Surf. B: Biointerfaces 198 (2021) 111478, https://doi.org/10.1016/j.colsurfb.2020.111478.
[155] R. Singh, S. Singh, Role of phosphate on stability and catalase mimetic activity of cerium oxide nanoparticles, Colloids Surf. B: Biointerfaces 132 (2015) 78–84, https://doi.org/10.1016/j.colsurfb.2015.05.005.
[156] X. Xia, J. Zhang, N. Lu, M.J. Kim, K. Ghale, Y. Xu, E. McKenzie, J. Liu, H. Ye, Pd–Ir core–shell nanocubes: a type of highly efficient and versatile peroxidase mimic, ACS Nano 9 (2015) 9994–10004, https://doi.org/10.1021/acsnano.5b03525.
[157] M. Liu, L. Huang, X. Xu, X. Wei, X. Yang, X. Li, B. Wang, Y. Xu, L. Li, Z. Yang, Copper doped carbon dots for addressing bacterial biofilm formation, wound infection, and tooth staining, ACS Nano 16 (2022) 9479–9497, https://doi.org/10.1021/acsnano.2c02518.
[158] Q. Liang, J. Xi, X.J. Gao, R. Zhang, Y. Yang, X. Gao, X. Yan, L. Gao, K. Fan, A metal-free nanozyme-activated prodrug strategy for targeted tumor catalytic therapy, Nano Today 35 (2020) 100935, https://doi.org/10.1016/j.nantod.2020.100935.
[159] S. Luo, M. Sha, F. Tian, X. Li, L. Fu, Y. Gu, L.-L. Qu, G.-H. Yang, C. Zhu, Nitrogen and boron Co-doped graphene nanoribbons as peroxidase-mimicking nanozymes for enhanced biosensing, Chin. Chem. Lett. 33 (2022) 344–348, https://doi.org/10.1016/j.cclet.2021.06.018.
[160] N. Dhiman, S. Ghosh, Y.K. Mishra, K.M. Tripathi, Prospects of nano-carbons as emerging catalysts for enzyme-mimetic applications, Mater. Adv. 3 (2022) 3101–3122, https://doi.org/10.1039/D2MA00034B.
[161] K. Fan, J. Xi, L. Fan, P. Wang, C. Zhu, Y. Tang, X. Xu, M. Liang, B. Jiang, X. Yan, L. Gao, In vivo guiding nitrogen-doped carbon nanozyme for tumor catalytic therapy, Nat. Commun. 9 (2018) 1440, https://doi.org/10.1038/s41467-018-03903-8.
[162] W. Zhu, N. Hao, J. Lu, Z. Dai, J. Qian, X. Yang, K. Wang, Highly active metal-free peroxidase mimics based on oxygen-doped carbon nitride by promoting electron transfer capacity, Chem. Commun. 56 (2020) 1409–1412, https://doi.org/10.1039/C9CC08311A.
[163] K.M. Tripathi, H.T. Ahn, M. Chung, X.A. Le, D. Saini, A. Bhati, S.K. Sonkar, M. I. Kim, T. Kim, N, S, and P-co-doped carbon quantum dots: intrinsic peroxidase activity in a wide pH range and its antibacterial applications, ACS Biomater Sci. Eng. 6 (2020) 5527–5537, https://doi.org/10.1021/acsbiomaterials.0c00831.
[164] V.K. Bajpai, I. Khan, S. Shukla, S.M. Kang, F. Aziz, K.M. Tripathi, D. Saini, H. J. Cho, N. Su Heo, S.K. Sonkar, L. Chen, Y. Suk Huh, Y.K. Han, Multifunctional N-P-doped carbon dots for regulation of apoptosis and autophagy in B16F10 melanoma cancer cells and in vitro imaging applications, Theranostics 10 (2020) 7841–7856, https://doi.org/10.7150/thno.42291.
[165] J. Sheng, Y. Wu, H. Ding, K. Feng, Y. Shen, Y. Zhang, N. Gu, Multienzyme-like Nanozymes: regulation, rational design, and application, Adv. Mater. 36 (2024) 2211210, https://doi.org/10.1002/adma.202211210.
[166] C. Liang, J.Y. Cheong, G. Sitaru, S. Rosenfeldt, A.S. Schenk, S. Gekle, I.-D. Kim, A. Greiner, Size-dependent catalytic behavior of gold nanoparticles, Adv. Mater. Interfaces 9 (2022) 2100867, https://doi.org/10.1002/admi.202100867.
[167] H. Zhang, X. Liang, L. Han, F. Li, "Non-naked" gold with glucose oxidase-like activity: a nanozyme for tandem catalysis, Small 14 (2018) 1803256, https://doi.org/10.1002/smll.201803256.
[168] J. Yang, X. Ren, X. Zhang, X. Wang, R. Zhang, P. Bai, B. Du, L. Li, S. Zhao, Y. Qin, R. Zhang, Mechanistic and kinetic insights into size-dependent activity in ultra-small Pt/CNTs nanozymes during antibacterial process, Arab. J. Chem. 15 (2022) 104238, https://doi.org/10.1016/j.arabjc.2022.104238.
[169] S. Ghosh, P. Roy, N. Karmodak, E.D. Jemmis, G. Mugesh, Nanoisozymes: crystal-facet-dependent enzyme-mimetic activity of V_2O_5 nanomaterials, Angew. Chem. Int. Ed. 57 (2018) 4510–4515, https://doi.org/10.1002/anie.201800681.
[170] F.M. De Oliveira, L.R.B.D.A. Nascimento, C.M.S. Calado, M.R. Meneghetti, M.G. A. Da Silva, Aqueous-phase catalytic chemical reduction of p-nitrophenol employing soluble gold nanoparticles with different shapes, Catalysts 6 (2016) 215, https://doi.org/10.3390/catal6120215.
[171] W. Zhang, J. Dong, Y. Wu, P. Cao, L. Song, M. Ma, N. Gu, Y. Zhang, Shape-dependent enzyme-like activity of Co_3O_4 nanoparticles and their conjugation with his-tagged EGFR single-domain antibody, Colloids Surf. B: Biointerfaces 154 (2017) 55–62, https://doi.org/10.1016/j.colsurfb.2017.02.034.
[172] Y. Wang, Z. Tan, Z. Zhang, P. Zhu, S.W. Tam, Z. Zhang, X. Jiang, K. Lin, L. Tian, Z. Huang, S. Zhang, Y.-K. Peng, K.K.L. Yung, Facet-dependent activity of CeO_2 nanozymes regulate the fate of human neural progenitor cell via redox homeostasis, ACS Appl. Mater. Interfaces 14 (2022) 35423–35433, https://doi.org/10.1021/acsami.2c09304.
[173] E. Marin, C. Tapeinos, S. Lauciello, G. Ciofani, J.R. Sarasua, A. Larrañaga, Encapsulation of manganese dioxide nanoparticles into layer-by-layer polymer capsules for the fabrication of antioxidant microreactors, Mater. Sci. Eng. C 117 (2020) 111349, https://doi.org/10.1016/j.msec.2020.111349.
[174] L. Jiao, W. Xu, H. Yan, Y. Wu, W. Gu, H. Li, D. Du, Y. Lin, C. Zhu, A dopamine-induced au hydrogel nanozyme for enhanced biomimetic catalysis, Chem. Commun. 55 (2019) 9865–9868, https://doi.org/10.1039/C9CC04436A.
[175] A.P. Fatrekar, A.A. Vernekar, A self-assembled nanozyme featuring precise active centers and topography exhibits controlled catalytic interplay with mitochondrial protein while regulating electron flow during bioinspired oxygen reduction, J. Mater. Chem. A 13 (2025) 4299–4308, https://doi.org/10.1039/D4TA06131D.
[176] Z. Wang, Y. Zhang, E. Ju, Z. Liu, F. Cao, Z. Chen, J. Ren, X. Qu, Biomimetic nanoflowers by self-assembly of nanozymes to induce intracellular oxidative damage against hypoxic tumors, Nat. Commun. 9 (2018) 3334, https://doi.org/10.1038/s41467-018-05798-x.
[177] P. Hu, J. Zheng, H. Wang, Y. Li, T. Ye, Q. Li, X. Lan, C. Liu, C. Liu, Supramolecular nanozymes based on Self-assembly of biomolecule for Cancer therapy, Int. J. Nanomedicine 20 (2025) 2043–2057, https://doi.org/10.2147/IJN.S496831.
[178] Y. Xu, D. Hou, M. Zhao, T. Zhao, Y. Ma, Y. Zhang, Y. Guo, W. Tao, H. Wang, Amino acid and au(III) Self-assembled supramolecular Nanozymes for antimicrobial applications, ACS Appl. Nano Mater. 7 (2024) 22505–22516, https://doi.org/10.1021/acsanm.4c02397.
[179] J. Zhou, D. Xu, G. Tian, Q. He, X. Zhang, J. Liao, L. Mei, L. Chen, L. Gao, L. Zhao, G. Yang, W. Yin, G. Nie, Y. Zhao, Coordination-driven Self-assembly strategy-activated cu single-atom nanozymes for catalytic tumor-specific therapy, J. Am. Chem. Soc. 145 (2023) 4279–4293, https://doi.org/10.1021/jacs.2c13597.
[180] X. Zhang, S. Lin, Y. Wang, F. Xia, Y. Dai, Cofactor-free organic nanozyme with assembly-induced catalysis and light-regulated activity, Chem. Eng. J. 426 (2021) 130855, https://doi.org/10.1016/j.cej.2021.130855.
[181] Y. Huang, Z. Liu, C. Liu, E. Ju, Y. Zhang, J. Ren, X. Qu, Self-assembly of multi-nanozymes to mimic an intracellular antioxidant defense system, Angew. Chem. Int. Ed. 55 (2016) 6646–6650, https://doi.org/10.1002/anie.201600868.
[182] M. Kumawat, H. Madhyastha, A. Umapathi, M. Singh, N. Revaprasadu, H. K. Daima, Surface engineered peroxidase-mimicking gold nanoparticles to subside cell inflammation, Langmuir 38 (2022) 1877–1887, https://doi.org/10.1021/acs.langmuir.1c03088.
[183] G. Rattu, N. Khansili, P. Krishna, Polyacrylic acid modified cerium oxide nanoparticles: synthesis and characterization as a peroxidase mimic for non-enzymatic H_2O_2 sensor, Curr. Nanosci. 15 (2019) 816–828, https://doi.org/10.2174/1573413715666191204124329.
[184] W.A. Arcos Rosero, A. Bueno Barbezan, C. Daruich de Souza, M.E. Chuery Martins Rostelato, Review of advances in coating and functionalization of gold nanoparticles: from theory to biomedical application, Pharmaceutics 16 (2024) 255, https://doi.org/10.3390/pharmaceutics16020255.
[185] K. Fan, H. Wang, J. Xi, Q. Liu, X. Meng, D. Duan, L. Gao, X. Yan, Optimization of Fe_3O_4 nanozyme activity via single amino acid modification mimicking an enzyme active site, Chem. Commun. 53 (2017) 424–427, https://doi.org/10.1039/C6CC08542C.
[186] S. Yang, J. Ji, M. Luo, H. Li, Z. Gao, Poly(tannic acid) nanocoating based surface modification for construction of multifunctional composite CeO_2NZs to enhance cell proliferation and antioxidative viability of preosteoblasts, Nanoscale 13 (2021) 16349–16361, https://doi.org/10.1039/D1NR02799A.
[187] C.-P. Liu, T.-H. Wu, Y.-L. Lin, C.-Y. Liu, S. Wang, S.-Y. Lin, Tailoring enzyme-like activities of gold nanoclusters by polymeric tertiary amines for protecting neurons against oxidative stress, Small 12 (2016) 4127–4135, https://doi.org/10.1002/smll.201503919.
[188] P.T. Nguyen, J. Lee, A. Cho, M.S. Kim, D. Choi, J.W. Han, M.I. Kim, J. Lee, Rational development of co-doped mesoporous ceria with high peroxidase-mimicking activity at neutral pH for paper-based colorimetric detection of multiple biomarkers, Adv. Funct. Mater. 32 (2022) 2112428, https://doi.org/10.1002/adfm.202112428.
[189] G.S. Das, K.M. Tripathi, G. Kumar, S. Paul, S. Mehara, S. Bhowmik, B. Pakhira, S. Sarkar, M. Roy, T. Kim, Nitrogen-doped fluorescent graphene nanosheets as visible-light-driven photocatalysts for dye degradation and selective sensing of ascorbic acid, New J. Chem. 43 (2019) 14575–14583, https://doi.org/10.1039/C9NJ02344E.
[190] H. Sun, A. Zhao, N. Gao, K. Li, J. Ren, X. Qu, Deciphering a nanocarbon-based artificial peroxidase: chemical identification of the catalytically active and substrate-binding sites on graphene quantum dots, Angew. Chem. Int. Ed. 54 (2015) 7176–7180, https://doi.org/10.1002/anie.201500626.
[191] A.-X. Zheng, Z.-X. Cong, J.-R. Wang, J. Li, H.-H. Yang, G.-N. Chen, Highly-efficient peroxidase-like catalytic activity of graphene dots for biosensing, Biosens. Bioelectron. 49 (2013) 519–524, https://doi.org/10.1016/j.bios.2013.05.038.
[192] L. Hou, G. Jiang, Y. Sun, X. Zhang, J. Huang, S. Liu, T. Lin, F. Ye, S. Zhao, Progress and trend on the regulation methods for Nanozyme activity and its application, Catal 9 (2019) 1057, https://doi.org/10.3390/catal9121057.
[193] Z. Chen, J.-J. Yin, Y.-T. Zhou, Y. Zhang, L. Song, M. Song, S. Hu, N. Gu, Dual enzyme-like activities of Iron oxide nanoparticles and their implication for diminishing cytotoxicity, ACS Nano 6 (2012) 4001–4012, https://doi.org/10.1021/nn300291r.
[194] Y. Huang, X. Ran, Y. Lin, J. Ren, X. Qu, Self-assembly of an organic–inorganic hybrid nanoflower as an efficient biomimetic catalyst for self-activated tandem reactions, Chem. Commun. 51 (2015) 4386–4389, https://doi.org/10.1039/C5CC00040H.
[195] L. Luo, L. Huang, X. Liu, W. Zhang, X. Yao, L. Dou, X. Zhang, Y. Nian, J. Sun, J. Wang, Mixed-valence Ce-BPyDC metal–organic framework with dual enzyme-

like activities for colorimetric biosensing, Inorg. Chem. 58 (2019) 11382–11388, https://doi.org/10.1021/acs.inorgchem.9b00661.
[196] X. Xiong, Y. Tang, C. Xu, Y. Huang, Y. Wang, L. Fu, C. Lin, D. Zhou, Y. Lin, High carbonization temperature to trigger enzyme mimicking activities of silk-derived nanosheets, Small 16 (2020) 2004129, https://doi.org/10.1002/smll.202004129.
[197] S. Rasheed, M. Ikram, D. Ahmad, M. Naseer Abbas, M. Shafique, Advancements in colorimetric and fluorescent-based sensing approaches for point-of-care testing in forensic sample analysis, Microchem. J. 206 (2024) 111438, https://doi.org/10.1016/j.microc.2024.111438.
[198] X. Ma, Y. Ge, N. Xia, Overview of the design and application of dual-signal immunoassays, Molecules 29 (2024) 4551, https://doi.org/10.3390/molecules29194551.
[199] A. Thamilselvan, M.I. Kim, Recent advances on nanozyme-based electrochemical biosensors for cancer biomarker detection, TrAC Trends Anal. Chem. 177 (2024) 117815, https://doi.org/10.1016/j.trac.2024.117815.
[200] F. Zhao, L. Wang, M. Li, M. Wang, G. Liu, J. Ping, Nanozyme-based biosensor for organophosphorus pesticide monitoring: functional design, biosensing strategy, and detection application, TrAC Trends Anal. Chem. 165 (2023) 117152, https://doi.org/10.1016/j.trac.2023.117152.
[201] H. Han, C. Wang, X. Yang, S. Zheng, X. Cheng, Z. Liu, B. Zhao, R. Xiao, Rapid field determination of SARS-CoV-2 by a colorimetric and fluorescent dual-functional lateral flow immunoassay biosensor, Sensors Actuators B Chem. 351 (2022) 130897, https://doi.org/10.1016/j.snb.2021.130897.
[202] L. Jiao, H. Yan, Y. Wu, W. Gu, C. Zhu, D. Du, Y. Lin, When nanozymes meet single-atom catalysis, Angew. Chem. Int. Ed. 132 (2020) 2585–2596, https://doi.org/10.1002/ange.201905645.
[203] S.Y. Lim, W. Shen, Z. Gao, Carbon quantum dots and their applications, Chem. Soc. Rev. 44 (2015) 362–381, https://doi.org/10.1039/C4CS00269E.
[204] M. Wu, Y. Lv, Z. Lin, Dual-mode colorimetric and fluorescence sensing system for the detection of captopril based on Fe/NC nanozymes and carbon dots, Spectrochim. Acta A Mol. Biomol. Spectrosc. 282 (2022) 121683, https://doi.org/10.1016/j.saa.2022.121683.
[205] C. Hu, Y. Yin, C. Huang, Y. Dong, J. Liu, F. Xiao, S. Yang, Cobalt-nitrogen co-doped carbon dots for the colorimetric and fluorometric dual-mode detection of gallic acid, Microchem. J. 197 (2024) 109735, https://doi.org/10.1016/j.microc.2023.109735.
[206] Y. Zhang, M. Wang, C. Shao, T. Liu, M. Sun, C. Wu, G. Su, Y. Wang, J. Ye, H. Hu, Y. Li, H. Rao, Z. Lu, Nanozyme-induced deep learning-assisted smartphone integrated colorimetric and fluorometric dual-mode for detection of tetracycline analogs, Anal. Chim. Acta 1297 (2024) 342373, https://doi.org/10.1016/j.aca.2024.342373.
[207] X. Ding, W. Ahmad, Y. Rong, J. Wu, Q. Ouyang, Q. Chen, A dual-mode fluorescence and colorimetric sensing platform for efficient detection of ofloxacin in aquatic products using iron alkoxide nanozyme, Food Chem. 442 (2024) 138417, https://doi.org/10.1016/j.foodchem.2024.138417.
[208] L. Nie, L. Jiang, S. Li, D. Song, G. Dong, L. Bu, C. Chen, Q. Zhou, Smartphone-assisted array discrimination of sulfur-containing compounds and colorimetric−fluorescence dual-mode sensor for detection of 1,4-benzenedithiol based on peroxidase-like nanozyme g-C_3N_4@Cu, N-CDs, Talanta 275 (2024) 126119, https://doi.org/10.1016/j.talanta.2024.126119.
[209] G. Fu, S.T. Sanjay, M. Dou, X. Li, Nanoparticle-mediated photothermal effect enables a new method for quantitative biochemical analysis using a thermometer, Nanoscale 8 (2016) 5422–5427, https://doi.org/10.1039/C5NR09051B.
[210] G. Cai, Z. Yu, P. Tong, D. Tang, Ti_3C_2 MXene quantum dot-encapsulated liposomes for photothermal immunoassays using a portable near-infrared imaging camera on a smartphone, Nanoscale 11 (2019) 15659–15667, https://doi.org/10.1039/C9NR05797H.
[211] P.K. Gupta, S.E. Son, J. Venkatesan, G.H. Seong, Cauliflower-like platinum nanostructures mediated photothermal and colorimetric dual-readout biosensor for sensitive cholesterol detection, Sensors Actuators B Chem. 386 (2023) 133741, https://doi.org/10.1016/j.snb.2023.133741.
[212] W. Jiang, Y. Feng, C. Jiang, H. Li, Z. Wang, Y. Xiao, W. Lan, Y. Liu, Platinum-nickel nanoparticle-based oxidase-like nanozyme for colorimetric/photothermal dual-mode detection of organophosphorus pesticides, Sensors Actuators B Chem. 412 (2024) 135861, https://doi.org/10.1016/j.snb.2024.135861.
[213] G. Marucci, M. Buccioni, D.D. Ben, C. Lambertucci, R. Volpini, F. Amenta, Efficacy of acetylcholinesterase inhibitors in Alzheimer's disease, Neuropharmacology 190 (2021) 108352, https://doi.org/10.1016/j.neuropharm.2020.108352.
[214] L. Lu, X. Hu, R. Zeng, Q. Lin, X. Huang, M. Li, D. Tang, Dual-mode colorimetric-photothermal sensing platform of acetylcholinesterase activity based on the peroxidase-like activity of Fe–N–C nanozyme, Anal. Chim. Acta 1229 (2022) 340383, https://doi.org/10.1016/j.aca.2022.340383.
[215] H. Shang, X. Zhang, M. Ding, A. Zhang, C. Wang, A smartphone-assisted colorimetric and photothermal probe for glutathione detection based on enhanced oxidase-mimic CoFeCe three-atom nanozyme in food, Food Chem. 423 (2023) 136296, https://doi.org/10.1016/j.foodchem.2023.136296.
[216] R. Li, M. He, Y. Cui, X. Ji, L. Zhang, X. Lan, L. Wang, Z. Han, H. Xiao, Silver-palladium bimetallic nanoparticles stabilized by elm pod polysaccharide with peroxidase-like properties for glutathione detection and photothermal anti-tumor ability, Int. J. Biol. Macromol. 264 (2024) 130673, https://doi.org/10.1016/j.ijbiomac.2024.130673.
[217] Z. Yu, H. Gong, M. Li, D. Tang, Hollow prussian blue nanozyme-richened liposome for artificial neural network-assisted multimodal colorimetric-photothermal immunoassay on smartphone, Biosens. Bioelectron. 218 (2022) 114751, https://doi.org/10.1016/j.bios.2022.114751.
[218] S. Huang, W. Lai, B. Liu, M. Xu, J. Zhuang, D. Tang, Y. Lin, Colorimetric and photothermal dual-mode immunoassay of aflatoxin B1 based on peroxidase-like activity of Pt supported on nitrogen-doped carbon, Spectrochim. Acta A Mol. Biomol. Spectrosc. 284 (2023) 121782, https://doi.org/10.1016/j.saa.2022.121782.
[219] Y.H. Soung, S. Ford, V. Zhang, J. Chung, Exosomes in Cancer diagnostics, Cancers 9 (2017) 8, https://doi.org/10.3390/cancers9010008.
[220] X. Zhang, X. Zhu, Y. Li, X. Hai, S. Bi, A colorimetric and photothermal dual-mode biosensing platform based on nanozyme-functionalized flower-like DNA structures for tumor-derived exosome detection, Talanta 258 (2023) 124456, https://doi.org/10.1016/j.talanta.2023.124456.
[221] X. Wang, X. Tang, C. Ji, L. Wu, Y. Zhu, Advances and future trends in nanozyme-based SERS sensors for food safety, environmental and biomedical applications, Int. J. Mol. Sci. 26 (2025) 709, https://doi.org/10.3390/ijms26020709.
[222] P. Wen, F. Yang, L. Tang, X. Hu, H. Zhao, B. Tang, L. Chen, Precise regulation and control of hotspots in nanoparticle multilayer SERS substrates, Microchem. J. 187 (2023) 108371, https://doi.org/10.1016/j.microc.2022.108371.
[223] M. Arabi, L. Chen, Technical challenges of molecular-imprinting-based optical sensors for environmental pollutants, Langmuir 38 (2022) 5963–5967, https://doi.org/10.1021/acs.langmuir.2c00935.
[224] M. Arabi, A. Ostovan, Z. Zhang, Y. Wang, R. Mei, L. Fu, X. Wang, J. Ma, L. Chen, Label-free SERS detection of Raman-inactive protein biomarkers by Raman reporter indicator: toward ultrasensitivity and universality, Biosens. Bioelectron. 174 (2021) 112825, https://doi.org/10.1016/j.bios.2020.112825.
[225] L. Liang, Y. Jiang, F. Liu, J. Wu, L. Tian, S. Zhao, F. Ye, Smartphone flashlight-triggered covalent organic framework nanozyme activity: a universal scheme for visual point-of-care testing, Sensors Actuators B Chem. 381 (2023) 133422, https://doi.org/10.1016/j.snb.2023.133422.
[226] X. Wang, X. Chen, R. Zhou, P. Hu, K. Huang, P. Chen, Filter-assisted separation of multiple nanomaterials: mechanism and application in atomic/mass spectrometry/fluorescence label-free multimode bioassays, Anal. Chem. 93 (2021) 3889–3897, https://doi.org/10.1021/acs.analchem.0c04562.
[227] Y. Li, P. Li, Y. Chen, Y. Wu, J. Wei, Interfacial deposition of ag nanozyme on metal-polyphenol nanosphere for SERS detection of cellular glutathione, Biosens. Bioelectron. 228 (2023) 115200, https://doi.org/10.1016/j.bios.2023.115200.
[228] X. Xia, Y. Weng, L. Zhang, R. Tang, X. Zhang, A facile SERS strategy to detect glucose utilizing tandem enzyme activities of Au@Ag nanoparticles, Spectrochim. Acta A Mol. Biomol. Spectrosc. 259 (2021) 119889, https://doi.org/10.1016/j.saa.2021.119889.
[229] S. Wen, X. Ma, H. Liu, G. Chen, H. Wang, G. Deng, Y. Zhang, W. Song, B. Zhao, Y. Ozaki, Accurate monitoring platform for the surface catalysis of nanozyme validated by surface-enhanced Raman-kinetics model, Anal. Chem. 92 (2020) 11763–11770, https://doi.org/10.1021/acs.analchem.0c01886.
[230] M.Y. Chan, W. Leng, P.J. Vikesland, Surface-enhanced Raman spectroscopy characterization of salt-induced aggregation of gold nanoparticles, ChemPhysChem 19 (2018) 24–28, https://doi.org/10.1002/cphc.201700798.
[231] W. Wang, B. Zhang, Y. Zhang, P. Ma, X. Wang, Y. Sun, D. Song, Q. Fei, Colorimetry and SERS dual-mode sensing of serotonin based on functionalized gold nanoparticles, Spectrochim. Acta A Mol. Biomol. Spectrosc. 261 (2021) 120057, https://doi.org/10.1016/j.saa.2021.120057.
[232] M. Qi, B. Wang, H. Jiang, Y. Li, P. Li, X. Zhang, L. Han, Smartphone readable colorimetry and surface-enhanced raman scattering (SERS) dual-mode sensing platform for ascorbic acid detection based on GeO_2 composite nanozymes, J. Food Compos. Anal. 125 (2024) 105740, https://doi.org/10.1016/j.jfca.2023.105740.
[233] Y. Cui, Q. Li, D. Yang, Y. Yang, Colorimetric-SERS dual-mode sensing of Pb(II) ions in traditional chinese medicine samples based on carbon dots-capped gold nanoparticles as nanozyme, Spectrochim. Acta A Mol. Biomol. Spectrosc. 313 (2024) 124100, https://doi.org/10.1016/j.saa.2024.124100.
[234] X. Tan, K. Kang, R. Zhang, J. Dong, W. Wang, W. Kang, An ultrasensitive dual-mode approach for AFB1 detection: colorimetric/label-free SERS aptasensor based on a self-assembled core-shell structured Ag@Au IP6 bifunctional nanozyme, Sensors Actuators B Chem. 412 (2024) 135854, https://doi.org/10.1016/j.snb.2024.135854.
[235] Y. Huang, Y. Gu, X. Liu, T. Deng, S. Dai, J. Qu, G. Yang, L. Qu, Reusable ring-like Fe_3O_4/au nanozymes with enhanced peroxidase-like activities for colorimetric-SERS dual-mode sensing of biomolecules in human blood, Biosens. Bioelectron. 209 (2022) 114253, https://doi.org/10.1016/j.bios.2022.114253.
[236] D.-K. Lim, K.-S. Jeon, J.-H. Hwang, H. Kim, S. Kwon, Y.D. Suh, J.-M. Nam, Highly uniform and reproducible surface-enhanced Raman scattering from DNA-tailorable nanoparticles with 1-nm interior gap, Nat. Nanotechnol. 6 (2011) 452–460, https://doi.org/10.1038/nnano.2011.79.
[237] H. Imanzadeh, Y. Sefid-Sefidehkhan, H. Afshary, A. Afruz, M. Amiri, Nanomaterial-based electrochemical sensors for detection of amino acids, J. Pharm. Biomed. Anal. 230 (2023) 115390, https://doi.org/10.1016/j.jpba.2023.115390.
[238] C. Gu, L. Bai, T. Hou, L. Zhang, P. Gai, F. Li, Dual-mode colorimetric and homogeneous electrochemical detection of intracellular/extracellular H_2O_2 based on FeSx/SiO_2 nanoparticles with high peroxidase-like activity, Anal. Chim. Acta 1265 (2023) 341332, https://doi.org/10.1016/j.aca.2023.341332.
[239] W. Wang, S. Xiao, M. Zeng, H. Xie, N. Gan, Dual-mode colorimetric-electrochemical biosensor for vibrio parahaemolyticus detection based on CuO_2 nanodot-encapsulated metal-organic framework nanozymes, Sensors Actuators B Chem. 387 (2023) 133835, https://doi.org/10.1016/j.snb.2023.133835.
[240] Z. Xi, K. Wei, Q. Wang, M.J. Kim, S. Sun, V. Fung, X. Xia, Nickel–platinum nanoparticles as peroxidase mimics with a record high catalytic efficiency, J. Am. Chem. Soc. 143 (2021) 2660–2664, https://doi.org/10.1021/jacs.0c12605.

[241] J. Wu, Q. Yang, Q. Li, H. Li, F. Li, Two-dimensional MnO_2 nanozyme-mediated homogeneous electrochemical detection of organophosphate pesticides without the interference of H_2O_2 and color, Anal. Chem. 93 (2021) 4084–4091, https://doi.org/10.1021/acs.analchem.0c05257.
[242] Y. Zhang, Y. Han, Z. Liu, L. Fan, Y. Guo, Colorimetric and electrochemical assay for dual-mode detection of di-2-ethylhexyl phthalate based on hemin-graphene nanocomposites, Microchem. J. 191 (2023) 108788, https://doi.org/10.1016/j.microc.2023.108788.
[243] P. Lei, N. Wu, Y. Zhou, C. Dong, Y. Liu, S. Shuang, Cu/Zr metal–organic frameworks with high peroxidase-like activity for sensitive electrochemical and colorimetric dual-mode detection of hydrogen peroxide released from living cells, ACS Appl. Nano Mater. 7 (2024) 6556–6563, https://doi.org/10.1021/acsanm.4c00321.
[244] S. Chen, P. Zhao, L. Jiang, S. Zhou, J. Zheng, X. Luo, D. Huo, C. Hou, Cu_2O-mediated assembly of electrodeposition of Au nanoparticles onto 2D metal-organic framework nanosheets for real-time monitoring of hydrogen peroxide released from living cells, Anal. Bioanal. Chem. 413 (2021) 613–624, https://doi.org/10.1007/s00216-020-03032-6.
[245] H. Cheng, Z. Wang, H. Sun, B. Chen, J. Huang, R. Jia, X. He, K. Wang, Colorimetric and electrochemical integrated dual-mode detection of glucose by utilizing CoOOH@Cu nanosheets as peroxidase mimetics, Chem. Commun. 58 (2022) 13487–13490, https://doi.org/10.1039/D2CC05578C.
[246] J.U. Kim, J.M. Kim, A. Thamilselvan, K.-H. Nam, M.I. Kim, Colorimetric and electrochemical dual-mode detection of Thioredoxin 1 based on the efficient peroxidase-mimicking and electrocatalytic property of Prussian blue nanoparticles, Biosensors 14 (2024) 185, https://doi.org/10.3390/bios14040185.
[247] M. Chen, P.L. Burn, P.E. Shaw, Luminescence-based detection and identification of illicit drugs, Phys. Chem. Chem. Phys. 25 (2023) 13244–13259, https://doi.org/10.1039/D3CP00524K.
[248] M. Liang, K. Fan, Y. Pan, H. Jiang, F. Wang, D. Yang, D. Lu, J. Feng, J. Zhao, L. Yang, X. Yan, Fe_3O_4 magnetic nanoparticle peroxidase mimetic-based colorimetric assay for the rapid detection of organophosphorus pesticide and nerve agent, Anal. Chem. 85 (2013) 308–312, https://doi.org/10.1021/ac302781r.
[249] G. Zhu, L. Singh, Y. Wang, R. Singh, B. Zhang, F. Liu, B.K. Kaushik, S. Kumar, Tapered optical fiber-based LSPR biosensor for ascorbic acid detection, Photonic Sens. 11 (2021) 418–434.
[250] B.-B. Wang, X. Zhao, L.-J. Chen, C. Yang, X.-P. Yan, Functionalized persistent luminescence nanoparticle-based aptasensor for autofluorescence-free determination of kanamycin in food samples, Anal. Chem. 93 (2021) 2589–2595, https://doi.org/10.1021/acs.analchem.0c04648.
[251] L.-M. Pan, X. Zhao, X. Wei, L.-J. Chen, C. Wang, X.-P. Yan, Ratiometric luminescence Aptasensor based on dual-emissive persistent luminescent nanoparticles for autofluorescence- and exogenous interference-free determination of trace aflatoxin B1 in food samples, Anal. Chem. 94 (2022) 6387–6393, https://doi.org/10.1021/acs.analchem.2c00861.
[252] J. Liu, J. Chen, D. Wu, M. Huang, J. Chen, R. Pan, Y. Wu, G. Li, CRISPR-/Cas12a-mediated liposome-amplified strategy for the surface-enhanced Raman scattering and naked-eye detection of nucleic acid and application to food authenticity screening, Anal. Chem. 93 (2021) 10167–10174, https://doi.org/10.1021/acs.analchem.1c01163.
[253] H. Shang, X. Zhang, M. Ding, A. Zhang, Dual-mode biosensor platform based on synergistic effects of dual-functional hybrid nanomaterials, Talanta 260 (2023) 124584, https://doi.org/10.1016/j.talanta.2023.124584.
[254] G. Xing, J. Zhao, J. Tang, Y. Zhao, J. Liu, Lanthanide-grafted covalent organic framework as a colorimetric and luminescence dual-mode nanoprobe for tetracycline detection, Sensors Actuators B Chem. 411 (2024) 135724, https://doi.org/10.1016/j.snb.2024.135724.
[255] L.-X. Yan, Z.-Y. Yan, X. Zhao, L.-J. Chen, X.-P. Yan, Highly efficient persistent luminescent nanozymes-based luminescence-colorimetric dual-mode sensor for total antioxidant capacity assay, Sensors Actuators B Chem. 405 (2024) 135333, https://doi.org/10.1016/j.snb.2024.135333.
[256] X. Chen, H. Zhang, X. Liang, L. Li, Dual-responsive persistent luminescence nanoflowers for glutathione detection and imaging, Sensors Actuators B Chem. 403 (2024) 135200, https://doi.org/10.1016/j.snb.2023.135200.
[257] N. Song, Y. Zhang, S. Ren, C. Wang, X. Lu, Rational design of conducting polymer-derived tubular carbon nanoreactors for enhanced enzyme-like catalysis and Total antioxidant capacity bioassay application, Anal. Chem. 94 (2022) 11695–11702, https://doi.org/10.1021/acs.analchem.2c02511.
[258] J. Yan, B. Yin, Q. Zhang, C. Li, J. Chen, Y. Huang, J. Hao, C. Yi, Y. Zhang, S.H. D. Wong, M. Yang, A CRISPR-Cas12a-mediated dual-mode luminescence and colorimetric nucleic acid biosensing platform based on upconversion nanozyme, Biosens. Bioelectron. 270 (2025) 116963, https://doi.org/10.1016/j.bios.2024.116963.
[259] L. Zhao, J. Xu, L. Xiong, S. Wang, C. Yu, J. Lv, J.-M. Lin, Recent development of chemiluminescence for bioanalysis, TrAC Trends Anal. Chem. 166 (2023) 117213, https://doi.org/10.1016/j.trac.2023.117213.
[260] Y. Guo, X. Wang, X. Liu, S. Wei, C. Le, J. Wang, C. Zhao, Preprint a Colorimetric and Chemiluminescence Dual-Mode Sensing Strategy Detecting *Staphylococcus Aureus* Based on Bacteria-Imprinted Composite Film and Aunps Embedded Covalent Organic Framework Nanozyme, 2023.
[261] K. Liu, Y. Wang, H. Zhu, F. Shi, Z. Lai, Y. Long, C. Ren, J. Li, Z. Yang, Inert-remodeling strategy to build bimetal-confined nitrogen-doped carbon nanozyme for colorimetric-chemiluminescent imaging dual-mode cascade enzyme sensing, Talanta 288 (2025) 127698, https://doi.org/10.1016/j.talanta.2025.127698.
[262] N. Gupta, K. Todi, T. Narayan, B.D. Malhotra, Graphitic carbon nitride-based nanoplatforms for biosensors: design strategies and applications, Mater. Today Chem. 24 (2022) 100770, https://doi.org/10.1016/j.mtchem.2021.100770.
[263] Y. Tang, N. Qiu, L. Pi, Y. Li, X. Yang, An electrochemiluminescent/colorimetric dual-mode biosensor for ultrasensitive detection of amyloid β based on Cu^{2+}-g-C_3N_4 nanomaterials, Microchem. J. 207 (2024) 111680, https://doi.org/10.1016/j.microc.2024.111680.
[264] M. Sun, R. Li, J. Zhang, K. Yan, M. Liu, One-pot synthesis of a CdS-reduced graphene oxide–carbon nitride composite for self-powered photoelectrochemical aptasensing of PCB72, Nanoscale 11 (2019) 5982–5988, https://doi.org/10.1039/C9NR00966C.
[265] A. Devadoss, P. Sudhagar, C. Terashima, K. Nakata, A. Fujishima, Photoelectrochemical biosensors: new insights into promising photoelectrodes and signal amplification strategies, J Photochem. Photobiol. C: Photochem. Rev. 24 (2015) 43–63, https://doi.org/10.1016/j.jphotochemrev.2015.06.002.
[266] B. Çakıroğlu, M. Özacar, A self-powered photoelectrochemical glucose biosensor based on supercapacitor Co_3O_4-CNT hybrid on TiO_2, Biosens. Bioelectron. 119 (2018) 34–41, https://doi.org/10.1016/j.bios.2018.07.049.
[267] M. Sun, Y. Zhu, K. Yan, J. Zhang, Dual-mode visible light-induced aptasensing platforms for bleomycin detection based on CdS–In_2S_3 heterojunction, Biosens. Bioelectron. 145 (2019) 111712, https://doi.org/10.1016/j.bios.2019.111712.
[268] Y. Cheng, R.-M. Kong, W. Hu, X. Tian, L. Zhang, L. Xia, F. Qu, Colorimetric-assisted photoelectrochemical sensing for dual-model detection of sialic acid via oxidation-power mediator integration, Chin. Chem. Lett. 34 (2023) 107502, https://doi.org/10.1016/j.cclet.2022.05.016.
[269] J. Wei, S. Liu, A. Qileng, W. Qin, W. Liu, K. Wang, Y. Liu, A photoelectrochemical/colorimetric immunosensor for broad-spectrum detection of ochratoxins using bifunctional copper oxide nanoflowers, Sensors Actuators B Chem. 330 (2021) 129380, https://doi.org/10.1016/j.snb.2020.129380.
[270] L. Li, Y. Zhang, L. Zhang, S. Ge, H. Liu, N. Ren, M. Yan, J. Yu, Paper-based device for colorimetric and Photoelectrochemical quantification of the flux of H_2O_2 releasing from MCF-7 cancer cells, Anal. Chem. 88 (2016) 5369–5377, https://doi.org/10.1021/acs.analchem.6b00693.
[271] J. Xia, Z. Li, Y. Ding, L.A. Shah, H. Zhao, D. Ye, J. Zhang, Construction and application of Nanozyme sensor arrays, Anal. Chem. 96 (2024) 8221–8233, https://doi.org/10.1021/acs.analchem.4c00670.
[272] X. Wang, L. Qin, M. Zhou, Z. Lou, H. Wei, Nanozyme sensor arrays for detecting versatile Analytes from small molecules to proteins and cells, Anal. Chem. 90 (2018) 11696–11702, https://doi.org/10.1021/acs.analchem.8b03374.
[273] W. Jing, Y. Wang, Q. Shi, Y. Yang, Y. Dai, F. Liu, $Cu_2(OH)_3NO_3$ nanozyme sensor array for the discrimination of multiple sulfides in food, Biosens. Bioelectron. 262 (2024) 116529, https://doi.org/10.1016/j.bios.2024.116529.
[274] H. Huang, M. Li, M. Hao, L.L. Yu, Y. Li, A novel selective detection method for sulfide in food systems based on the GMP-cu nanozyme with laccase activity, Talanta 235 (2021) 122775, https://doi.org/10.1016/j.talanta.2021.122775.
[275] X. Zhang, D. Wu, Y. Wu, G. Li, Bioinspired nanozyme for portable immunoassay of allergenic proteins based on a smartphone, Biosens. Bioelectron. 172 (2021) 112776, https://doi.org/10.1016/j.bios.2020.112776.
[276] J. Xu, Y. Wang, Z. Li, F. Liu, W. Jing, Machine learning assisted multi-signal nanozyme sensor array for the antioxidant phenolic compounds intelligent recognition, Food Chem. 471 (2025) 142826, https://doi.org/10.1016/j.foodchem.2025.142826.
[277] Q. Shi, Y. Wang, Q. Zhang, Y. Dai, F. Liu, W. Jing, $Cu_2Cl(OH)_3$ nanozyme-based colorimetric sensor array for phosphates discrimination and disease identification, Talanta 280 (2024) 126724, https://doi.org/10.1016/j.talanta.2024.126724.
[278] X. Yang, Z. Bi, C. Yin, H. Huang, Y. Li, A novel hybrid sensor array based on the polyphenol oxidase and its nanozymes combined with the machine learning based dual output model to identify tea polyphenols and Chinese teas, Talanta 272 (2024) 125842, https://doi.org/10.1016/j.talanta.2024.125842.
[279] H. Lv, X. Ma, G. Zhang, H. Wang, X. Hai, S. Bi, A bimetallic peroxidase-mimicking nanozyme with antifouling property for construction of sensor array to identify phosphoproteins and diagnose cancers, Biosens. Bioelectron. 258 (2024) 116370, https://doi.org/10.1016/j.bios.2024.116370.
[280] K. Tang, W. Zuo, Y. Tan, X. Wang, Q. Zhou, Z. Zhang, Microvolume ratiometric fluorescence capillary imprinted array sensor based on bimetallic-nanozyme for rapid intelligent visual detection of five glucocorticoids, Sensors Actuators B Chem. 432 (2025) 137483, https://doi.org/10.1016/j.snb.2025.137483.
[281] K. Dashtian, F. Afshar Gheshlaghi, R. Zare-Dorabei, M. Mahdavi, Prussian blue analogues-derived molecularly imprinted Nanozyme Array for septicemia detection, ACS Appl. Bio Mater. 7 (2024) 3346–3357, https://doi.org/10.1021/acsabm.4c00297.
[282] W. Kroutil, M. Rueping, Introduction to ACS catalysis virtual special issue on cascade catalysis, ACS Catal. 4 (2014) 2086–2087, https://doi.org/10.1021/cs500622h.
[283] J.H. Schrittwieser, S. Velikogne, M. Hall, W. Kroutil, Artificial biocatalytic linear cascades for preparation of organic molecules, Chem. Rev. 118 (2018) 270–348, https://doi.org/10.1021/acs.chemrev.7b00033.
[284] K.S. Rabe, J. Müller, M. Skoupi, C.M. Niemeyer, Cascades in compartments: En route to machine-assisted biotechnology, Angew. Chem. Int. Ed. 56 (2017) 13574–13589, https://doi.org/10.1002/anie.201703806.
[285] G. Guan, L. Yang, Q. Mei, K. Zhang, Z. Zhang, M.-Y. Han, Chemiluminescence switching on peroxidase-like Fe_3O_4 nanoparticles for selective detection and simultaneous determination of various pesticides, Anal. Chem. 84 (2012) 9492–9497, https://doi.org/10.1021/ac302341b.

[286] B. Ding, S. Shao, H. Xiao, C. Sun, X. Cai, F. Jiang, X. Zhao, P.A. Ma, J. Lin, $MnFe_2O_4$-decorated large-pore mesoporous silica-coated upconversion nanoparticles for near-infrared light-induced and O_2 self-sufficient photodynamic therapy, Nanoscale 11 (2019) 14654–14667, https://doi.org/10.1039/C9NR04858H.
[287] Y. Huang, M. Zhao, S. Han, Z. Lai, J. Yang, C. Tan, Q. Ma, Q. Lu, J. Chen, X. Zhang, Z. Zhang, B. Li, B. Chen, Y. Zong, H. Zhang, Growth of au nanoparticles on 2D metalloporphyrinic metal-organic framework nanosheets used as biomimetic catalysts for cascade reactions, Adv. Mater. 29 (2017) 1700102, https://doi.org/10.1002/adma.201700102.
[288] Z. Cao, L. Zhang, J. Liu, D. Wang, K. Liang, Y. Chen, Z. Gu, A dual enzyme-mimicking radical generator for enhanced photodynamic therapy via series–parallel catalysis, Nanoscale 13 (2021) 17386–17395, https://doi.org/10.1039/D1NR04104E.
[289] J. Kim, H.R. Cho, H. Jeon, D. Kim, C. Song, N. Lee, S.H. Choi, T. Hyeon, Continuous O_2-evolving $MnFe_2O_4$ nanoparticle-anchored mesoporous silica nanoparticles for efficient photodynamic therapy in hypoxic Cancer, J. Am. Chem. Soc. 139 (2017) 10992–10995, https://doi.org/10.1021/jacs.7b05559.
[290] M. Chang, Z. Wang, C. Dong, R. Zhou, L. Chen, H. Huang, W. Feng, Z. Wang, Y. Wang, Y. Chen, Ultrasound-amplified Enzyodynamic tumor therapy by perovskite Nanoenzyme-enabled cell Pyroptosis and Cascade catalysis, Adv. Mater. 35 (2023) 2208817, https://doi.org/10.1002/adma.202208817.
[291] Y. Zhu, Y. Pan, Z. Guo, D. Jin, W. Wang, M. Liu, M. Zong, X. Zheng, Y. Wu, L. Wang, C. Tian, J. Cheng, Y. Liu, Photothermal enhanced and tumor microenvironment responsive nanozyme for amplified cascade enzyme catalytic therapy, Adv. Healthc. Mater. 12 (2023) 2202198, https://doi.org/10.1002/adhm.202202198.
[292] S. Dong, Y. Dong, T. Jia, S. Liu, J. Liu, D. Yang, F. He, S. Gai, P. Yang, J. Lin, GSH-depleted Nanozymes with hyperthermia-enhanced dual enzyme-mimic activities for tumor nanocatalytic therapy, Adv. Mater. 32 (2020) 2002439, https://doi.org/10.1002/adma.202002439.
[293] M. Huo, L. Wang, Y. Chen, J. Shi, Tumor-selective catalytic nanomedicine by nanocatalyst delivery, Nat. Commun. 8 (2017) 357, https://doi.org/10.1038/s41467-017-00424-8.
[294] Q. Xu, H. Yuan, X. Dong, Y. Zhang, M. Asif, Z. Dong, W. He, J. Ren, Y. Sun, F. Xiao, Dual nanoenzyme modified microelectrode based on carbon fiber coated with AuPd alloy nanoparticles decorated graphene quantum dots assembly for electrochemical detection in clinic cancer samples, Biosens. Bioelectron. 107 (2018) 153–162, https://doi.org/10.1016/j.bios.2018.02.026.
[295] Y. Zhao, Y. Huang, H. Zhu, Q. Zhu, Y. Xia, Three-in-one: sensing, self-assembly, and cascade catalysis of cyclodextrin modified gold nanoparticles, J. Am. Chem. Soc. 138 (2016) 16645–16654, https://doi.org/10.1021/jacs.6b07590.
[296] J. Zhang, J. Wang, J. Liao, Y. Lin, C. Zheng, J. Liu, In situ fabrication of Nanoceria with oxidase-like activity at neutral pH: mechanism and boosted bio-nanozyme cascades, ACS Appl. Mater. Interfaces 13 (2021) 50236–50245, https://doi.org/10.1021/acsami.1c14831.
[297] X. Zhang, F. Zhang, Z. Lu, Q. Xu, C. Hou, Z. Wang, Coupling two sequential biocatalysts with close proximity into metal–organic frameworks for enhanced cascade catalysis, ACS Appl. Mater. Interfaces 12 (2020) 25565–25571, https://doi.org/10.1021/acsami.0c04317.
[298] G. Pant, S. Singh, P.K. Choudhary, P.C. Ramamurthy, H. Singh, D. Garlapati, J. Singh, G. Kumar, N.A. Khan, S. Zahmatkesh, Nanozymes: advance enzyme-mimicking theragnostic tool: a review, Clean Techn. Environ. Policy 26 (2024) 3685–3695, https://doi.org/10.1007/s10098-023-02716-8.
[299] H. Wang, W. Ouyang, H. Liu, Tumor microenvironment responsive nanozymes for multimodal imaging of tumors, Nano TransMed. 3 (2024) 100032, https://doi.org/10.1016/j.ntm.2024.100032.
[300] R. Singh, A. Sharma, J. Saji, A. Umapathi, S. Kumar, H.K. Daima, Smart nanomaterials for cancer diagnosis and treatment, Nano Converg. 9 (2022) 21, https://doi.org/10.1186/s40580-022-00313-x.
[301] L. Li, Z. Lin, X. Xu, W. Wang, H. Chen, Z. Feng, Z. Yang, J. Hao, A pH/GSH/glucose responsive nanozyme for tumor cascade amplified starvation and chemodynamic theranostics, ACS Appl. Mater. Interfaces 15 (2023) 41224–41236, https://doi.org/10.1021/acsami.3c05412.
[302] D. Liang, Y. Yang, G. Li, Q. Wang, H. Chen, X. Deng, Endogenous H_2O_2-sensitive and weak acidic pH-triggered nitrogen-doped graphene nanoparticles (N-GNMs) in the tumor microenvironment serve as peroxidase-mimicking Nanozymes for tumor-specific treatment, Materials 14 (2021) 1933, https://doi.org/10.3390/ma14081933.
[303] C. Wen, H. Chen, X. Guo, Z. Lin, S. Zhang, X.-C. Shen, H. Liang, Lysosome-targeted gold Nanotheranostics for in situ SERS monitoring pH and multimodal imaging-guided phototherapy, Langmuir 37 (2021) 569–577, https://doi.org/10.1021/acs.langmuir.0c03290.
[304] J. Han, J. Yoon, Supramolecular nanozyme-based cancer catalytic therapy, ACS Appl. Bio Mater. 3 (2020) 7344–7351, https://doi.org/10.1021/acsabm.0c01127.
[305] J. He, J. Chen, D. Niu, X. Jia, Q. Wang, J. Hao, J. Gu, Y. Li, J. Shi, GSH/pH dual-responsive supramolecular hybrid vesicles for synergistic enzymatic/chemo-tumor therapy, Appl. Mater. Today 18 (2020) 100458, https://doi.org/10.1016/j.apmt.2019.100458.
[306] K. Zhang, Z. Yang, X. Meng, Y. Cao, Y. Zhang, W. Dai, H. Lu, Z. Yu, H. Dong, X. Zhang, Peroxidase-like Fe_3O_4 nanocomposite for activatable reactive oxygen species generation and cancer theranostics, Mater. Chem. Front. 2 (2018) 1184–1194, https://doi.org/10.1039/C8QM00098K.